A STUDY OF THE SILICA-UNDERSATURATED ALKALINE ROCKS OF THE LAACHER SEA AREA, EAST EIFEL VOLCANIC FIELD, WEST GERMANY

by

ANGELA C. DOBSON

Submitted in partial fulfillment of the requirements for a Bachelor of Science (Honours) Degree at Dalhousie University, Halifax, Nova Scotia, May, 1983

DALHOUSIE UNIVERSITY
Department of Geology
Halifax, N.S. Canada B3H 3J5 Telephone (902) 424-2358 Telex: 019-21863

DALHOUSIE UNIVERSITY, DEPARTMENT OF GEOLOGY

B.Sc. HONOURS THESIS

Author: ANGELA C. DOBSON

Title: THE ALKALINE ROCKS OF THE LAACHER SEE AREA

Signature of author

Date: 1983 05 19

Distribution License

DalSpace requires agreement to this non-exclusive distribution license before your item can appear on DalSpace.

NON-EXCLUSIVE DISTRIBUTION LICENSE

You (the author(s) or copyright owner) grant to Dalhousie University the non-exclusive right to reproduce and distribute your submission worldwide in any medium.

You agree that Dalhousie University may, without changing the content, reformat the submission for the purpose of preservation.

You also agree that Dalhousie University may keep more than one copy of this submission for purposes of security, back-up and preservation.

You agree that the submission is your original work, and that you have the right to grant the rights contained in this license. You also agree that your submission does not, to the best of your knowledge, infringe upon anyone's copyright.

If the submission contains material for which you do not hold copyright, you agree that you have obtained the unrestricted permission of the copyright owner to grant Dalhousie University the rights required by this license, and that such third-party owned material is clearly identified and acknowledged within the text or content of the submission.

If the submission is based upon work that has been sponsored or supported by an agency or organization other than Dalhousie University, you assert that you have fulfilled any right of review or other obligations required by such contract or agreement.

Dalhousie University will clearly identify your name(s) as the author(s) or owner(s) of the submission, and will not make any alteration to the content of the files that you have submitted.

If you have questions regarding this license please contact the repository manager at dalspace@dal.ca.

Grant the distribution license by signing and dating below.

_____ _____

Name of signatory Date

TABLE OF CONTENTS

List of Figures

List of Tables

ABSTRACT

The generation of alkaline rocks is a complex process. The East Eifel volcanic field in West Germany represents the most alkalic rocks in the alkaline province of Central Europe and France. The area of particular interest, in this study, is the Laacher See.

The rocks in this study include phonolites (including selbergites), tephritic phonolites, nephelinites and phonolitic tuffs. They have been divided into two major groups; mafic (M) and felsic (F) on the basis of petrographical, major and trace element geochemical and mineralogical analyses. Group M can be further subdivided into two subgroups: Group M-1 is composed of nephelinites and Group M-2 is composed of phonolites.

The samples of Group M and F are intricately related in space and are approximately the same age. These observations together with the experimental results indicate that all the groups are petrogenetically related.

CHAPTER 1

INTRODUCTION

1.1 Occurrence of Alkaline Volcanic Rocks

Alkaline rocks are generally defined on the basis of the following relationship, K + Na > Ca. They are characterized by the presence of feldspathoids and alkali pyroxenes (Sorensen, 1974). The magmas are more differentiated in continental areas eg. phonolite, rhyolite, than in oceanic areas eg. alkali basalt, tholeiitic basalt.

Magmas of alkalic affinity are relatively rare, but are distributed worldwide. Sahama (1974) has suggested that although the processes involved are unusual, they must be reproducible in order to generate such widespread distribution. Alkaline magmatism is generally related to major tectonic structures (Sorensen, 1974). The most predominant occurrences are associated with rift zones, for example the East African Rift system, the Rhine-Oslo graben system, Southern Greenland and the Monteregion area of Quebec (Sorensen, 1974). Another favourable site for alkaline magmatism is the junction of fault zones, eg. Kola Peninsula, Northwestern Soviet Union, Gardar Province and Southwestern Greenland (Sorensen, 1974). Alkaline rocks also occur at curves in the strike of monoclines eg.

Nuanetsi Province, South East Africa and Eastern Greenland (Sorensen, 1974). In some areas eg. Western North America and Siberia, the related tectonic lineament is not evident. Sorensen (1974) assumes that in these cases, zones of crustal weakness or concealed fault zones are associated with the alkaline rocks. The final association of alkaline magmatism is with the updoming of the crust eg. Siberian alkaline province and rift valleys (Sorensen, 1974).

The provinces of alkaline rocks often display chemical zoning eg. the African Rift system and/or bimodal magmatism eg. the Tertiary alkaline province of Central Europe and the Roman Province of Italy.

1.2 Eifel District - Study Area

A belt of alkaline rocks, Cretaceous to Pleistocene in age, extends through Central Europe and France (Fig. 1.1). The belt stretches from the Pyrenees to Southwestern Germany, Bohemia and Silesia. Volcanic activity was restricted to areas of Tertiary grabens or graben-like structures (Wimmenauer, 1974). This activity, however, occurs on adjoining horst blocks and is not found directly in the grabens (Wimmenauer, 1974).

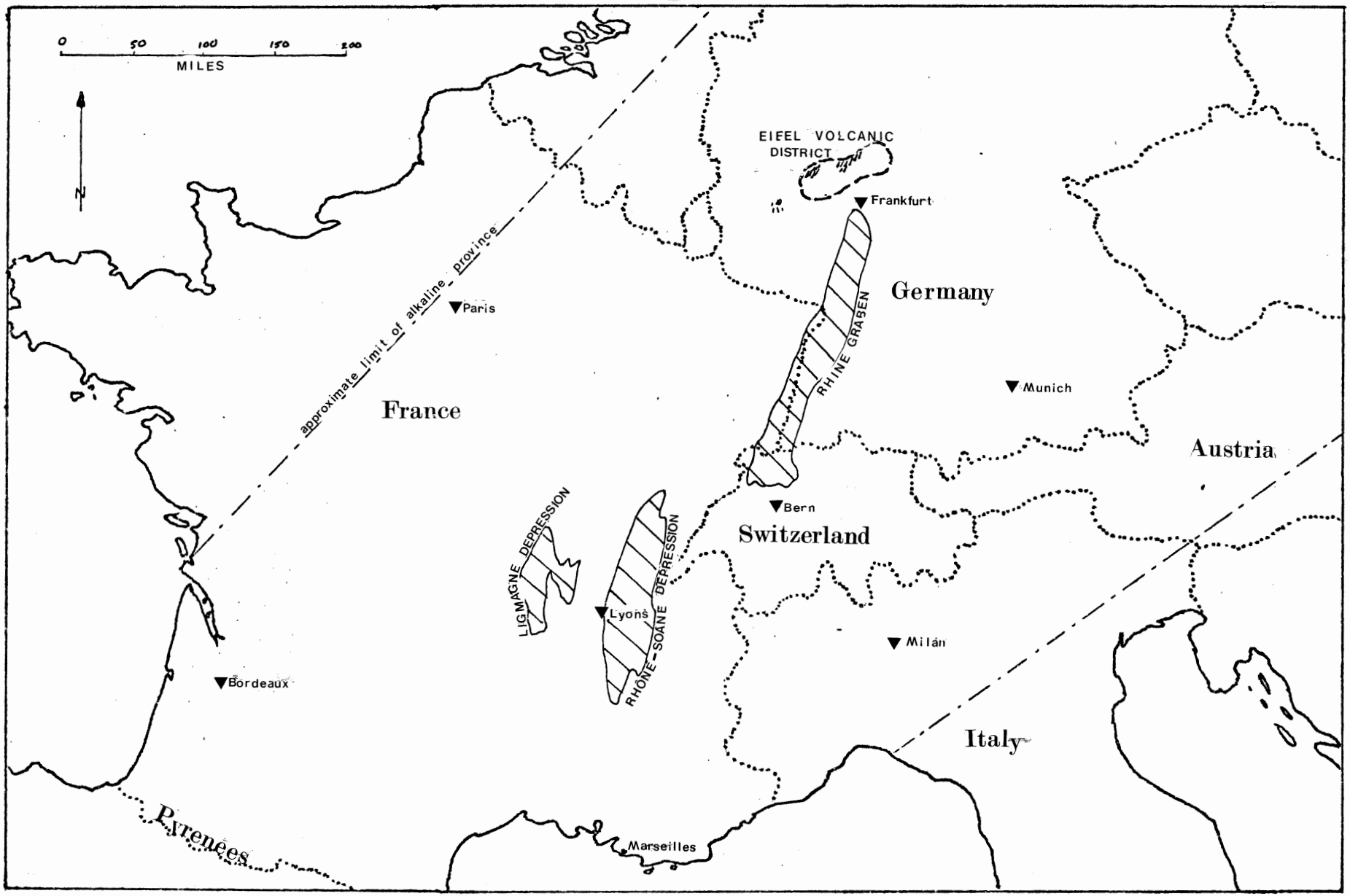

Figure 1.1. Map of the Central Europe and France Alkaline Belt. (After Wimmenauer, 1969).

The area of particular interest in this study is situated in the Eifel district of the German volcanic subprovince. The Eifel region is underlain by the Rheinish Shield which is composed of folded slates, greywackes, quartzites and limestones of Lower Devonian to Upper Carboniferous age (Illies et al., 1979). The fold axes trend in an east-northeasterly direction (Ahrens, 1928). During the Mesozoic, the area underwent extensive erosion. Uplift, commencing in the Tertiary was preceded by clastic and argillic sedimentation (Illies et al., 1979). These events were then followed by disruptive volcanism in the Quaternary (Duda and Schmincke, 1978). Illies et al. (1979), believe that the widespread volcanism was generated by the regional upwarping of the Rheinish Shield.

There are two volcanic fields of Quaternary age occurring in the Eifel area (Fig. 1.2). The larger western field is less alkaline and less differentiated than the smaller eastern field (Illies et al., 1979).

The Laacher See volcanic field is located in the eastern region of the Eifel district (Fig. 1.3). Volcanism occurred throughout the Quaternary (420,000 to 10,000 years ago), as determined by Frechen (1962) who performed K/Ar studies on the lavas and subvolcanic intrusions. These dates have been supported by the correlation of loesses and fluviatile sediments of the Rhine River (Frechen, 1965).

The volcanic field is roughly 200 km^2 and contains approximately seventy volcanic centers (Duda and Schmincke, 1978). Volcanism began in the western part of the field, extruding alkali phonolites and leucitites, and gradually progressed eastward yielding basanitic and tephritic lavas resulting in widespread, thick, phonolitic, pyroclastic deposits centered in the Laacher See basin (Duda and Schmincke, 1978).

Phonolites, which are the dominant magma type, are associated with subvolcanic foidites and carbonatites. Isotopic studies conducted on these subvolcanics and carbonatites (Taylor et al., 1967) have revealed that the $\delta^{18}O$ and $\delta^{13}C$ values vary minimally. This suggests that these rocks are closely related. The isotopic values of the CO_2 now issued at the Laacher See vent, are very similar to the ones of the carbonatites (Wimmenauer, 1974).

Three of the major phonolitic vents are thought to have a plinian origin (Illies et al., 1979) (Fig. 1.3). In this process, groundwater contacts the uprising magma causing vaporization. The addition of water to the phonolitic magma reduces its viscosity and facilitates the release of volatiles (Sood, 1981). The pressure in the vent is suddenly increased, causing rapid, disruptive ascent of the magma (Lorenz, 1973).

Extrusion at the surface is extremely violent, and magmatic debris and country rock can be found at great distances

from the vent eg. debris from the Laacher See vent has been distributed over much of Central Europe (Illies et al., 1979). The resulting crater surrounding the vent is encased by a tuff ring. Upon cessation of volcanic activity, the crater often fills with water forming a circular lake or maar. These maars lie on valley floors at the intersection of fissures (Lorenz, 1973). The bulk of the volcanic centers produce cinder cones which lie on hills or valley slopes (Lorenz, 1973).

The Laacher See area is well known for the occurrence of country rock fragments in tuffs and pyroclastics of Pleistocene age (Okrusch et al., 1979). Many of the xenoliths have undergone pyrometamorphic alteration, producing the famous Sanidinites (Okrusch et al., 1979). The alteration has occurred under high temperature, low pressure conditions which may or may not involve the metasomatic addition of alkalis (Okrusch, 1979). Some xenoliths however, remain relatively unaltered, enabling the metamorphic grade of the underlying crystalline basement to be determined at an amphibolite facies grade (Okrusch et al., 1979).

It has been postulated that crustal bodies of magma have been generated due to extensional forces in the East Eifel area. As previously stated, the volcanism is thought to be related to the uplift of the Rheinish Shield. As the crust was uplifted due to rising mantle geotherms, an area of

reduced pressure is thought to attract volatiles and other highly mobile elements causing the generation of an alkalic magma. The magma forces its way to the surface, due to its reduced density, along a zone of weakness generated by the uplift. Xenoliths are incorporated in the magma as it ascends. Studies conducted on these xenoliths (Illies, et al., 1979) indicate that the more differentiated lavas contain xenoliths from higher crustal levels than do less differentiated magmas (Fig. 1.3).

1.2.1 Previous Work

Previous work on the volcanics of the Laacher See area has been conducted by various authors. Braums (1921) published twenty-three chemical analyses, Frechen (1962, 1965, 1971) added additional data. Lorenz (1973), Schmincke and Duda and Schmincke (1978) have studied the volcanic centers. Illies et al. (1979) have done a study on the Quaternary uplift of the Rheinish Shield and Okrusch et al. (1979) have studied the xenoliths in the pyroclastics. Much of the work has been published in German.

1.3 Petrogenic Problems

The petrogenesis of an alkaline magma is a complex problem. Many authors believe that they are generated by partial melting of the deep seated crust or mantle. Ringwood (1975) and

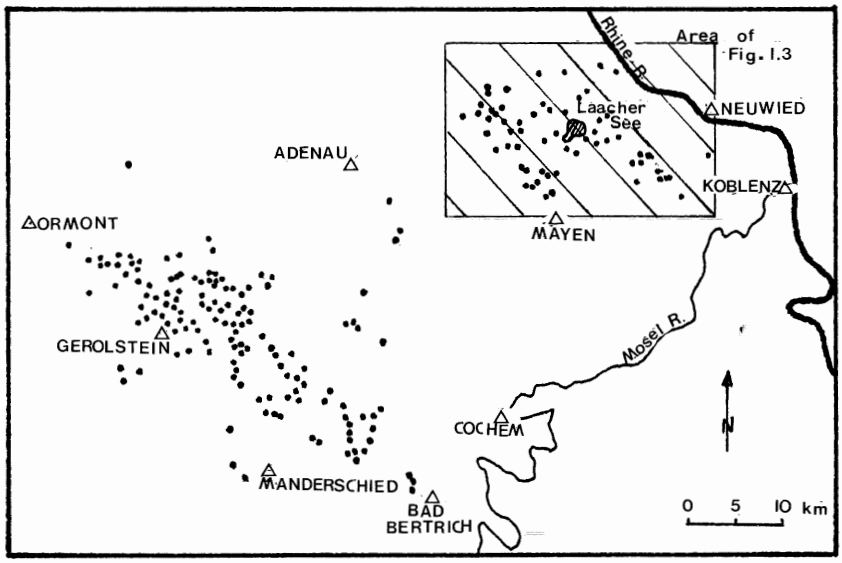

Figure 1.2. Late Quaternary West Eifel and East Eifel volcanic fields. The dots represent volcanic centers. (After Illies, et al., 1979).

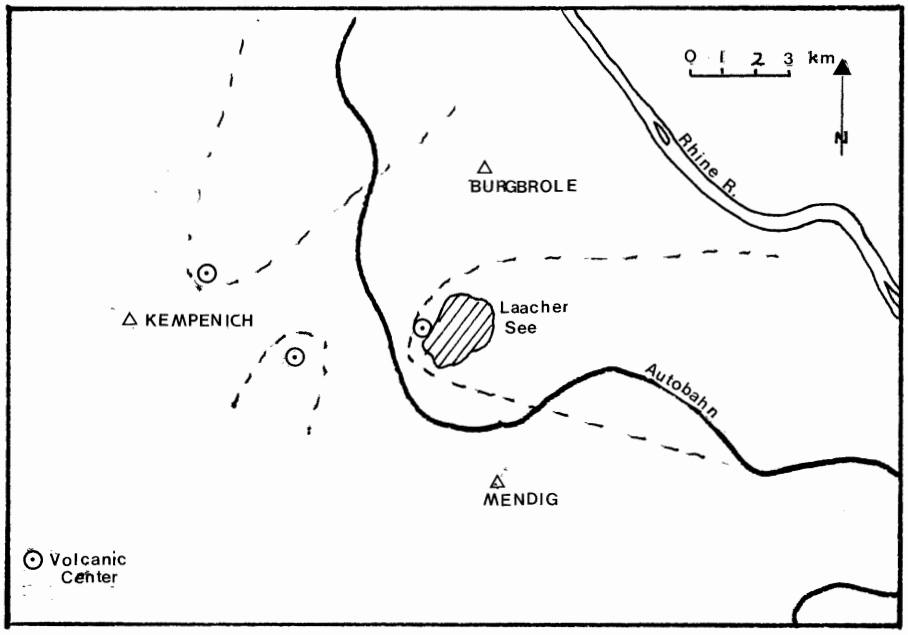

Figure 1.3. Map of the East Eifel volcanic district. The three main phonolitic centers are outlined and the distribution of their corresponding tephra are schematically shown. (After Duda and Schmincke, 1978).

Kushiro (1972) have determined, by experimental study on silicate systems, that the formation of alkaline silica-undersaturated magmas becomes dominant with depth eg. a depth of 100 km corresponds to a partial melting of 3%. Bailey (1974) states, however, that this process is not sufficient to produce floods of magma of constant composition over large areas. Thus many processes are probably involved. Harker (1909) and Wood (1968) suggest the process of zone refining to enrich the magma in incompatibles. Daly (1933), O'Hara (1968) and Wood (1968) discuss the importance of crystal fractionation in the role of differentiating an alkaline magma. Daly (1933) also suggested the introduction of alkalis by gaseous transfer.

The influence of assimilation of carbonate rocks to produce an alkaline magma is seen to be only of local importance (Barker and Long, 1969; Wyllie, 1974). This process was considered to be of major importance in the production of the Mt. Vesuvius lavas (Rittman, 1973). Savelli, however, disproved Rittman's theory because, although the major elements of the limestone and magma correlated, the trace elements did not.

Liquid immiscibility is thought to be of minor importance, especially during late stage crystallization processes (Kogarko, et al., 1974).

Korzhinsky (1955) and Bailey (1982) have proposed the process of metasomatism. Mobile elements are introduced eg.

volatiles, water, which cause the expansion of the fields of crystallization of the minerals and thus influence the crystallization trend of the magma.

The generation of an alkaline magma is thus a complex process, and only a few of the influencing processes have been outlined above.

1.4 Purpose of the Present Work

Petrographic analyses will help to determine the mineralogy and geochemistry of the selbergites, tephritic phonolites and nephelinites of the Laacher See area. Microprobe analyses of the major elements, substantiated by the analyses of the rare earth and trace elements will be examined in order to make an attempt to understand the petrogenesis of the source magma(s).

CHAPTER 2

LOCAL GEOLOGY

2.1 Local Geology

As previously stated, volcanism in the East Eifel district began in the western section, extruding phonolites, and progressed eastward extruding basinites and nephelinites. During this period of late Quaternary volcanism (40,000 yr to 200,000 yr. ago), approximately forty-four volcanoes were formed (Duda and Schmincke, 1978). Thirty-three of these are leucite basinites, eight are leucite tephrites and three are nephelinites. The character and structure of the volcanoes has been described by Frechen (1971), Lorenz (1973), Schmincke (1977b) and Duda and Schmincke (1978). The volcanic cones are approximately 150 m in height and 100 to 500 m in diameter. The cones are largely composed of unwelded scoria and agglutinates. In some cases the agglutinates grade into lava flows which can extend up to five kilometers. Poorly sorted block tuffs may contain up to 50% xenoliths and dense mafic lapilli and bombs. These dense mafic ejecta are interpreted to be the products of phreatomagmatic eruptions, which were succeeded by lava fountaining (Duda and Schmincke, 1978).

The latest volcanic episode was of a phonolitic-pyroclastic nature, which centered around the Laacher See. The type of eruption predominant at this time was of phreato-magmatic character. The deposits of these maar volcanoes are fine to coarse-grained, and poorly to well bedded (Lorenz, 1973). Individual beds, representing air-fall and base surge deposits, are 1 to 40 cm in thickness. The ejecta contain up to 80% country rock debris (Lorenz, 1973). These xenoliths are generally similar in composition. They are composed of plagioclase, pyroxene and minor amounts of brown hornblende, opaques and scapolite (Okrusch et al., 1979). These rocks have been named garnet pyroclastites. Studies on these ejecta (Okrusch et al., 1979) have been conducted in order to determine the composition of the crust below the Laacher See area. Results indicate that the xenoliths are of deep crustal origin, about forty kilometers depth (Okrusch et al., 1979).

2.2 Field Work

The twenty-one samples used in this study were collected by Dr. D.B. Clarke during his sabbatical in Bonn, West Germany in 1982.

The sample locations are shown in Figure 2.1.

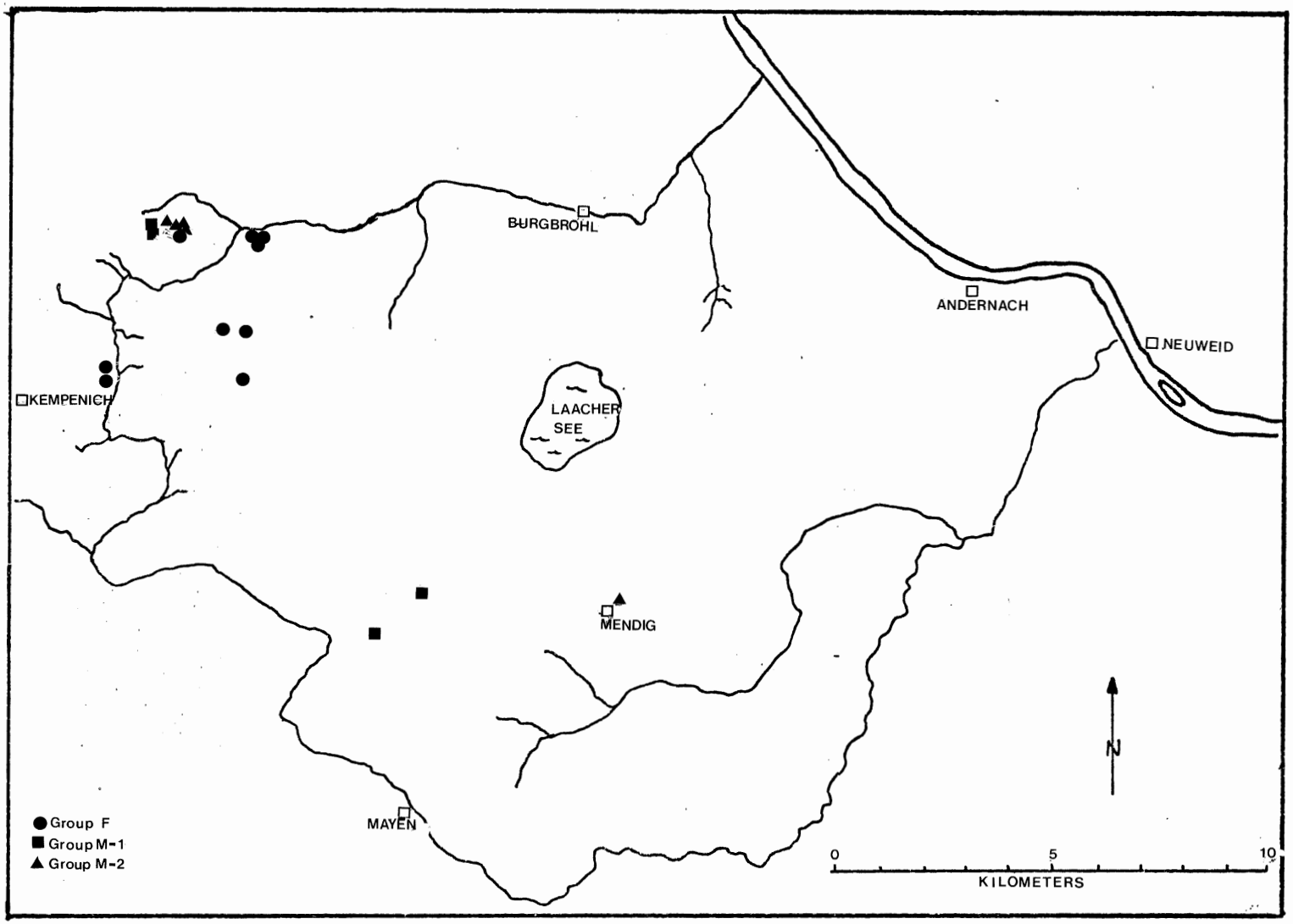

Figure 2.1. Location map of the samples selected for this study. (After Frechen, 1976).

2.3 Analysis

Twenty-one polished thin sections were prepared for mineralogical analysis using the electron microprobe at Dalhousie University. Petrographic descriptions were also conducted on these thin sections. Nineteen samples, excluding two tuffs, were then crushed and powdered, and submitted for trace element analyses using X-ray fluorescence and neutron activation, to X-Ray Assay Laboratories, Don Mills, Ontario. These samples were also melted to form a homogeneous glass which was then analysed for its whole rock composition using the electron microprobe.

Structural formulas were determined for all minerals obtained, and CIPW normative programs were computed on the whole rock data and selected feldspathoids and alkali minerals.

CHAPTER 3

GENERAL PETROLOGY

The major rock types dealt within this study are phonolites (including selbergites), tephritic phonolites and nephelinites. They occur as porphyritic and fine-grained basic rocks, and as felsic tuffs.

Selbergites were defined in 1922 by Brauns as "... hypabyssal phonolite(s) containing phenocrysts of leucite, nosean (hauyne), sanidine, acmite-augite, (and) biotite in a fine-grained groundmass of nepheline, alkali feldspar and acmite. The phenocrysts comprise a higher percentage of the volume of the rock than the groundmass ...."[1]

Classification according to Streckeisen's diagram results in two main groups (Fig. 3.1). One group (M), is more melanocratic eg. samples 50, 51, 57, 116 and 117, than the other (F), which consists of samples 64, 69, 76, 77, 78, 79, 82, 83, 101, 104, 107, 108, 109. Full petrographic descriptions may be found in Appendix A.

3.1 Group "M"

The main rock type constituting Group M is nephelinite.

---

1. Bates and Jackson. Glossary of Geology. American Geological Institute, Virginia (1980).

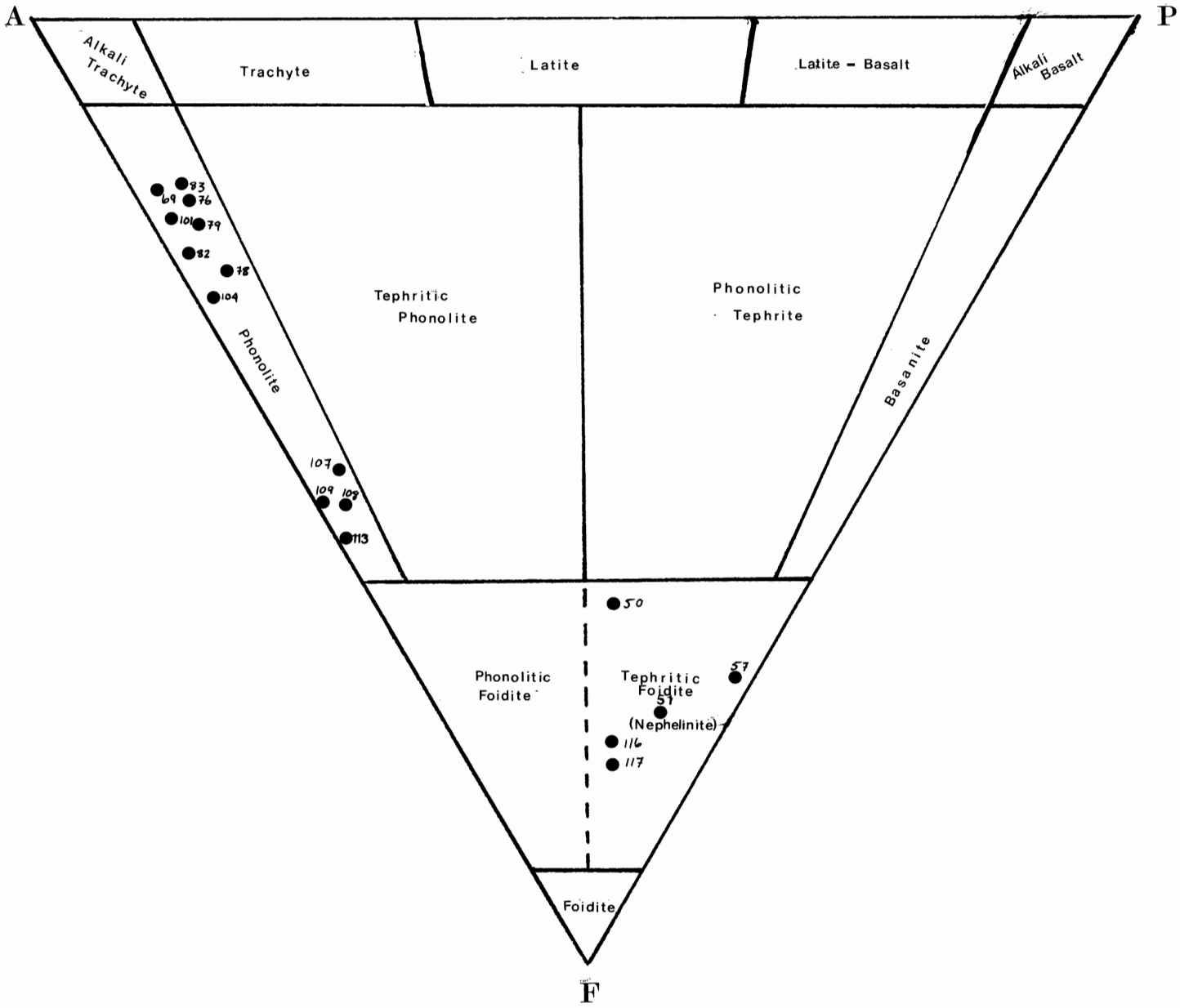

Figure 3.1. Streckheisen's classification scheme for igneous rocks. The samples are plotted according to modal mineralogy.

3.1.1 Nephelinites

The nephelinites or tephritic foidites (Streckeisen) are of two distinct types. Samples 51 and 52 are porphyritic nephelinites, and samples 116 and 117 are vesicular lava flows. All of the samples collected contain xenoliths. The xenoliths in the porphyries are approximately two centimeters in diameter, and are leucocratic, possibly phonolitic in composition. The xenoliths in the flows are rich in pyroxene and are approximately one centimeter in diameter.

3.1.1a Porphyritic Nephelinites

Samples 51 and 57 are holocrystalline and the groundmass is pilotaxitic. The phenocrysts present are titanaugite, biotite and olivine and are minimally poikilitic. The biotite present indicates that the rocks have been under strain at some time in their history (Plate 3.1). The pyroxene comprises 30 to 40% of the slide and generally occurs in euhedral form, displaying fine oscillatory zoning (Plate 3.2). Many of the pyroxenes exhibit dark anhedral cores. This is probably the result of the overgrowth of an unstable pyroxene by a more stable one. This effect may be caused by magma mixing, which causes an originally stable mineral to become unstable by the introduction of a magma of different composition or the reincorporation of a fractionated crystal in the magma. The unstable mineral may undergo resorption in the melt. Crystallization


BT

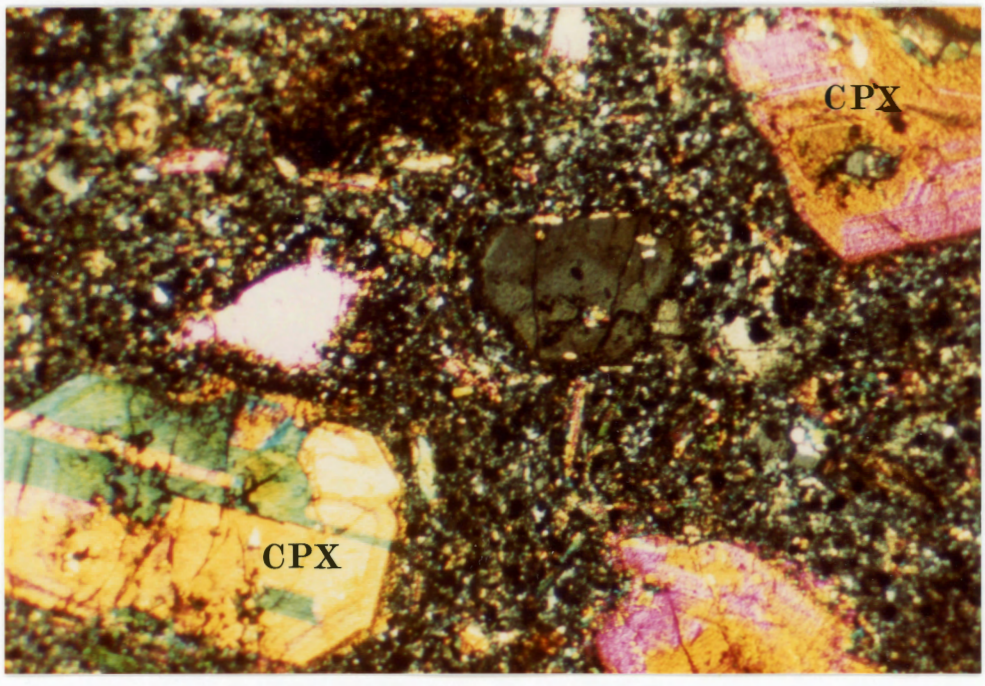
CPX
CPX

Plate 3.1. 57 Nephelinite (porphyritic) Mag. x20 (x-nicols) Group M

- straining evident in the extinction of the biotite phenocryst
- microcrystalline groundmass altering to clays

Plate 3.2. 51 Nephelinite (porphyritic) Mag. x20 (x-nicols) Group M

- fine oscillatory zoning of clinopyroxene phenocrysts
- small laths of clinopyroxene in the groundmass

of a more stable mineral will occur on the surface of this reacting crystal and will effectively prevent the melt from further reaction. There is some twinning among the pyroxene crystals.

The groundmass is generally composed of nepheline, sanidine, leucite, magnetite and felty masses of clinopyroxene. Alteration is restricted to the borders of the olivine crystals and some biotite laths. Secondary calcite is present along some fractures.

3.1.1b Flows

Samples 116 and 117 are vesicular lava flows. The groundmass is aphanitic and holocrystalline. The pyroxene often displays an ophitic and microglomeroporphyritic texture. These augite crystals are generally well zoned, poikilitic and are subhedral to euhedral. Small secondary or late forming aegirine-augite crystals form part of the groundmass and are most obvious protruding into vesicles (Plate 3.3). The groundmass is again composed mainly of nepheline and augite laths, altered leucite crystals and anhedral magnetite. Sample 117 is a more altered equivalent of sample 116. Calcite occurs along fractures and in vesicles, and sulphide weathering stains are prominent on the surface of the rock specimens.

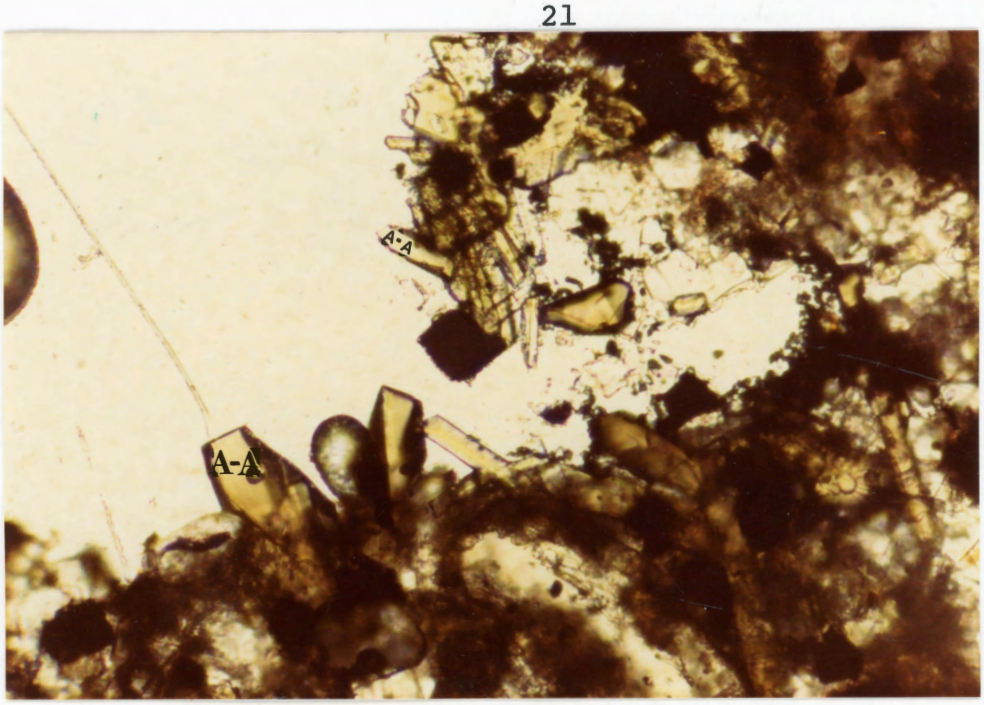
A-A
A-A

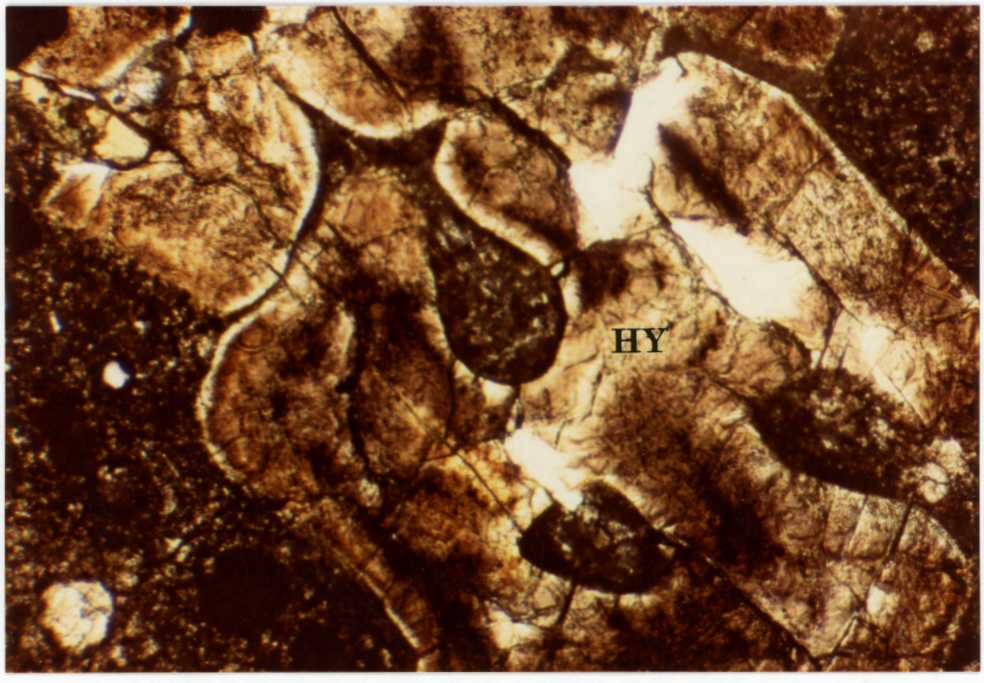
HY

Plate 3.3 116 Nephelinite (flow) Mag. x80 (ppl) Group M

- aegirine-augite crystals protruding into a cavity

Plate 3.4. 77 Selbergite Mag. x20 (ppl) Group F

- embayed hauyne phenocryst due to skeletal growth (?)

3.2 Group "F"

The dominant rock type in this more leucocratic group is phonolite. There are eight samples of true selbergites - 77, 78, 79, 101, 104, 108, 109 and 113, three porphyritic phonolites - 69, 76, 82 and three tephritic phonolites - 50, 83, 107.

3.2.1 Selbergites

The samples classified in this category are strictly selbergites because the phenocrysts comprise more of the volume of the rock than the groundmass. The main phenocryst phases are hauyne, sanidine and leucite with minimal clinopyroxene and biotite. These crystals were generally idiomorphic, but have since been altered or corroded by the magma. The groundmass generally displays a pilotaxitic texture and is composed of felty sanidine crystals and nepheline prisms, with minor appearances of magnetite, clinopyroxene and biotite. Alteration is most evident in the transition of leucite to pseudoleucite. The hauyne phenocrysts are often highly altered, displaying either dark cores with light rims or light cores surrounded by dark rims. The light cores have generally been altered to a felty mass of crystals - probably alkali feldspar. Some of the hauyne crystals display embayed crystal boundaries (Plate 3.4). This texture is more likely to be the result of skeletal crystal growth than magma reaction, because during

the latter process the corners would have been removed first, however this is not the case, thus skeletal growth is preferred. The rectangular nepheline crystals in the groundmass also display altered grain boundaries as well as rows of inclusions in the core. The phenocrysts of sanidine and the smaller crystals in the groundmass display Carlsbad twinning. Small quantities of apatite are present in the groundmass of some samples, in subhedral to anhedral crystal forms. Secondary calcite and zeolite have crystallized along fractures and in voids.

A xenolith which is a hauyne-apatite-augite cumulate is present in sample 108. The composition of this cumulate is very similar to the rest of the slide, thus the xenolith has probably been derived from the same melt as the selbergites rather than from the country rock.

3.2.2 Porphyritic Phonolites

Samples 69, 76 and 82 are classified as porphyritic phonolites because although the mineralogy is generally the same as the selbergites, the groundmass constitutes a larger volume of the rock than do the phenocrysts. The main phenocrysts are again hauyne, leucite and sanidine, and the groundmass is composed mainly of fine grained nepheline and sanidine crystals. Alteration has affected these minerals in the same way as the selbergites. Around some of the hauyne crystals in

sample 82 are alteration halos consisting of felty intergrowths, probably alkali feldspathic in composition (Plate 3.5). A small, acicular green mineral - aegirine-augite - is present in some of the leucites and also in the groundmass. Secondary zeolite has crystallized along fractures.

3.2.3 Tephritic phonolites

The three samples which fall into this category are 50, 83 and 107. Sample 50 is a lava flow, and samples 83 and 107 are porphyritic phonolites.

3.2.3a Flows

Sample 50 represents a highly vesicular lava flow which has a holocrystalline, aphanitic texture. The main phases of phenocrysts are zoned augites, sanidine and hauyne crystals. The groundmass is composed of nepheline, sanidine, augite and magnetite. Much of the groundmass has been altered to clays. Secondary calcite has crystallized along fractures and in vesicules.

3.2.3b Porphyritic Tephrite Phonolites

Samples 83 and 107 are porphyritic, holocrystalline phonolites supported by a pilotaxitic groundmass. The porphyritic phases are the same as the selbergites and porphyritic phonolites. They are generally idiomorphic in shape, but display some evidence of magma corrosion for example the

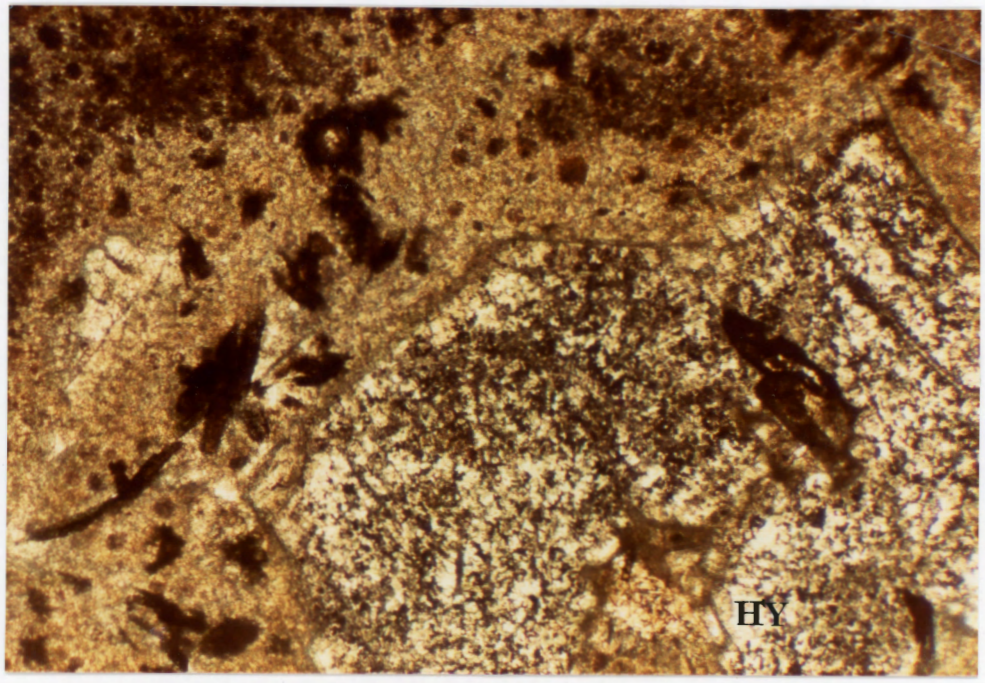

Plate 3.5. 82 Phonolite (porphyry) Mag. x20 (ppl)
Group F

- alteration halo surrounding a poikilitic hauyne phenocryst in an altered holocrystalline groundmass

development of mantles around the sanidine, hauyne and leucite crystals. Portions of these samples have been highly fractured and largely altered to red and brown clays. Zeolite, calcite and late stage aegirine-augite crystals, are present along fractures and in the vesicles.

3.3 Tuffs

There were three samples of tuffs studied in this survey - 52, 64, 96. Samples 52 and 96 are generally phonolitic in composition, and sample 64 is a trachytic tuff. The tuffs are composed of crystal and lithic fragments, as well as fine grained ash.

3.3.1 Phonolitic Tuff

Sample 52 is a selbergite tuff. It contains augite, hauyne, leucite and sanidine phenocrysts, as well as assorted xenocrysts and lithic fragments. The groundmass is composed of sanidine, biotite and volcanic ash. There are several types of xenoliths present; one type is highly siliceous, another is felsic but of approximate trachyte composition, another type is mafic, possibly of nephelinite composition and some fragments are of well lineated metasediments/volcanics (?). The highly siliceous and metamorphic rock fragments are probably derived from the country rock. The felsic and mafic fragments are probably genetically associated with the magmas generating the rocks in Group F and M.

Sample 96 is more mafic than 52. It contains sanidine and biotite phenocrysts, zoned augite aggregates and a wide variety of xenoliths similar to those found in sample 52. The rock fragments and ash are highly altered.

3.3.2 Trachyte Tuff

Many of the rock fragments in sample 64 have developed alteration rims and have progressed to clays in most cases. Sanidine, augite and biotite occur as zoned, fractured phenocrysts. Nepheline is present as microscopic felty intergrowths. The rock fragments are again similar to those of samples 52 and 96.

Summary

Group M is composed of two types of nephelinites; vesicular flows and porphyries. The main constituents of these rocks are clinopyroxene, olivine, biotite and nepheline. The accessory minerals include sanidine, leucite and magnetite. Alteration is evident at the crystal boundaries of olivine and biotite. All of the samples contain xenoliths.

Group F is composed of various types of phonolites. These include selbergites, porphyritic phonolites and trachytic phonolites. The main phenocryst phases are hauyne, leucite and sanidine with minor clinopyroxene and biotite. The groundmass is composed generally of nepheline, sanidine, clino-

pyroxene and rare apatite and magnetite.

The three tuffs in the study are composed of augite, hauyne, leucite, sanidine, nepheline and biotite crystals and crystal fragments. There are two main types of rock fragments; those derived from the country rock and those of close petrogenetic relationship to that of Groups M and F.

CHAPTER 4

WHOLE ROCK GEOCHEMISTRY - MAJOR AND TRACE ELEMENTS

Nineteen samples representing nine volcanic vents studied in this paper, were analysed for trace elements using X-ray fluorescence and neutron activation at the X-Ray Assay Laboratories Ltd., Don Mills, Ontario. These samples were also analysed for major elements using the electron microprobe at Dalhousie University.

4.1 Major Elements

The whole rock analyses for major elements were performed by the author, on homogeneous glasses produced from the powdered rocks (Table 4.1). These analyses were run through a CIPW norm program and the results were plotted on Streckeisen's diagram for the classification of volcanic rocks (Fig. 4.1). Three main rock types have been distinguished - phonolites, tephritic phonolites and nephelinites. Sample 64 is a tuff, incorporating many xenoliths and plots as a trachyte. Chemically this sample is not representative of the extruding lava and will be left out of further geochemical studies.

TABLE 4.1

MAJOR ELEMENT WHOLE ROCK ANALYSIS

	50	51	57	107	108	109	113	116	117	
SiO_2	49.19	41.69	40.95	51.91	49.66	50.04	49.57	42.03	42.28	
TiO_2	1.91	2.85	2.88	.94	1.03	1.05	1.07	2.29	2.28	
Al_2O_3	17.41	14.08	13.98	20.94	19.19	19.41	19.42	16.13	15.91	
FeO	8.05	10.48	11.05	5.81	6.52	6.55	6.30	11.02	11.04	
MnO	0.19	0.25	0.21	.37	.34	.37	.36	.35	.28	
MgO	4.14	9.02	7.79	.98	1.18	1.17	1.05	4.50	4.26	
CaO	8.66	12.73	14.14	5.94	6.47	6.48	7.66	13.49	12.48	
Na_2O	5.10	3.74	2.91	6.93	8.42	8.11	7.97	5.56	5.59	
K_2O	4.13	3.42	3.95	5.46	5.64	5.62	5.53	3.30	3.70	
P_2O_5	.51	.61	.85	.46	.49	.43	.41	.93	.96	
Total	99.30	98.87	98.71	99.74	98.94	99.23	99.34	99.60	98.79	
	64	69	76	77	78	79	82	83	101	104
SiO_2	58.90	54.52	55.39	56.35	54.25	54.41	59.34	59.77	54.39	53.84
TiO_2	.39	.42	.36	.27	.19	.22	.23	.12	.22	.23
Al_2O_3	21.68	22.36	22.75	23.11	22.69	22.54	22.61	23.14	22.76	22.48
FeO	3.04	3.38	3.64	3.12	2.99	3.12	2.91	2.85	2.81	2.86
MnO	0.19	0.27	0.23	0.24	0.24	.23	.25	.23	.20	.23
MgO	0.77	-	.41	-	-	-	-	-	-	-
CaO	2.40	1.56	1.62	1.16	1.46	1.50	1.40	3.10	1.55	1.93
Na_2O	5.55	7.81	8.39	8.11	8.31	7.90	8.77	5.29	8.25	8.47
K_2O	7.17	9.03	6.31	8.64	9.44	9.52	9.23	9.32	8.90	9.15
P_2O_5	-	-	-	-	-	-	-	-	-	-
Total	100.09	99.35	99.09	101.0	99.52	99.44	99.74	98.82	99.08	99.19

Mafic Group: 50, 51, 57, 107, 108, 109, 113, 116, 117
Felsic Group: 69, 76, 77, 78, 79, 82, 83. 101, 104
Tuff: 64

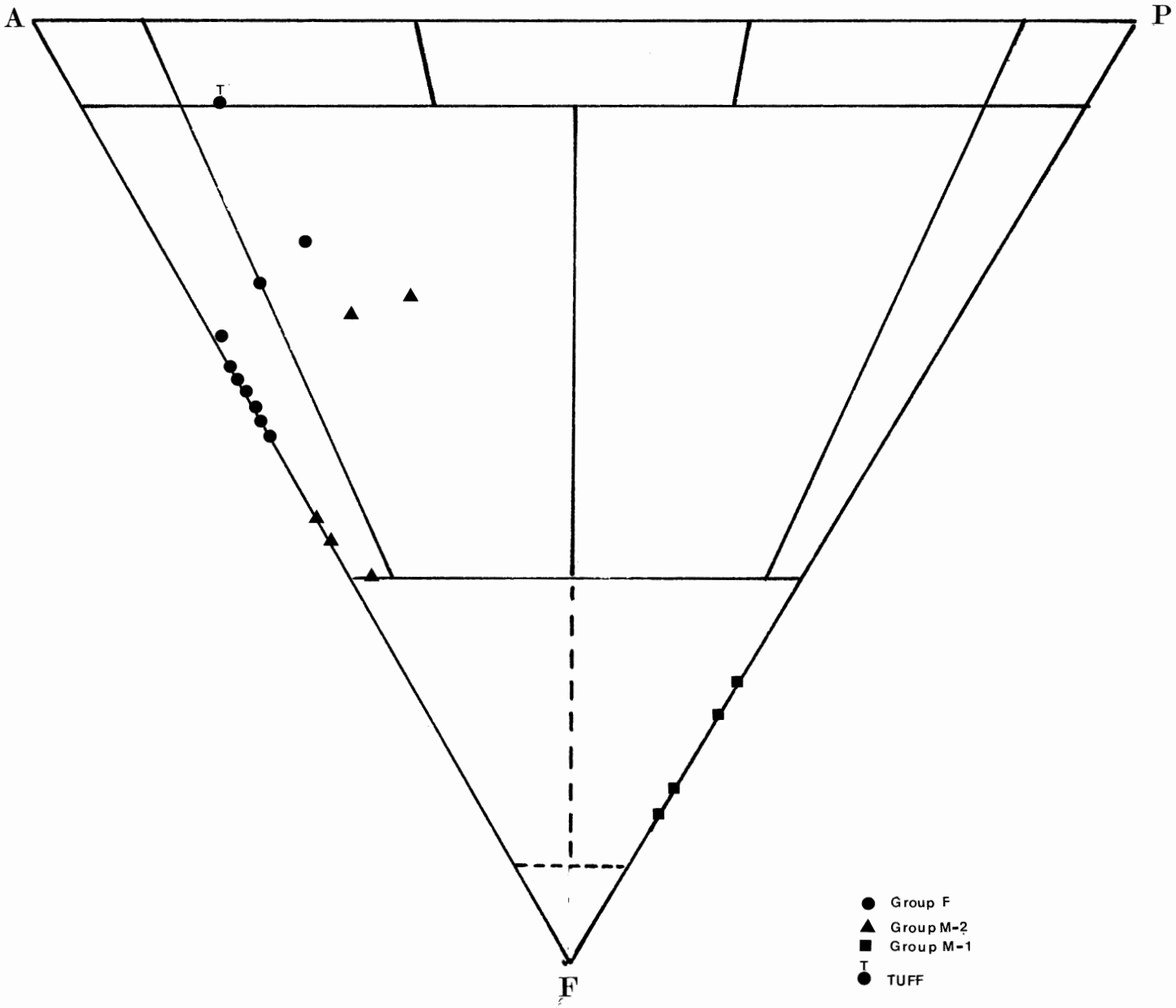

Figure 4.1. Streckeisen's diagram for the classification of Igneous Rocks. The samples are plotted on the basis of the CIPW normative analysis.

4.1.1 CIPW

The CIPW values of the samples are plotted on the quartz-kalsilite-nepheline residua system (Fig. 4.2). This diagram reveals the presence of two distinct groups. One group clusters around the center of the diagram and the other group plots on the nepheline apex. The felsic and mafic groups of the third chapter will be redefined here. The felsic group will correspond to the rocks which plot in the center of the residua system and the other rocks will be classified in the mafic group. This definition groups some selbergites and trachytic phonolites in the "mafic" group which will be defined as Group M-2. Group M-1 represents the nephelinites. The points of Group F indicate the possible position of a reaction point. This reaction point could provide an estimation on the physical conditions of formation of the volcanic rocks.

The CIPW norms were also plotted on the tetrahedral projections of the alkali basalt system (Figs. 4.3 - 4.6). In this set of diagrams it is only possible to plot Group M-1. These points describe a linear trend which corresponds to the nepheline-diopside cotectic boundary and the diopside-olivine cotectic boundary which are especially obvious in the diopside projection (Fig. 4.3) and the olivine projection (Fig. 4.4). The presence of these cotectics is observable in the hand samples by the co-existence of nepheline and clinopyroxene, phenocrysts, and clinopyroxene and olivine phenocrysts.

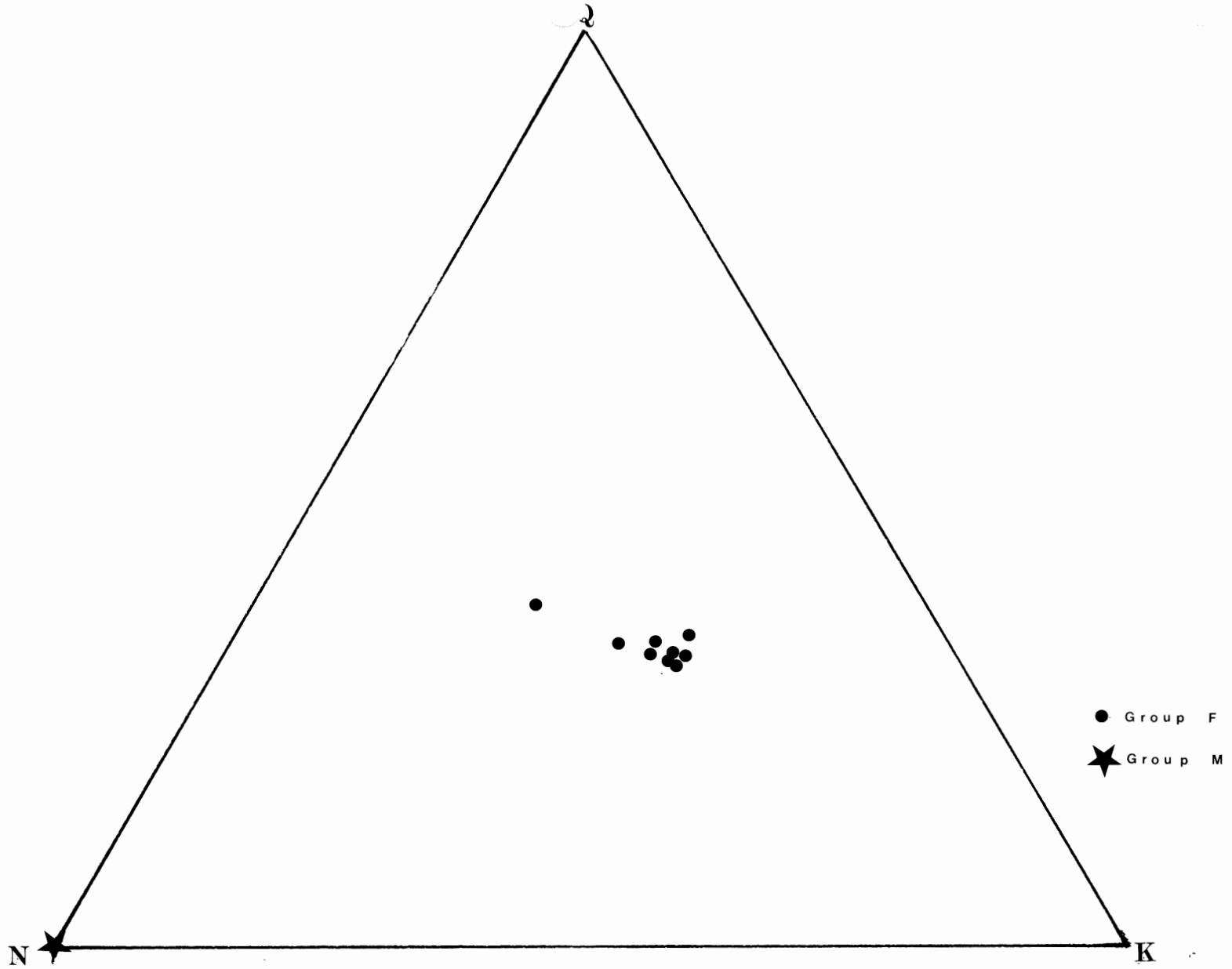

Figure 4.2. Quartz-Kalsilite-Nepheline Residua System. The samples of Group M-1 and M-2 plot on the nepheline apex. A reaction point is indicated by the clustering of the points.

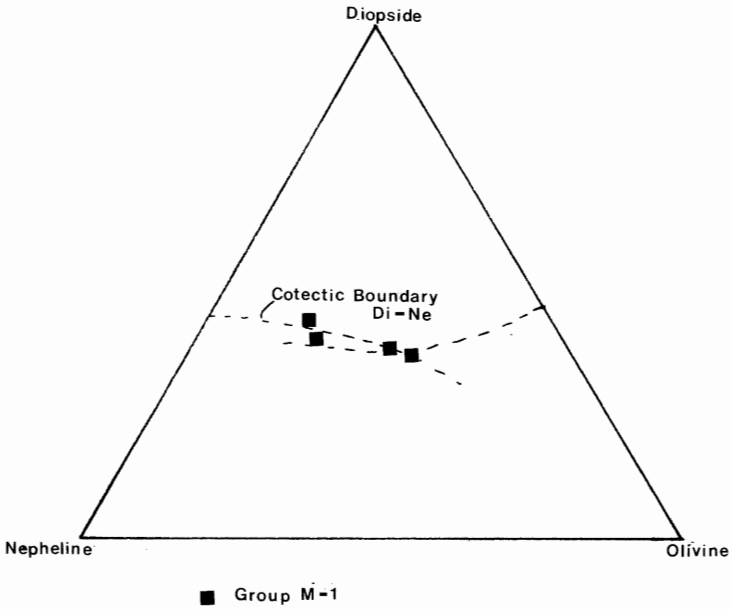

Figure 4.3. Alkali Basalt System - Plagioclase Projection

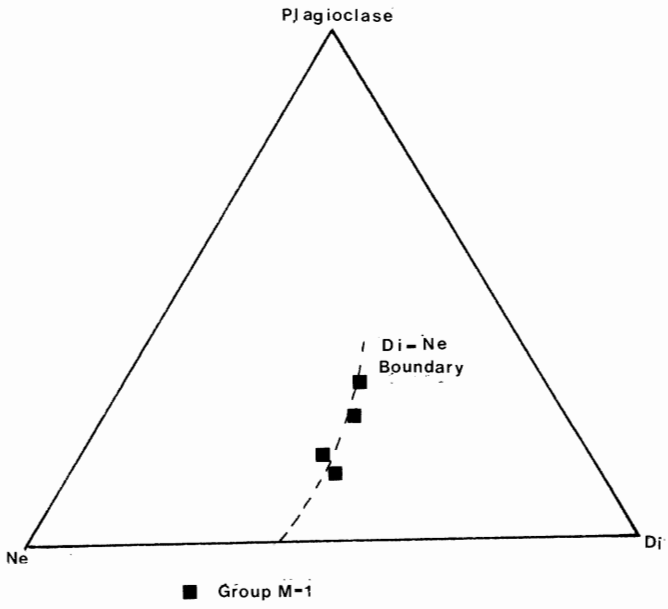

Figure 4.4. Alkali Basalt System - Olivine Projection

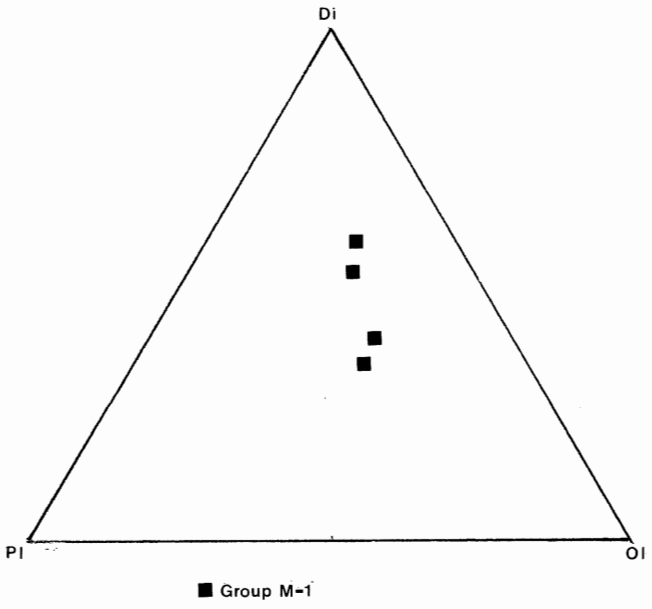

Figure 4.5. Alkali Basalt System - Nepheline Projection

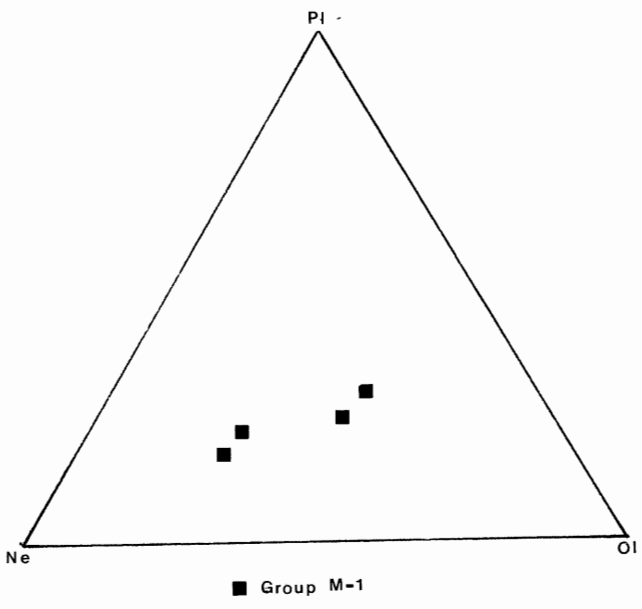

Figure 4.6. Alkali Basalt System - Diopside Projection

4.1.2 Variation Diagrams

The microprobe analyses of the major elements were plotted on Harker (Fig. 4.7, 4.8) and Power (Fig. 4.9, 4.10) variation diagrams. The Harker diagrams indicate the expected decrease of CaO, FeO, TiO_2 and P_2O_5 and the increase of Al_2O_3, Na_2O and K_2O with the increase of SiO_2 in the samples. The Power diagrams display the predictable tendency of the samples to decrease in FeO, CaO, TiO_2, P_2O_5 and the corresponding increase in Na_2O, Al_2O_3 and K_2O with decreasing MgO. The division of the samples into the felsic and mafic groups is again apparent. Group F is higher in SiO_2, Al_2O_3, Na_2O and K_2O than Group M which is correspondingly higher in MgO, CaO, FeO, TiO_2 and P_2O_5 (Fig. 4.7 - 4.10). The further subdivision into Group M-1 and M-2 can be established in the mafic group. Group M-1 is enriched in MgO, FeO, CaO, TiO_2 and P_2O_5 relative to Group M-2 which contains a higher percentage of SiO_2, Al_2O_3, Na_2O and K_2O.

Chemical analyses from the sanidine, olivine, pyroxene and magnetite crystals studied have been plotted on Figures 4.9 and 4.10. From these analyses, control lines delineating the possible paths of fractionation of the melt can be determined assuming that all the samples are genetically related. Olivine, clinopyroxene and sanidine mineral analyses have been plotted on Fig. 4.9 and 4.10 to establish mineral control lines.

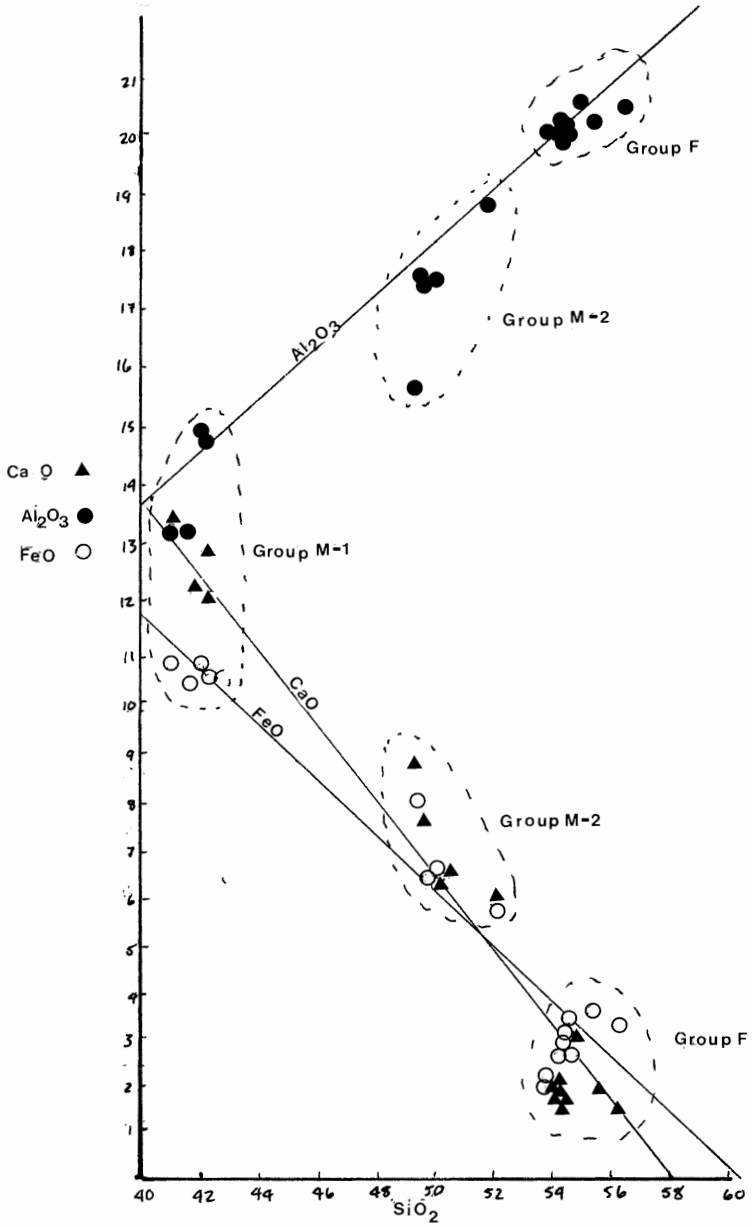

Figure 4.7. Harker Variation Diagram CaO, Al_2O_3, FeO vs SiO_2

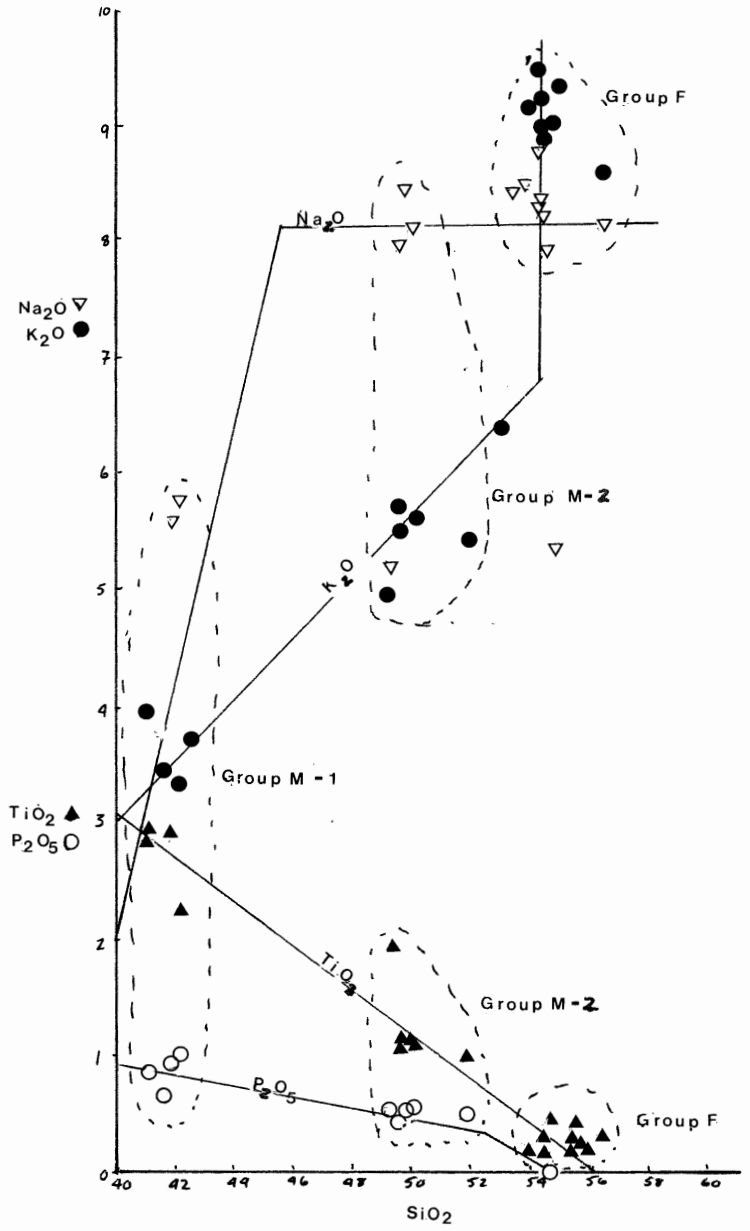

Figure 4.8. Harker Variation Diagram Na_2O, K_2O, TiO_2, P_2O_5 vs SiO_2

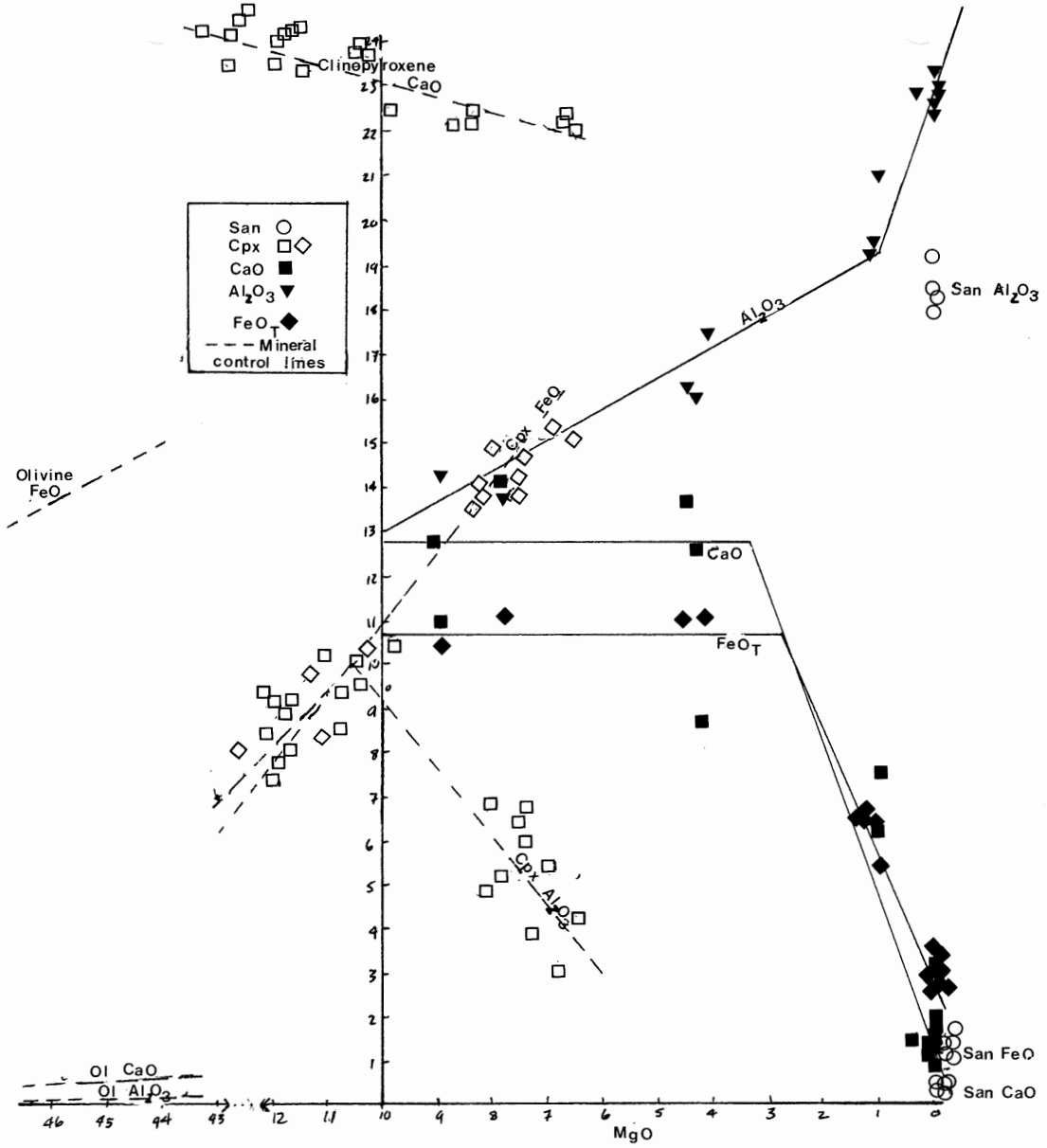

Figure 4.9. Power Variation Diagram
CaO, Al_2O_3, FeO vs MgO
- mineral analyses are plotted to establish control lines for the elements

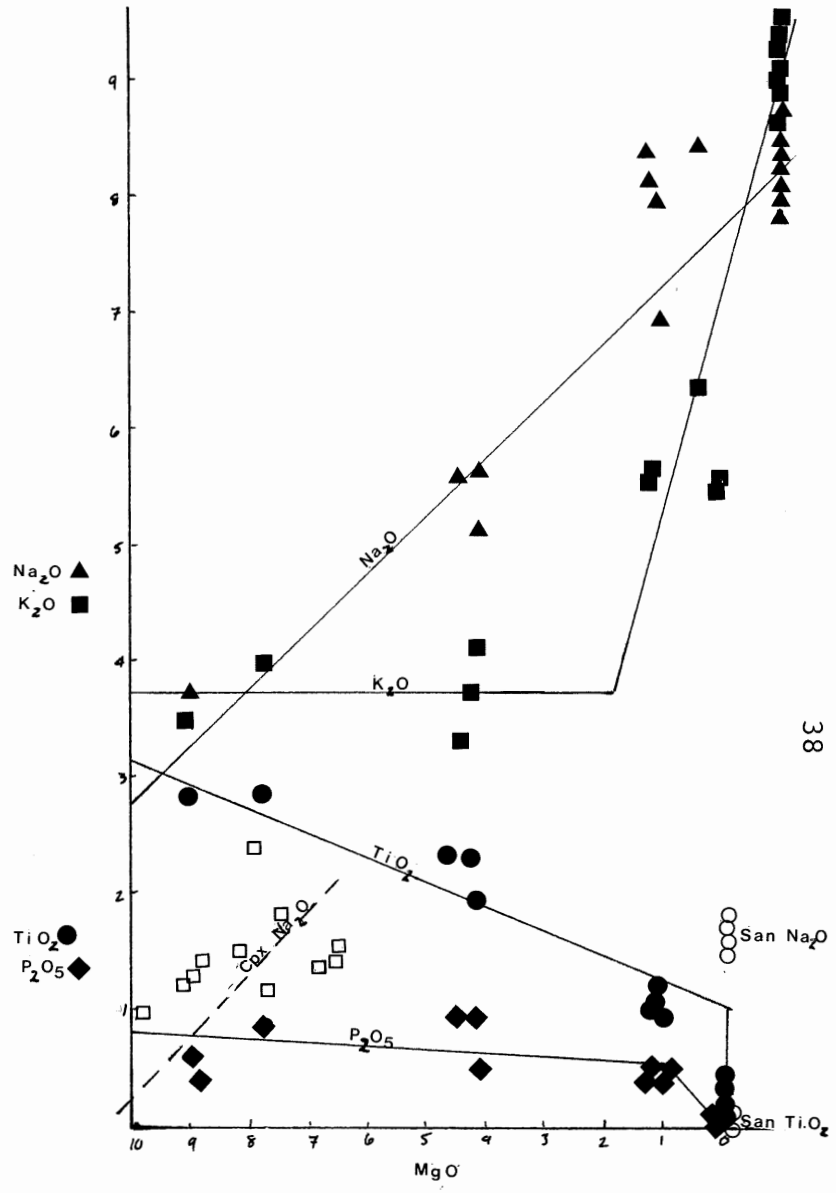

Figure 4.10. Power Variation Diagram
Na_2O, K_2O, TiO_2, P_2O_5 vs MgO
- mineral analyses are plotted to establish control lines for the elements

The trend of the CaO and Al_2O_3 (Fig. 4.9) lines, where MgO is greater than 6%, might be attributed to the fractionation of olivine. The possible effects of the removal of clinopyroxene can be observed in the trend lines of CaO, Al_2O_3, Na_2O and TiO_2 where MgO is greater than or equal to 1% (Fig. 4.9, 4.10). At MgO $\leq$ 2 the CaO, Al_2O_3, FeO, Na_2O, CaO_2, TiO_2 and P_2O_5 trend lines rapidly become much steeper. The controls for this sudden change may be the crystallization of sanidine, hauyne, leucite and nepheline. It is probable that the removal of nepheline and hauyne are the major phases controlling the Na_2O trend. The P_2O_5 trend line is probably controlled by the fractionation of apatite and subsequently also by the fractionation of the more felsic materials (Fig. 4.10). The fractionation of apatite is a minor process and its effect on the other trend lines is probably minor. The K_2O trend line remains approximately constant until MgO = 2% (Fig. 4.10). Thus this trend line is probably only minimally affected until the felsic minerals begin to fractionate. Sood (1981) has indicated that the size of the potassium ion restricts its inclusion in mafic minerals such as olivine and clinopyroxene.

4.2 Trace Elements

The trace elements analysed were Cr, Ni, Cu, Zn, Rb, Sr, Y, Zr, Nb, Cs and the rare earth elements. These analyses are

presented in parts per million in Table 4.2.

4.2.1 Rare Earth Elements (REE)

The REE analyses are plotted in Fig. 4.11. The trend in light rare earth elements (LREE) is similar for all samples and is typical of highly evolved magmas. The samples of Group M are relatively enriched in LREE. A difference between the two groups is evident starting with the element terbium (Tb) (Fig. 4.11), where the concentration of successive elements in Group F is the same until the element ytterbium (Yb). At this point groups M and F again adopt similar trends. Group F is thus relatively enriched in the heavy rare earth elements (HREE). This trend is opposite to that expected, thus some process must have occurred which caused preferential enrichment of HREE in Group F.

4.2.2 Rb vs Sr

Figure 4.12 represents a plot of rubidium (Rb) vs strontium (Sr). It is obvious that Group F is enriched in Rb and depleted in Sr, relative to Group M. This is to be expected if Group F is a more felsic differentiate of the magma which also produced Group M. This is because Rb is a more incompatible and more mobile element than Sr. Group F plots between Rb/Sr ratios of 0.3 and 0.15, centering on 0.25. This Rb/Sr value corresponds to the mean Rb/Sr ratio of the crust

Element / Sample	Cr	Ni	Cu	Zn	Rb	Sr	Y	Zr	Nb	Cs	Ba	Za*	Ce*	Nd*	Sm*	Eu*	Tb*	Yb*	Lu*	Hf	Ta	Th	U
50	25	8	10.0	20.0	100	1340	30	230	140	1.6	1700	342.4	211.4	116.7	60.8	52.2	25.5	13	11.2	7.6	8.4	12.0	3.0
51	170	88	130	78.0	90	1150	30	180	130	1.6	1280	318.2	184.1	106.7	55.3	47.8	23.4	11	8.24	5.6	8.1	9.0	3.2
57	160	86	7.50	83.0	100	1360	30	160	130	2.1	1260									5.6	8.6		
107	11	3	11.0	120	100	1400	40	470	290	4.5	1020									8.1	12.6		
108	13	3	9.5	120	130	1300	40	500	280	4.9	1120	506.1	327.3	183.3	88.4	68.1	38.3	21	18.2	8.8	12.0	34.0	4.8
109	6	3	9.5	120	120	1390	30	470	270	4.2	960									8.8	12.0		
113	10	4	9.0	120	140	1390	40	480	270	4.3	1060									8.3	12.0		
116	14	18	82.0	120	90	1500	40	230	230	1.8	900									6.2	14.0		
117	13	21	85.0	120	90	1190	40	260	240	1.7	940									6.0	13.0		
69	2	2	3.0	150	140	850	30	510	150	3.8	680	218.2	138.6	66.7	37.0	30.4	17.0	15	13.8	6.2	11.0	28.0	5.6
76	3	2	3.0	140	150	1000	30	480	370	4.0	720	206.1	130.7	65.0	35.9	27.5	14.9	14	12.9	5.9	10.0	26.0	6.7
77	2	2	.5	150	190	650	30	610	350	3.7	320									7.1	3.9		
78	3	2	.5	150	170	690	20	550	240	3.8	320									6.9	4.2		
79	4	2	1.5	150	200	780	30	580	250	3.8	340									7.5	3.6		
82	2	2	.5	150	170	720	20	570	250	4.5	240	266.7	159.6	66.7	33.7	23.2	14.9	14	12.9	7.2	9.6	30.0	9.9
83	2	2	.5	140	170	1030	20	500	230	3.8	300									6.0	4.3		
101	3	2	.5	160	170	800	20	590	260	3.8	260									7.2	5.0		
104	2	2	.5	160	190	780	30	570	240	4.4	260									7.6	5.3		

Table 4.2. Analyses of the trace elements (ppm) as determined by X-Ray Assay Labs. Ltd., Don Mills, Ontario, 1982.

* REE Normalized to Type 1 Carbonaceous Chondrite

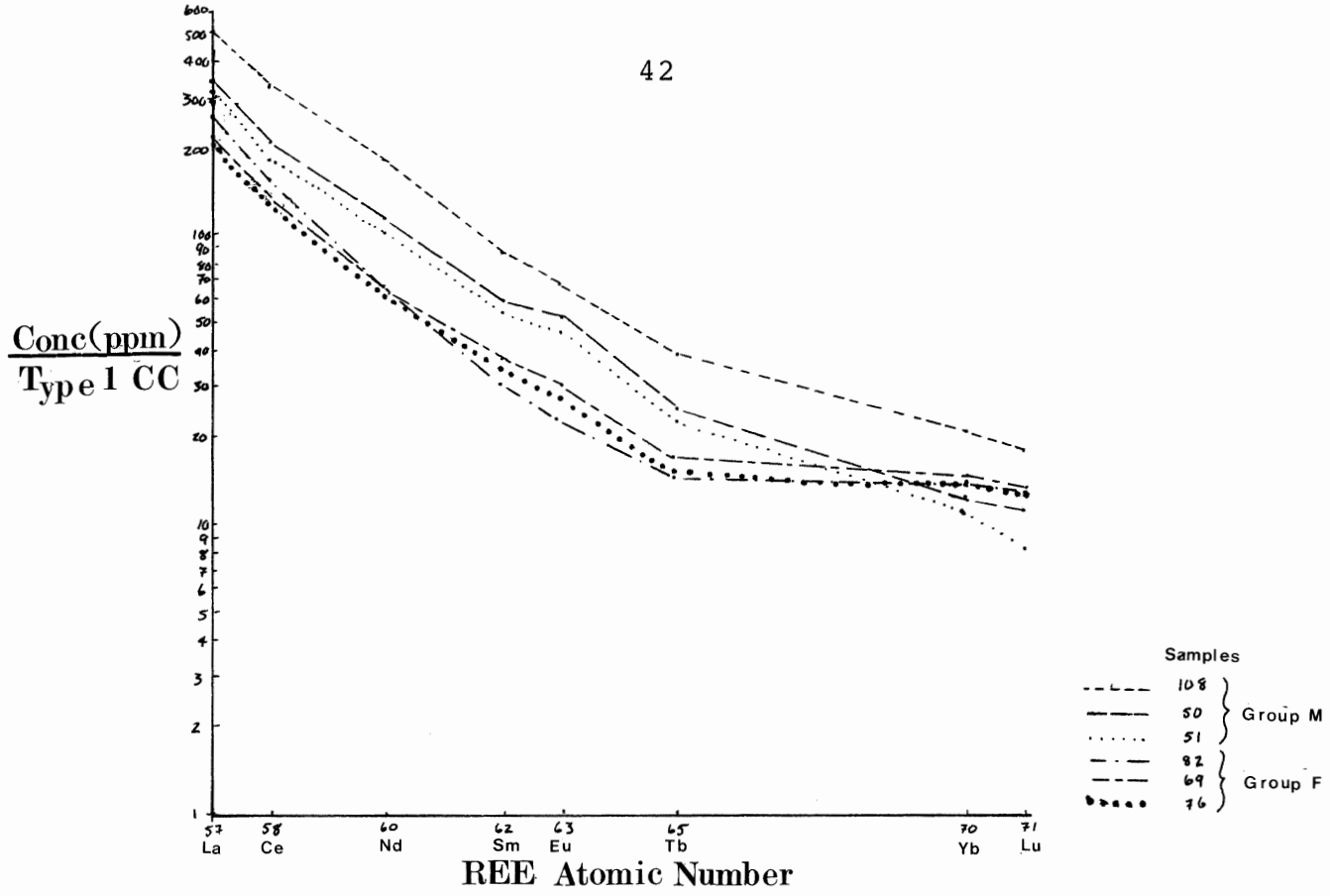

Figure 4.11. Concentration (ppm)/type 1 CC vs REE Atomic Number REE analyses of samples 50, 51, 108 (Group M) and 69, 76, 82 (Group F).

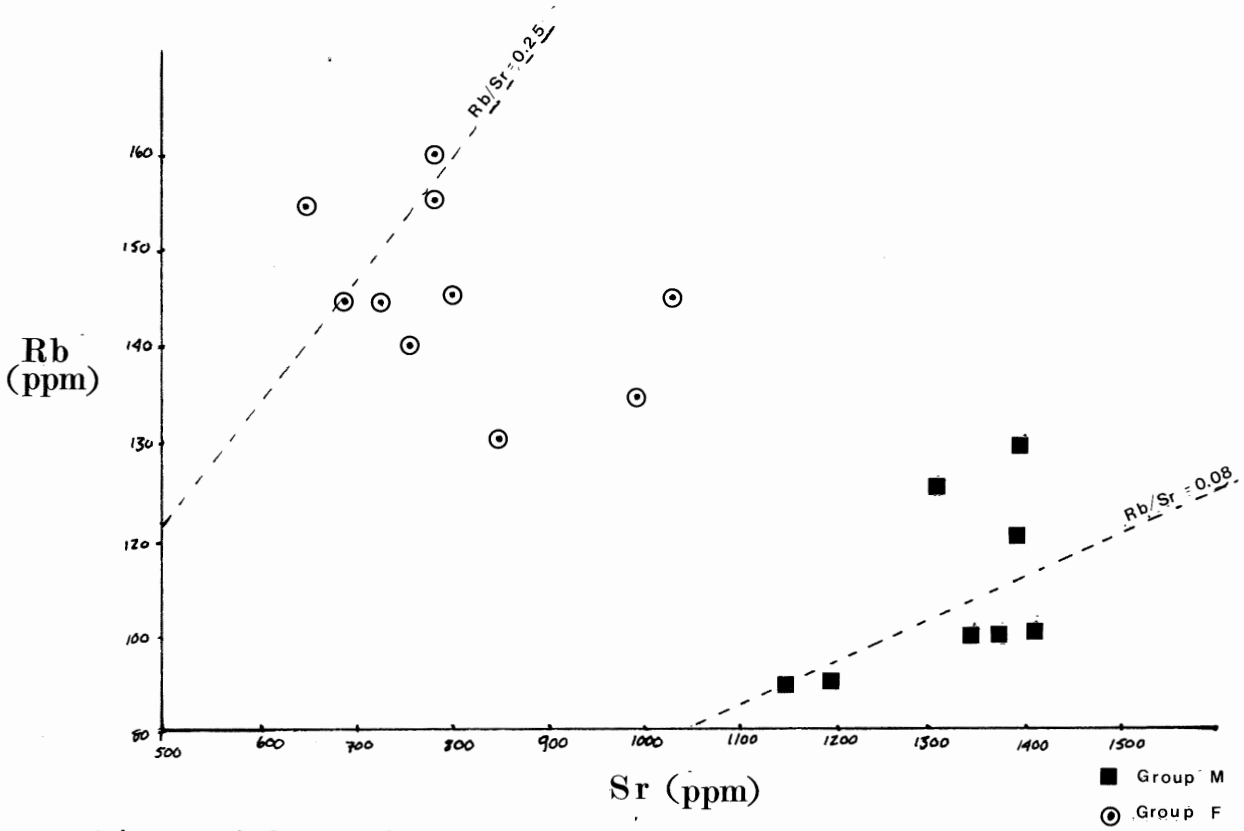

Figure 4.12. Plot of Rb vs Sr (ppm).

(alternatively a mantle exceptionally enriched in lithophile trace elements (Taylor, 1964)) as calculated by Taylor (1964). The mafic group plots between Rb/Sr ratios of 0.1 and 0.06 centering on 0.08. This indicates that the source rock of Group M was similar to mantle rocks (Rb/Sr - 0.025) (Fig. 4.13) (Cox et al., 1979). The Rb/Sr ratios indicate that the source of Group F is the crust and is the mantle for Group M.

4.2.3 Zr vs Hf

Figure 4.14 is a plot of zirconium (Zr) vs hafnium (Hf). The sample Groups M and F are separated by a Zr/Hf ratio of 90. Group F is enriched in Zr relative to Group M. This may indicate the tendency for the lighter incompatibles to accompany the lighter differentiates of a magma, assuming Groups F and M are petrogenetically related.

4.2.4 K/Rb vs K

In Figure 4.15 it is evident that as potassium (K) increases, the ratio K/Rb also increases. Group M contains a lower percentage of K than does Group F. The trend shown by the samples is opposite to that of Shaw (1968) who has indicated that as K increases, Rb increases (Fig. 4.15). The trend of the samples in this study indicate the decrease of Rb relative to K. The mechanism responsible for this process is unknown at this point, however, a possibility is the metasomatism of

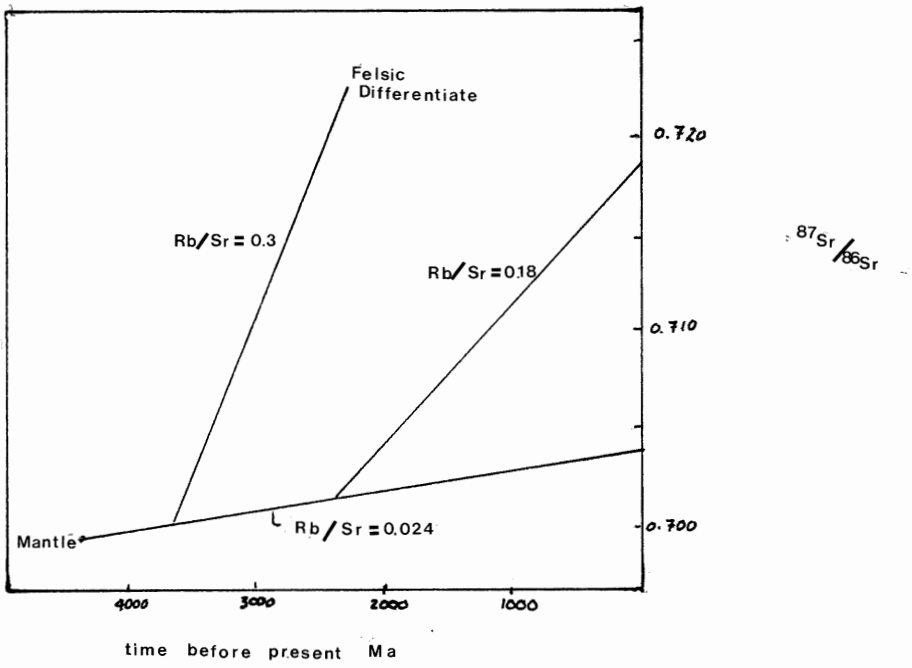

Figure 4.13. Schematic diagram illustrating the Sr-isotope evolution in the Earth with time. The rate of growth is linearly dependent on the Rb/Sr ratio. (After Cox et al., 1979).

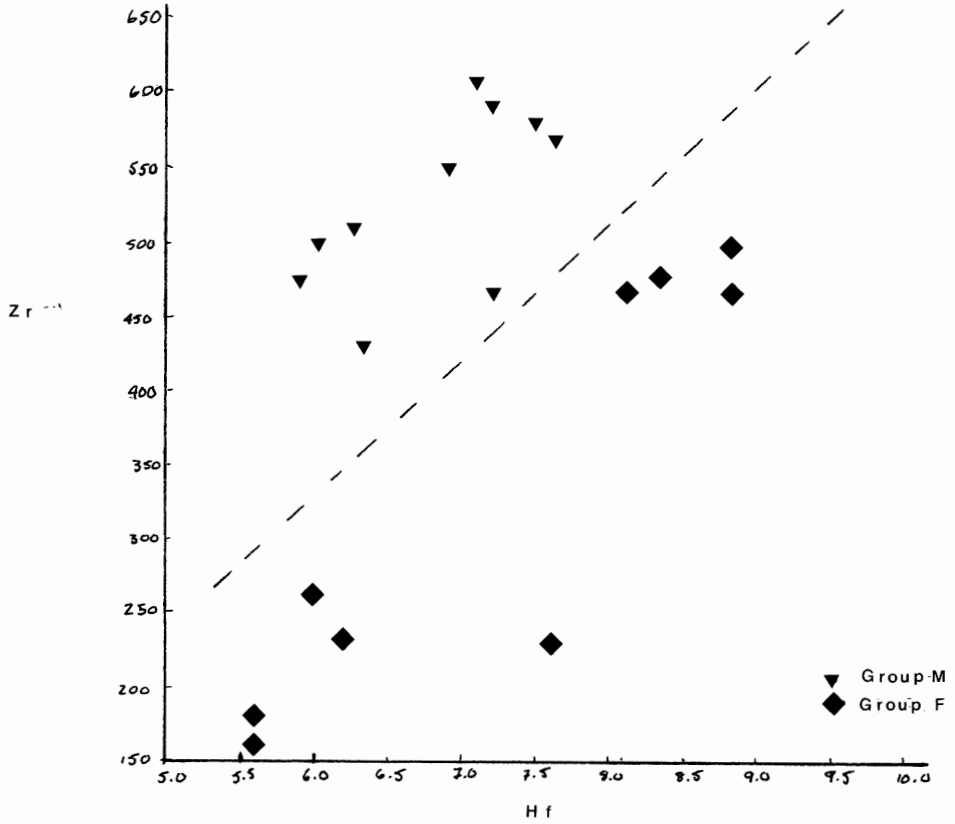

Figure 4.14. Plot of Zirconium (Zr) vs Hafnium (Hf) (ppm).

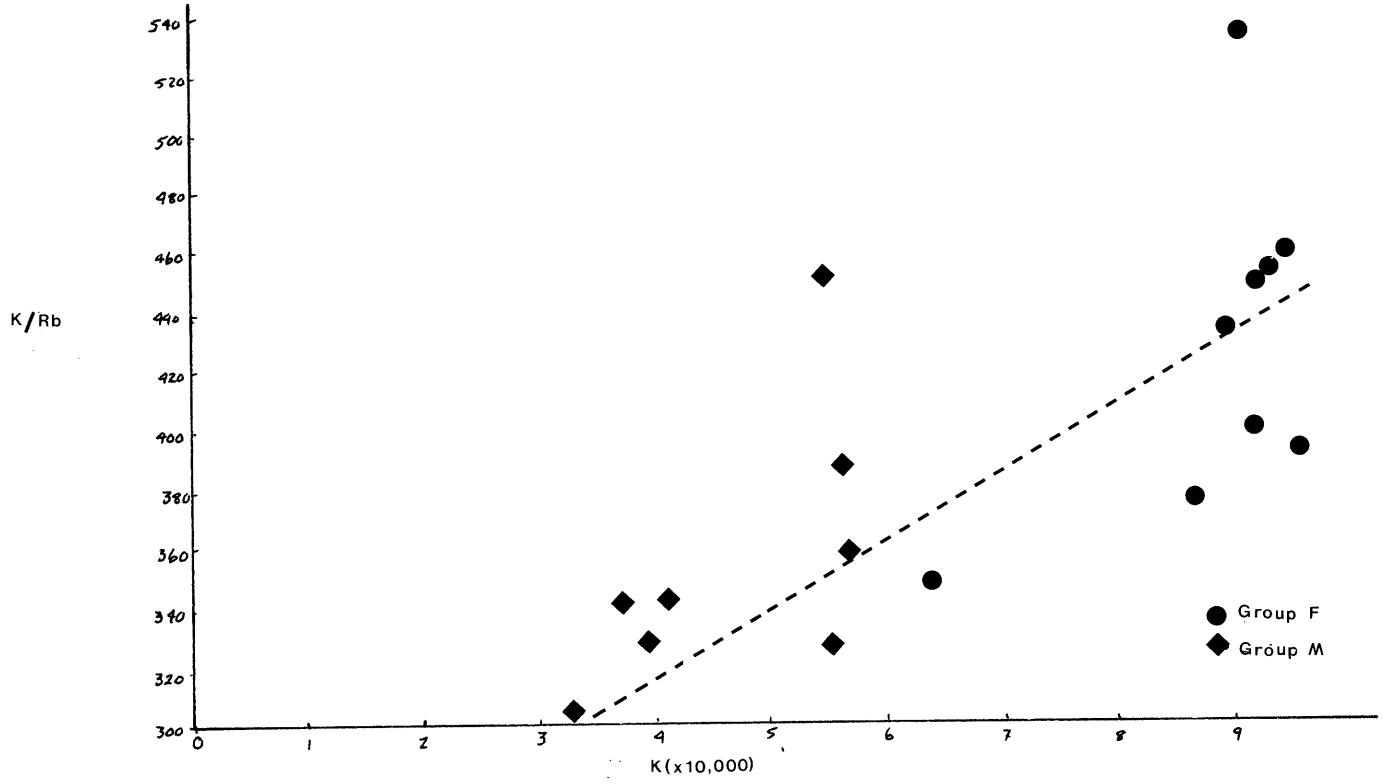

Figure 4.15. K/Rb vs K (ppm).

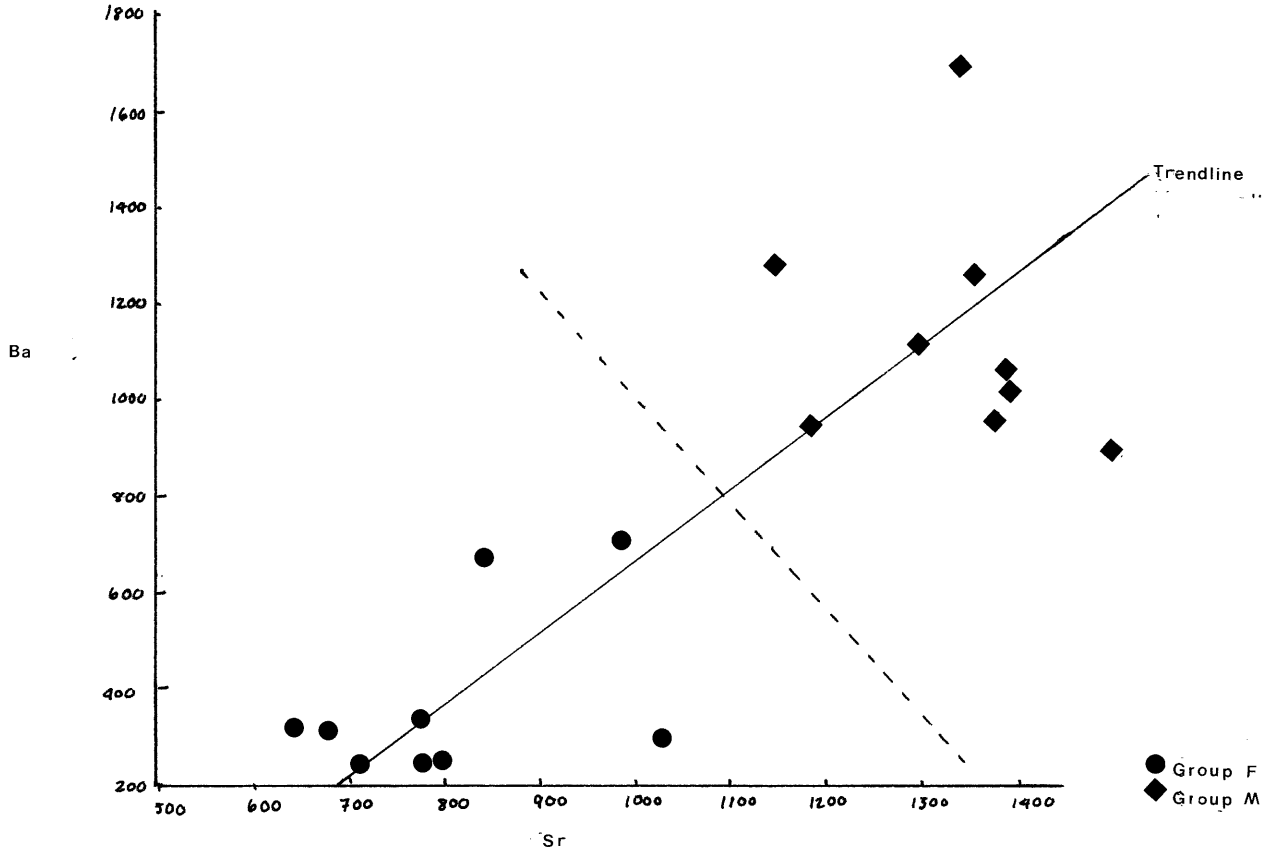

Figure 4.16. Barium (Ba) vs Strontium (Sr) (ppm).

the magma by a K-rich fluid which has been depleted in Rb.

4.2.5 Ba vs Sr

Group F is relatively poor in both barium (Ba) and strontium (Sr) (Fig. 4.16). The abundance of these trace elements is dictated, to a large extent, by the major elements present eg. Ba substitutes for K in an alkali feldspar and Sr substitutes for Ca in plagioclase and pyroxene. Group M is enriched in Ba and Sr relative to Group F.

4.2.6 Ta vs Nb

The felsic and mafic groups are separated by a tantalum/niobium (Ta/Nb) ratio of about 4.0×10^{-2} (Fig. 4.17). The points of Group M plot in the area where $Ta/Nb \geq 4.0 \times 10^{-2}$, and Group F plots in the area where $Ta/Nb \leq 4.0 \times 10^{-2}$. This effect may again illustrate the preference of the lighter incompatibles (Nb) to differentiate with the more felsic portions of magma.

4.3 Conclusions

On the basis of the major and trace element geochemistry, the samples in this study can be divided into two main groups (Table 4.3). By referring to Streckeisen's classification diagram (Fig. 4.1), the felsic group is composed of phonolites.

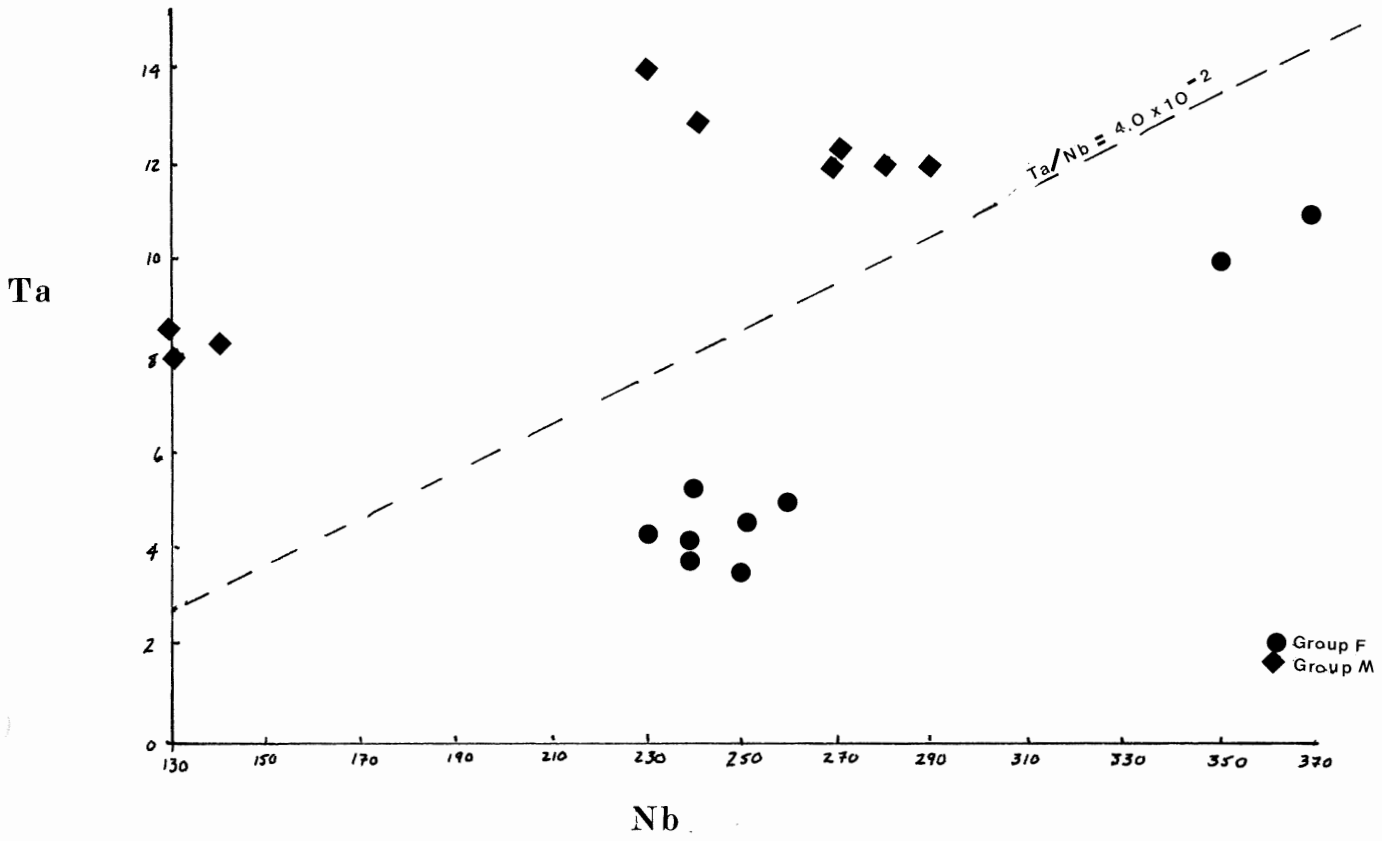

Figure 4.17. Tantalum (Ta) vs Niobium (Nb) (ppm)
$Ta/Nb \simeq 4.0 \times 10^{-2}$

TABLE 4.3

COMPILATION OF WHOLE ROCK DATA

Elements	GROUP F	GROUP M-1	GROUP M-2
	69,76,77,78,79, 82,83,101,104	51,57,116,117	50,107,108,109, 113
SiO_2	>53%	<43%	49%< x <52%
TiO_2	<.50%	>2.2%	.9%< x <2.0%
Al_2O_3	>22%	>16.2%	17%< x <21%
FeO	< 4%	>10.5%	5%< x <8.5%
MnO	.20%< x <.30%	.20%< x <.35%	.15%< x <.40%
MgO	0	>4.2%	<4.2%
CaO	<3.0%	>12%	5.0%< x <9.0%
Na_2O	5.0< x <9.0%	≤6.0%	5.0%< x <8.5%
K_2O	>5.0%	<4.0%	4.0%< x <6.0%
P_2O_5	0	>.60%	<.55%
Rb	140< x <200	<100	100< x <140
Sr	<700	1150< x <1300	1300< x <1400
Zr	>500	<260	230< x <500
Nb	>240	<240	140< x <300
Ba	<750	900< x <1300	900< x <1700
Hf	5.9< x <7.6	<6.2	>7.6
Ta	<11	8.0< x <14.0	8.0< x <12
La	206, 218, 267	318	342, 506
Ce	131, 139, 155	184	211, 327
Nd	65, 67, 67	107	117, 183
Sm	34, 36, 37	55	61, 88
REE* Eu	23, 28, 30	48	52, 68
Tb	15, 15, 17	23	26, 38
Yb	14, 14, 15	11	13, 21
Lu	13, 13, 14	8	11, 18

*The REE have been normalized with respect to Type 1 CC.

The mafic group consists of two distinct rock types; nephelinites and phonolites. The previous subdivision into M-1 (nephelinites) and M-2 (phonolites) is then justified. The division of the samples into the two groups is based on the differences between Groups M and F, which are greater than the similarities.

CHAPTER 5

MINERAL CHEMISTRY

Mineral analyses were conducted using the electron microprobe at Dalhousie. Analyses were obtained for the following minerals - clinopyroxene, biotite, magnetite/ilmenite, olivine, hauyne, sanidine, nepheline and leucite.

5.1 Clinopyroxene

The results from forty-four analyses include those of homogeneous crystals, and rims and cores of zoned crystals. Three types of clinopyroxene can be distinguished: augite ($\leq$3% TiO_2), titanaugite ($\geq$3% TiO_2) and late stage aegirine augite. The augite and titanaugite often occur as euhedral, zoned phenocrysts and are also present in the groundmass. Titanaugite is distinguished from augite by its stronger birefringence and pleochroism. Titanaugite is generally restricted to the nephelinites of Group M-1, while augite is the prominant pyroxene in Groups M-2 and F. The small, euhedral aegirine-augite crystals occur throughout Groups M and F. They are most prominant protruding into vesicles and along fractures. In general the difference in composition between the core and the rim seems to be the loss of SiO_2, TiO_2, Al_2O_3, MgO and CaO in the core accompanied by the gain

of FeO, MnO and Na_2O in the rim. These observations were based on the core-rim analyses of the same crystal (Table 5.1) (Fig. 5.1). The main chemical differences between the late-stage pyroxenes (aegirine-augite) and the primary pyroxenes (titanaugite, augite) are marked increases in iron and sodium coupled by significant decreases in calcium and magnesium (Table 5.1) (Fig. 5.1). The trend of Fig. 5.1 toward the FeO + MnO apex is typical of the crystallization of pyroxene in basalts (Deer, et al., 1980). Often the first pyroxenes to crystallize are close to diopside in composition and as crystallization proceeds the calcium content decreases (Deer et al., 1980).

Hughes (1982) has indicated that the fractionation of pyroxene or presence of pyroxene as a stable phase in equilibrium with the melt will depress the silica content of the melt. This is not a major process contributing to the silica undersaturated state of the magma, merely an accessory process.

5.2 Mica

Four analyses of mica are presented in Table 5.2. Two of the analyses have been determined to be phlogopite due to their relatively high MgO content and relatively low FeO content. The remaining analyses are of biotite crystals.

TABLE 5.1

PYROXENE ANALYSES

	1	2	3	4	5	6	7	8	9	10	11	12	13	14	15
SiO_2	46.07	43.97	44.85	42.56	45.1	44.02	43.41	46.1	44.24	46.80	45.80	46.17	44.7	47.37	48.76
TiO_2	1.38	2.50	1.79	3.37	1.75	2.16	2.14	1.58	2.65	1.20	1.58	1.64	1.93	1.10	1.65
Al_2O_3	4.85	6.73	6.31	9.25	5.97	7.27	7.94	3.49	7.52	4.87	4.64	4.65	6.20	3.74	4.98
FeO	13.91	13.45	14.68	12.19	14.05	14.10	15.11	19.06	12.96	14.07	16.28	16.12	16.01	16.01	6.13
MnO	.80	.51	.66	.21	.55	.51	.48	1.17	.44	.77	.84	.98	.64	1.01	.07
MgO	8.33	8.00	7.43	8.07	7.65	7.47	6.63	5.18	8.27	8.32	6.50	6.72	7.28	7.09	13.87
CaO	22.33	22.66	22.44	22.51	27.17	22.39	22.26	21.07	22.83	22.08	21.6	21.58	22.3	21.97	24.11
Na_2O	1.00	.97	1.14	.92	1.15	.89	1.29	1.84	1.36	1.16	1.56	1.64	1.70	1.46	.23
TOTAL	98.64	98.81	99.3	99.08	98.4	98.8	99.25	99.49	100.26	99.36	98.79	99.50	99.17	99.75	99.79

Number of ions on the basis of 6 oxygens

SiO_2	1.814	1.731	1.763	1.659	1.782	1.734	1.712	1.897	1.712	1.829	1.822	1.752	1.752	1.860	1.820
TiO_2	.041	.074	.053	.099	.052	.064	.063	.048	.077	.035	.047	.049	.057	.032	.046
Al_2O_3	.224	.312	.292	.425	.278	.337	.369	.165	.343	.224	.218	.216	.286	.173	.219
FeO	.458	.443	.483	.397	.464	.465	.499	.639	.419	.459	.592	.532	.525	.526	.191
MnO	.027	.017	.022	.007	.018	.017	.016	.040	.014	.025	.028	.033	.021	.034	.002
MgO	.489	.469	.435	.469	.450	.438	.390	.309	.477	.484	.385	.395	.425	.415	.772
CaO	.442	.956	.945	.940	.938	.945	.941	.904	.946	.923	.921	.912	.936	.925	.965
Na_2O	.076	.074	.087	.070	.088	.068	.099	.143	.102	.088	.120	.125	.091	.111	.017
TOTAL	4.071	4.076	4.081	4.065	4.071	4.068	4.089	4.095	4.091	4.068	4.083	4.084	4.094	4.076	4.032

	16	17	18	19	20	21	22	23	24	25	26	27	28	29	30
SiO_2	45.27	47.22	42.70	44.86	48.51	48.52	46.5	46.71	44.6	46.63	47.32	49.12	48.77	45.34	44.16
TiO_2	2.58	1.98	3.84	3.08	1.59	1.8	2.25	2.32	3.00	2.05	2.26	1.52	1.65	2.51	3.41
Al_2O_3	7.78	6.68	10.12	8.01	5.36	5.78	7.25	6.35	8.89	6.50	5.93	4.77	5.22	7.94	9.36
FeO	7.43	6.51	8.08	9.6	6.00	5.96	6.53	7.93	8.43	7.69	7.5	6.38	6.41	7.41	8.27
MnO	.06	.10	.11	.23	.09	.06	.08	.23	.10	.13	.15	.14	.13	-	.13
MgO	11.89	13.05	10.56	10.19	13.74	13.84	12.57	12.41	10.92	12.42	12.97	14.31	14.01	11.89	11.23
CaO	24.66	24.5	24.04	23.7	29.52	24.33	24.36	24.29	24.02	24.54	24.71	23.13	23.29	23.05	23.19
Na_2O	.30	.47	.54	.96	.31	.40	.35	.47	.41	.36	.35	.42	.37	.70	.78
TOTAL	99.96	100.51	99.89	100.69	100.11	100.67	99.89	100.72	100.37	100.31	101.2	99.79	99.84	98.84	100.47

SiO_2	1.710	1.761	1.622	1.701	1.107	1.796	1.745	1.752	1.683	1.754	1.763	1.831	1.818	1.724	1.664
TiO_2	.073	.056	.110	.088	.045	.050	.063	.065	.085	.058	.063	.043	.046	.072	.097
Al_2O_3	.346	.294	.453	.358	.235	.252	.321	.281	.395	.288	.260	.210	.229	.356	.413
FeO	.235	.203	.257	.304	.187	.185	.205	.249	.266	.242	.234	.199	.20	.236	.261
MnO	.002	.003	.004	.007	.003	.002	.003	.007	.003	.004	.005	.004	.004	-	.004
MgO	.669	.725	.598	.576	.763	.764	.703	.694	.614	.696	.720	.795	.779	.674	.631
CaO	.998	.979	.979	.963	.979	.965	.979	.976	.971	.989	.986	.924	.930	.939	.936
Na_2O	.022	.034	.040	.071	.022	.029	.025	.034	.030	.026	.025	.030	.027	.052	.057
TOTAL	4.055	4.054	4.061	4.068	4.042	4.042	4.044	4.059	4.049	4.057	4.056	4.036	4.034	4.052	4.062

1 - augite - sample 113-8, solid, selbergite, Perlerkopf
2 - augite - sample 113-10, rim , selbergite, Perlerkopf
3 - augite - sample 113-2 core, selbergite, Perlerkopf
4 - augite - sample 113-14 solid, selbergite, Perlerkopf
5 - augite - sample 113-15 solid, selbergite, perlerkopf
6 - augite - sample 108-1 solid, selbergite, perlerkopf
7 - augite - sample 108-2 core, selbergite, Perlerkopf
8 - augite - sample 108-3 rim, selbergite, Perlerkopf
9 - augite - sample 108-5 rim, selbergite, Perlerkopf
10 - augite - sample 108-6 core, selbergite, Perlerkopf
11 - augite - sample 108-zeno-8 solid, selbergite, Perlerkopf
12 - augite - sample 108-zeno-9 rim, selbergite, Perlerkopf
13 - augite - sample 108-zeno-10 core, selbergite, Perlerkopf
14 - augite - sample 108-zeno-11 solid, selbergite, Perlerkopf
15 - augite - sample 96-1 solid, selbergite tuff, Brenk
16 - augite - sample 96-2 core, selbergite tuff, Brenk
17 - augite - sample 96-3 rim, selbergite tuff, Brenk
18 - titanaugite - sample 96-4 core, selbergite tuff, Brenk
19 - titanaugite - sample 96-5 rim, selbergite tuff, Brenk
20 - augite - sample 96-6 rim, selbergite tuff, Brenk
21 - augite - sample 96-7 core, selbergite tuff, Brenk
22 - augite - sample 96-12 solid, selbergite tuff, Brenk
23 - augite - sample 117-1 solid, Nephelinite, Hannebacher Ley
24 - augite - sample 117-2 solid, Nephelinite, Hannebacher Ley
25 - augite - sample 117-3 solid, Nephelinite, Hannebacher Ley
26 - augite - sample 117-4 solid, Nephelinite, Hannebacher Ley
27 - augite - sample Nied-1 solid, Tephritic phonolite, Niedermendig
28 - augite - sample Nied-3 core, Tephritic phonolite, Niedermendig
29 - augite - sample Nied-4 rim, Tephritic phonolite, Niedermendig
30 - titanaugite - sample Nied-5 solid, Tephritic phonolite, Niedermendig

TABLE 5.1 (continued)

	31	32	33	34	35	36	37	38	39	40	41	42	43	44	45	46
SiO_2	44.07	44.18	43.62	33.93	46.52	40.66	47.57	47.84	45.58	47.56	46.9	48.01	43.16	43.87	52.4	51.96
TiO_2	2.92	1.92	3.09	2.65	2.17	3.74	1.15	1.92	1.94	1.42	1.29	.89	4.01	3.07	.43	.67
Al_2O_3	9.32	7.62	9.16	8.41	6.37	10.95	4.51	5.80	6.55	4.85	4.96	4.26	10.34	8.62	-	.07
FeO	10.15	14.85	7.50	7.37	6.94	11.04	15.32	8.60	14.64	14.49	14.92	16.28	10.36	7.32	27.32	27.57
MnO	.18	.48	.15	.22	.07	.15	.79	.14	.49	.70	.73	1.02	.10	.09	2.06	1.21
MgO	9.9	7.8	12.05	12.23	13.20	8.80	8.51	8.6	8.23	8.94	8.49	7.51	9.80	11.56	.91	1.03
CaO	22.41	21.93	27.73	23.25	23.62	22.77	21.95	23.69	22.13	22.04	21.88	20.97	22.7	24.14	7.07	5.94
Na_2O	.88	1.13	.35	.29	.12	.47	1.23	.25	1.13	1.20	1.19	1.75	.86	-	10.77	11.38
TOTAL	99.82	99.90	99.62	99.22	99.01	98.59	101.02	100.75	100.67	101.21	100.35	100.71	101.33	98.67	100.96	99.81

Number of ions on the basis of 6 oxygens

SiO_2	1.681	1.724	1.654	1.491	1.761	1.588	1.833	1.857	1.760	1.822	1.817	1.862	1.627	1.678		
TiO_2	.084	.056	.088	.088	.062	.110	.033	.056	.056	.041	.038	.026	.114	.088		
Al_2O_3	.419	.350	.409	.436	.284	.504	.205	.265	.298	.219	.227	.195	.459	.389		
FeO	.324	.485	.238	.271	.220	.361	.494	.279	.473	.464	.484	.528	.327	.234		
MnO	.006	.016	.005	.008	.002	.005	.026	.005	.016	.023	.024	.034	.003	.003		
MgO	.563	.454	.681	.802	.745	.512	.489	.498	.474	.510	.490	.434	.551	.659		
CaO	.916	.917	.964	1.096	.958	.953	.906	.985	.916	.905	.908	.871	.917	.989		
Na_2O	.065	.085	.026	.025	.009	.036	.092	.019	.085	.089	.089	.132	.063	-		
TOTAL	4.058	4.087	4.066	4.216	4.04	4.068	4.077	3.964	4.077	4.073	4.077	4.081	4.061	4.090		

31 - titanaugite - sample 52-1 solid, selbergite tuff, Southern Bell
32 - augite - sample 52-2 solid, selbergite tuff, Southern Bell
33 - titanaugite - sample 52-3 core, selbergite tuff, Southern Bell
34 - augite - sample 52-13 solid, selbergite tuff, Southern Bell
35 - augite - sample 52-15 rim, selbergite tuff, Southern Bell
36 - titanaugite - sample 52-16 solid, selbergite tuff, Southern Bell
37 - augite - sample 109-1 solid, selbergite, Perlerkopf
38 - augite - sample 109-2 core, selbergite, Perlerkopf
39 - augite - sample 109-3 rim, selbergite, Perlerkopf
40 - augite - sample 109-4 core, selbergite, Perlerkopf
41 - augite - sample 109-5 rim, selbergite, Perlerkopf
42 - augite - sample 109-6 core, selbergite, Perlerkopf
43 - titanaugite - sample 109-7 rim, selbergite, Perlerkopf
44 - titanaugite - sample 57-1 solid, Nephelinite, Rodder Hofen
45 - aegirine-augite - sample 82-3, Phonolite, Brenk
46 - aegirine-augite - sample 82-4, Phonolite, Brenk

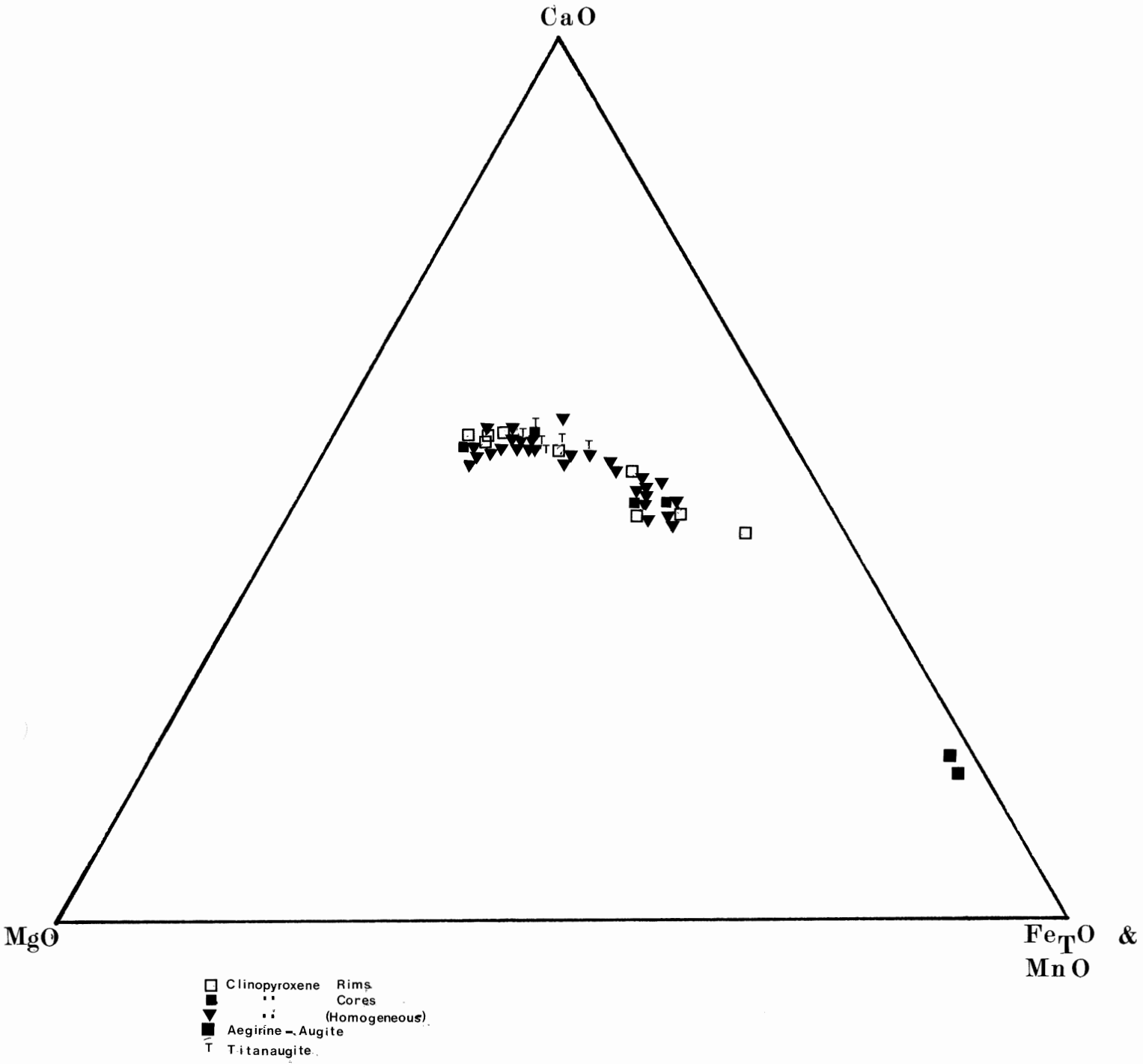

Figure 5.1. Variation diagram for the clinopyroxene analyses. The titanaugite analyses plot near the center of the triangle exhibiting little variation. The pyroxene cores are enriched in FeO and MnO and depleted in CaO and MgO relative to the rims. The late stage aegirine-augite crystals are greatly enriched in FeO and MnO and significantly depleted in MgO and CaO in comparison to the rest of the clinopyroxene analyses.

TABLE 5.2

MICA ANALYSES

	1	2	3	4
SiO_2	36.17	36.87	33.93	34.71
TiO_2	5.43	4.02	4.51	9.80
Al_2O_3	17.09	16.77	19.30	13.78
FeO	8.47	8.35	24.29	26.62
MnO	.07	-	1.17	1.71
MgO	17.94	19.84	8.73	7.08
CaO	.08	.07	.07	-
Na_2O	.31	.53	-	-
K_2O	9.67	9.61	9.17	9.73
TOTAL	95.24	96.03	96.17	98.43
Number of ions on the basis of 24 (O, OH, F)				
Si	5.743	5.798	5.009	5.888
Ti	.648	.475	.581	.612
Al	3.198	3.108	2.886	2.755
Fe^{2+}	1.125	1.085	3.479	3.777
Mn	.009	-	.170	.296
Mg	4.245	4.6	2.228	1.790
Ca	.014	.012	.013	-
Na	.095	.162	-	-
K	1.960	1.429	2.004	2.107
TOTAL	17.037	17.218	17.169	17.175

1. Biotite-phlogopite, sample 57-1, nephelinite, Rodder Hofen
2. Biotite-phlogopite, sample 96-10, selbergite tuff, Brenk
3. Biotite, sample 52-12, selbergite tuff, Bell
4. Biotite, sample 64-12, trachyte, Reiden

The phlogopite crystals may represent an early stage of crystallization. As crystallization proceeds the Mg content decreases causing late-stage crystallization of biotite (Deer et al., 1980). Deer, et al. (1980) have indicated that phlogopite is stable at depth and is not upon extrusion. The alteration of phlogopite/biotite to clays is evident in several thin sections eg. 64, 78, 96.

5.3 Olivine

Olivine was analysed in the nephelinites of samples 51 and 57. The results and structural formulas are available in Table 5.3. The chemical analyses indicate that the olivine present is chrysolite. Many rims of the olivine crystals have been altered to iddingsite.

5.4 Spinel

A super recal program was conducted on the spinel data and the resulting analyses indicated that both ilmenite and magnetite were present. For the chemical analyses and structural formulas see Table 5.4.

5.5 Hauyne

Eighteen samples were made of the generally euhedral, altered hauyne phenocrysts. In such a highly potassic magmas such as this, sodium is often replaced by potassium in the

TABLE 5.3

OLIVINE ANALYSES

	1	2	3	4	5	6	7
SiO_2	39.83	39.79	39.01	39.52	40.40	40.36	40.62
TiO_2	-	-	-	-	-	-	-
Al_2O_3	-	-	-	-	-	-	-
FeO	14.07	15.53	19.91	15.67	12.31	12.52	12.28
MnO	0.44	0.61	1.29	0.49	0.27	0.17	0.26
MgO	44.93	43.20	39.48	43.73	48.09	47.50	48.33
CaO	0.38	0.72	0.83	0.63	0.25	0.20	0.30
TOTAL	99.22	99.80	100.53	100.04	101.32	100.75	101.79
	Number of ions on the basis of 4 oxygens						
Si	1.001	1.005	1.003	.998	.990	.994	.990
Ti	-	-	-	-	-	-	-
Al	-	-	-	-	-	-	-
Fe^{2+}	.296	.329	.428	.331	.252	.258	.250
Mn	.009	.013	.028	.010	.006	.004	.005
Mg	1.683	1.629	1.514	1.646	1.756	1.744	1.756
Ca	.010	.020	.023	.017	.007	.005	.008
Total	2.999	2.995	2.997	3.002	3.010	3.006	3.010

1. Chrysolite, sample #51-6, Tephritic foidite (nephelinite), Southern Bell
2. Chrysolite, sample #51-7, Tephritic foidite (nephelinite), Southern Bell
3. Chrysolite, sample #51-8, Tephritic foidite (nephelinite), Southern Bell
4. Chrysolite, sample #51-9, Tephritic foidite (nephelinite), Southern Bell
5. Chrysolite, sample #57-6, Tephritic foidite (nephelinite), Rodder Hofen
6. Chrysolite, sample #57-10, Tephritic foidite (nephelinite), Rodder Hofen
7. Chrysolite, sample #57-11, Tephritic foidite (nephelinite), Rodder Hofen

TABLE 5.4

OXIDE ANALYSES

	1	2	3	4	5	6
SiO_2	-	-	-	-	-	-
TiO_2	10.28	8.29	10.31	8.98	5.56	12.93
Al_2O_3	5.13	2.19	.15	-	.72	2.10
Cr_2O_3	.06	-	.19	-	-	.06
Fe_2O_3	44.55	81.17	80.55	81.53	57.08	40.64
FeO	33.44	5.53	6.04	5.48	33.78	39.76
MnO	1.03	1.86	2.59	2.25	2.22	3.16
MgO	4.33	.89	.45	.18	.11	.06
CaO	-	-	.17	.08	-	.12
TOTAL	98.82	99.93	100.94	98.50	99.47	98.44
	Number of ions on the basis of 4 (O)					
Si	-	-	-	-	-	-
Ti	.281	.216	.269	.240	.160	.369
Al	.219	.089	.006	-	.033	.094
Cr	.002	-	.005	-	-	.002
Fe^{+3}	1.218	2.116	2.108	2.184	1.647	1.162
Fe^{+2}	1.015	.160	.176	.163	1.082	1.263
Mn	.032	.055	.076	.068	.072	.102
Mg	.234	.046	.023	.010	.006	.003
Ca	-	-	.006	.003	-	.005
TOTAL	3.000	2.682	2.671	2.660	3.000	3.000

1. Magnetite, sample #96-9, selbergite tuff, Brenk
2. Ilmenite, sample #96-11, selbergite tuff, Brenk
3. Ilmenite, sample #117-6, tephritic foidite (nephelinite), Hannebacher Ley
4. Ilmenite, sample #117-7, tephritic foidite (nephelinite), Hannebacher Ley
5. Magnetite, sample #52-17, selbergite tuff, Southern Bell
6. Magnetite, sample #52-19, selbergite tuff, Southern Bell

crystal structure, in the presence of chlorine and/or SO_3 (Rittman, 1973). Chlorine substitutes for the sulphide ion in the structure (Deer, et al., 1980). The structural formula based on twenty-one oxygens and omitting chlorine were calculated and are displayed in Table 5.5.

5.6 Sanidine

Twenty-nine sanidine analyses and structural formulas are available in Table 5.6. The chemical composition of the sanidine crystals is relatively the same in all the samples. Of these anaylses three are significantly more altered than the others; for example 12, 18 and 24. The main differences observed are the loss of silica and potassium and the gain of silica in the altered crystals (Table 5.6). The twenty-nine analyses are plotted on a quartz-nepheline-kalsilite ternary diagram (residua system) (Fig. 5.2). The alkali feldspar composition point is well delineated. The clustering of the points around this main compositional point represent the varying degrees of alteration or the differing conditions of crystallization. There are also a large number of points which follow a linear trend representing the presence of K-Na feldspar solid solution.

5.7 Leucite

Twenty-three analyses and structural formulas were

TABLE 5.5

SODALITE AND HAÜYNE ANALYSES

	1	2	3	4	5	6	7	8	9	10	11	12	13	14	15	16	17	18
SiO_2	37.75	38.31	38.14	36.28	36.54	36.55	36.33	38.9	37.20	36.79	37.39	36.77	36.53	37.11	35.58	36.26	35.50	35.96
TiO_2	-	-	-	-	-	-	-	-	-	-	-	-	-	-	-	-	-	-
Al_2O_3	31.10	31.19	31.40	30.04	30.59	30.54	30.59	27.69	30.34	30.01	30.65	29.85	29.67	30.45	29.30	29.8	29.13	29.79
Fe_2O_3	.08	.29	2.3	.15	.21	.20	.14	2.70	.19	-	.08	.13	.12	.13	.13	.27	.11	.23
CaO	.54	.15	.05	2.01	2.16	1.88	1.98	.33	.27	.28	.09	.09	.18	.13	1.89	1.52	1.83	1.90
Na_2O	18.15	18.48	18.66	17.61	15.36	16.32	15.47	21.28	18.30	19.91	20.28	22.13	21.10	20.56	17.74	16.64	18.31	17.15
K_2O	1.32	1.42	1.52	2.27	2.12	2.06	1.96	.95	1.56	2.00	1.59	1.63	1.51	1.58	2.13	1.82	2.11	1.21
SO_3	9.50	8.96	8.92	11.20	11.59	11.40	11.51	.14	9.41	8.95	8.70	8.58	8.72	8.70	11.10	11.20	11.28	11.60
Cl	.77	.85	.83	.55	.55	.54	.53	5.35	.76	1.02	.91	.85	.88	.94	.53	.78	.55	.58
TOTAL	99.21	99.61	100.74	100.16	99.20	99.98	98.50	100.44	98.24	98.91	99.78	100.16	98.84	99.73	98.55	98.61	98.94	98.68
	Number of ions on the basis of 21 oxygens																	
Si	6.075	6.106	6.077	6.062	6.034	6.039	6.019	6.427	6.101	6.013	6.088	6.113	6.112	6.003	6.076	6.082	6.086	6.061
Ti	-	-	-	-	-	-	-	-	-	-	-	-	-	-	-	-	-	-
Al	5.899	5.859	5.897	5.917	5.954	5.948	5.979	5.431	5.865	5.982	5.882	5.849	5.851	5.996	5.898	5.891	5.886	5.918
Fe^{3+}	.010	.031	.028	.019	.026	.025	.017	.336	.023	-	0.10	.016	.015	.016	.017	.034	.014	.029
Ca	.093	.026	.009	.360	.382	.333	.352	.058	.047	.049	.016	.016	.032	.023	.346	.273	.336	.343
Na	5.663	5.608	5.764	5.705	4.918	5.228	4.969	6.816	5.819	6.318	6.402	7.133	6.844	6.448	5.874	5.411	6.085	5.804
K	.271	.289	.309	.484	.447	.434	.415	.200	.327	.418	.330	.346	.322	.326	.464	.390	.462	.475
S	1.149	1.137	1.068	1.406	1.438	1.413	1.433	.017	1.159	1.10	1.064	1.072	1.096	1.057	1.424	1.411	1.453	1.469
TOTAL	11.975	11.965	11.974	11.979	11.989	11.987	11.994	11.858	11.966	11.996	11.971	11.962	11.963	11.999	11.975	11.973	11.971	11.98

1. haüyne, sample 104-5, Phonolite, Brenk
2. haüyne, sample 104-6, Phonolite, Brenk
3. haüyne, sample 104-7, Phonolite, Brenk
4. haüyne, sample 113-4, Phonolite, Perlerkopf
5. haüyne, sample 113-6, Phonolite, Perlerkopf
6. haüyne, sample 108-15, Phonolite, Perlerkopf
7. haüyne, sample 108-16, Phonolite, Perlerkopf
8. sodalite, sample 82-107, Phonolite, Brenk
9. haüyne, sample 82-110, Phonolite, Brenk
10. haüyne, sample 83-14, Tephritic phonolite, Brenk
11. haüyne, sample 104-5a Phonolite, Brenk
12. haüyne, sample 104-5a rastered, Phonolite, Brenk
13. haüyne, sample 104-6a Phonolite, Brenk
14. haüyne, sample 104-7a, Phonolite, Brenk
15. haüyne, sample 113-4a, Phonolite, Perlerkopf
16. haüyne, sample 109-5, Tephritic phonolite, Perlerkopf
17. haüyne, sample 107-2, Tephritic phonolite, Perlerkopf
18. haüyne, sample 107-2, Tephritic phonolite, Perlerkopf

TABLE 5.6

ALKALI FELDSPAR ANALYSIS

	1	2	3	4	5	6	7	8	9	10	11	12	13	14	15
SiO_2	65.61	65.18	64.44	65.39	63.04	63.98	64.67	64.57	62.11	62.25	63.54	59.46	64.06	64.30	64.55
TiO_2	-	-	-	-	-	-	-	-	-	-	-	-	-	-	-
Al_2O_3	18.88	18.44	18.42	17.70	19.22	17.87	17.81	18.24	18.14	17.97	18.19	19.80	17.20	18.18	17.44
FeO	.15	.28	.76	1.19	-	1.01	1.24	.23	1.40	1.08	.44	1.52	.96	.41	.87
CaO	.10	.09	.15	.14	.10	.06	.18	-	.05	-	.06	.23	.21	.10	-
Na_2O	1.44	.99	1.08	.00	-	1.47	1.00	.50	1.33	1.57	.66	4.14	.50	.72	.26
K_2O	14.16	14.86	14.13	14.72	16.01	14.15	14.84	15.79	15.47	15.14	15.44	13.44	15.57	15.71	16.30
TOTAL	100.33	99.84	98.99	100.13	98.36	98.53	99.79	99.32	98.51	98.01	98.32	98.68	98.49	99.41	99.43

Number of ions on the basis of 32 oxygens

Si	11.979	12.005	11.967	12.055	11.839	11.978	11.947	12.003	11.783	11.821	11.944	11.323	12.060	11.969	12.057
Ti	-	-	-	-	-	-	-	-	-	-	-	-	-	-	-
Al	4.063	4.003	4.032	3.846	4.255	3.943	3.894	3.997	4.056	4.022	4.032	4.444	3.817	3.989	3.840
Fe^{2+}	.023	.043	.117	.184	.020	.158	.192	.036	.222	.172	.069	.242	.151	.064	.136
Ca	.020	.018	.03	.029	.020	.012	.036	.180	.010	-	.012	.047	.042	.020	-
Na	.510	.354	.389	.354	-	.520	.360	-	.489	.530	.241	1.528	.182	.260	.094
K	3.300	3.494	3.35	3.464	3.838	3.382	3.514	3.747	3.745	3.670	3.706	3.267	3.741	3.733	3.886
TOTAL	19.894	19.917	19.886	19.931	19.952	20.007	19.993	19.962	20.307	20.210	20.009	20.852	19.994	20.033	20.013

	16	17	18	19	20	21	22	23	24	25	26	27	28	29
SiO_2	64.04	64.39	59.17	63.96	69.36	6.377	65.06	65.97	61.72	63.70	64.18	64.18	64.36	64.06
TiO_2	-	-	-	-	-	-	-	-	-	-	-	-	-	-
Al_2O_3	17.04	18.12	20.98	17.95	18.00	18.15	18.58	18.45	20.35	17.54	17.74	17.96	18.00	17.65
FeO	.68	.11	1.12	.24	.19	1.23	.21	.52	.96	.94	1.04	.98	1.01	1.01
CaO	.06	.12	-	.09	.06	.07	.05	.15	1.41	-	-	-	.13	-
Na_2O	.81	1.07	5.45	-	.47	1.77	1.91	1.95	5.50	1.45	.63	1.14	1.34	.96
K_2O	15.39	15.11	12.31	16.46	15.41	14.44	13.02	13.87	8.15	14.47	15.48	15.05	15.27	15.34
TOTAL	98.48	98.92	99.03	98.70	98.49	99.93	98.83	100.91	98.09	98.10	00.07	99.31	100.11	99.02

Si	12.094	11.997	11.170	12.007	12.040	11.84	12.005	12.001	11.465	12.002	12.004	11.965	11.934	11.995
Ti	-	-	-	-	-	-	-	-	-	-	-	-	-	-
Al	3.793	3.982	4.668	3.972	3.969	3.972	4.041	3.956	4.456	3.895	3.911	3.947	3.934	3.896
Fe^{2+}	.107	.017	.177	.038	.030	.172	.029	.079	.149	.148	.163	.153	.157	.158
Ca	.012	.024	-	.018	.012	.014	.010	.029	.280	-	-	-	.026	-
Na	.297	.387	1.995	-	.170	.637	.683	.688	1.981	.530	.228	.412	.482	.349
K	3.709	3.596	2.966	3.444	3.680	3.541	3.067	3.221	19.32	3.480	3.696	3.581	3.614	3.667
TOTAL	20.012	20.003	20.976	19.979	19.901	20.176	19.835	19.975	20.264	20.055	20.002	20.058	20.147	20.064

1 - Sanidine, sample 104-2, Phonolite, Brenk
2 - Sanidine, sample 104-3, Phonolite, Brenk
3 - Sanidine, sample 113-1, Phonolite, Perlerkopf
4 - Sanidine, sample 113-2, Phonolite, Perlerkopf
5 - Sanidine, sample 57-11, Nephelinite, Rodder Hofen
6 - Sanidine, sample 108-12, Phonolite, Perlerkopf
7 - Sanidine, sample 108-13, Phonolite, Perlerkopf
8 - Sanidine, sample 82-103, Phonolite, Brenk
9 - Sanidine, sample 82-104, Phonolite, Brenk
10 - Sandine, sample 82-118, Phonolite, Brenk
11 - Sanidine, sample 83-3, Tephritic phonolite, Brenk
12 - Sanidine, sample 83-4, Tephritic phonolite, Brenk
13 - Sanidine, sample 83-5, Tephritic phonolite, Brenk
14 - Sanidine, sample 83-8N, Tephritic phonolite, Brenk
15 - Sanidine, sample 83-13, Tephritic phonolite, Brenk

16 - Sanidine, sample 79-203, Phonolite, Olbruck
17 - Sanidine, sample 104-3a, Phonolite, Brenk
18 - Sanidine, sample 83-1, Tephritic phonolite, Brenk
19 - Sanidine, sample 52-13, Selbergite tuff, Southern Bell
20 - Sanidine, sample 52-7, Selbergite tuff, Bell
21 - Sanidine, sample 77-10, Phonolite, Olbruck
22 - Sanidine, sample 96-2, Selbergite tuff, Brenk
23 - Sanidine, sample 96-5, Selbergite tuff, Brenk
24 - Sanidine, sample 116-3, Nephelinite, Hannebacher Ley
25 - Sanidine, sample 109-2, Tephritic phonolite, Perlerkopf
26 - Sanidine, sample 107-4, Tephritic phonolite, Perlerkopf
27 - Sanidine, sample 107-5, Tephritic phonolite, Perlerkopf
28 - Sanidine, sample 107-6, Tephritic phonolite, Perlerkopf
29 - Sanidine, sample 107-11, Tephritic phonolite, Perlerkopf

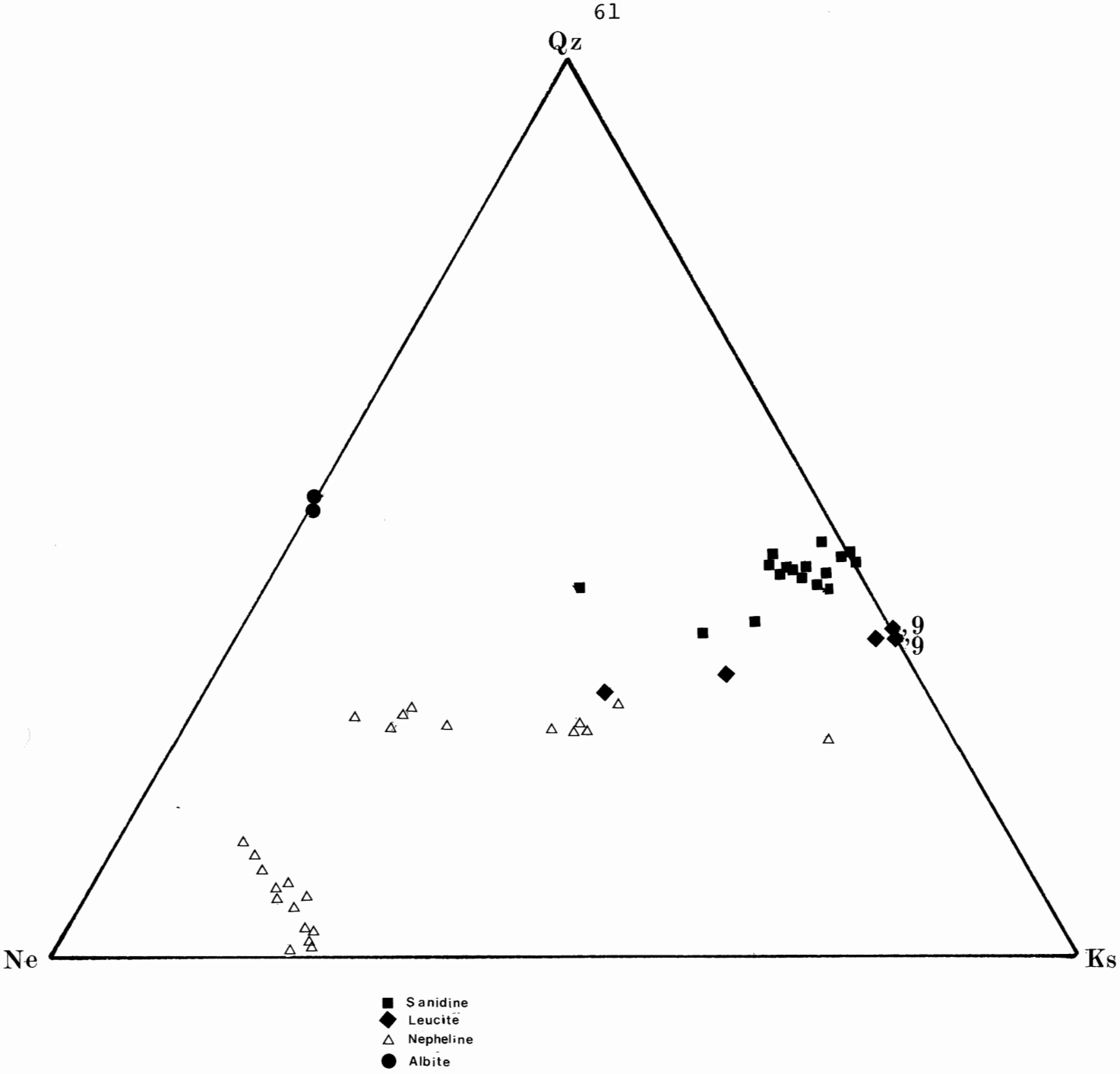

Figure 5.2. Quartz-Nepheline-Kalsilite Ternary Diagram - Residua System

The Albite composition point was defined using analyses from Deer, et al. (1980). Analyses of sanidine, leucite and nepheline are plotted from the CIPW normative values.

obtained for leucite (Table 5.7). Two of these analyses are pseudoleucite; for example 4 and 22. They differ from unaltered leucite by increased amounts of FeO and Na_2O and by decreased amounts of K_2O. Pseudoleucite is produced through the reaction of the liquid with leucite phenocrysts (Morse, 1980). Alternatively it can be produced by the subsolidus breakdown of sodium leucite (Fudali, 1963). Both processes may be of importance in this particular case. Pseudoleucite is composed of nepheline and alkali feldspar. Some of the leucite crystals display well defined grain boundaries which Deer, et al. (1980) believe to indicate rapid chilling. The CIPW norm values are plotted on the residua system (Fig. 5.2). The points indicate the relatively stable composition of leucite in this particular system. Deviation of the points from this major compositional point is probably due to alteration or K-Na solid solution.

5.8 Nepheline

Analyses of twenty-three nepheline crystals have been obtained (Table 5.8). The nepheline compositions vary considerably among the samples. Rittman (1973) states that the chemical composition of nepheline never corresponds to the theoretical formula $NaAlSiO_4$. He has used the alkali ratio: $K = K/(Na + K)$ to predict the order of formation of nepheline and leucite crystals in silica undersaturated magmas. If the

TABLE 5.7

LEUCITE AND PSEUDOLEUCITE ANALYSES

	1	2	3	4	5	6	7	8	9	10	11	12
SiO_2	55.09	55.57	55.82	56.39	54.68	54.95	55.01	54.97	54.70	54.66	52.04	54.96
TiO_2	-	-	-	-	-	-	-	-	-	-	.33	.08
Al_2O_3	22.74	23.14	22.72	21.33	22.35	22.65	22.79	22.41	22.47	22.42	24.98	22.78
FeO	.54	.58	.49	2.31	.62	.40	.45	.64	.80	.56	1.19	.75
MnO	-	-	-	-	-	-	-	-	-	-	-	-
MgO	-	-	-	.06	-	-	-	-	-	-	-	-
CaO	-	-	-	.14	.06	-	.11	-	.18	.13	.09	.07
Na_2O	-	-	-	5.95	-	-	-	-	-	-	2.73	-
K_2O	21.53	21.53	21.57	12.83	21.16	21.67	21.67	21.84	21.35	21.59	18.98	21.92
Total	99.89	100.82	100.6	99.01	98.88	99.67	100.03	99.86	99.50	99.36	100.34	100.63

Number of ions on the basis of 6 oxygens

Si	2.008	2.005	2.018	2.031	2.013	2.009	2.005	2.011	2.006	2.008	1.897	1.998
Ti	-	-	-	-	-	-	-	-	-	-	.009	.002
Al	.977	.984	.968	.905	.970	.976	.979	.966	.971	.971	1.073	.976
Fe^{2+}	.016	.018	.015	.070	.019	.012	.014	.020	.025	0.71	.036	.023
Mn	-	-	-	-	-	-	-	-	-	-	-	-
Mg	-	-	-	.003	-	-	-	-	-	-	-	-
Ca	-	-	-	.005	.002	-	.004	-	.007	.005	.004	.005
Na	-	-	-	.415	-	-	-	-	-	-	.193	-
K	1.002	.992	.995	.590	.994	1.011	1.008	1.020	.999	1.012	.883	1.017
Total												

	13	14	15	16	17	18	19	20	21	22	23
SiO_2	55.15	55.32	52.51	55.33	55.58	54.92	55.25	55.58	55.53	53.28	56.39
TiO_2	.19	.30	.15	-	-	-	-	-	-	.08	-
Al_2O_3	22.85	22.94	25.04	22.68	22.47	22.55	22.46	22.57	22.48	24.73	22.55
FeO	.58	.65	.69	.63	.65	.65	.63	.52	.52	2.98	.48
MnO	-	.11	-	-	.07	-	-	-	-	-	-
MgO	-	-	-	-	-	-	-	-	-	-	-
CaO	.22	.11	.17	-	.09	.07	.16	.09	.04	.19	-
Na_2O	-	-	2.64	-	.49	.07	-	-	-	10.89	-
K_2O	21.79	22.07	18.83	22.22	19.78	21.08	21.59	22.32	22.70	8.36	21.95
Total	100.78	101.5	100.03	100.86	99.13	99.34	100.09	101.08	100.77	100.51	101.37

Si	1.998	1.994	1.911	2.006	2.025	2.011	2.013	2.011	2.014	1.892	2.025
Ti	.005	.008	.004	-	-	-	-	-	-	.002	-
Al	.976	.974	1.074	.969	.965	.973	.964	.962	.961	1.035	.955
Fe	.018	.02	.021	.019	.020	.020	.019	.016	.016	.089	.014
Mn	-	.003	-	-	.002	-	-	-	-	-	-
Mg	-	-	-	-	-	-	-	-	-	-	-
Ca	.009	.004	.007	-	.004	.003	.006	.003	.002	.007	-
Na	-	-	.186	-	.035	.005	-	-	-	.750	-
K	1.008	1.015	.875	1.028	.920	.985	1.004	1.031	1.028	.379	1.006
Total	4.013	4.019	4.078	4.023	3.97	3.997	4.007	4.023	4.020	4.153	4.001

1 leucite, sample #79-1, phonolite, Olbruck
2 leucite, sample #79-2, phonolite, Olbruck
3 leucite, sample #79-3, phonolite, Olbruck
4 pseudoleucite, sample #82-101, phonolite, Brenk
5 leucite, sample #82-116, phonolite, Brenk
6 leucite, sample #83-10, tephritic phonolite, Brenk
7 leucite, sample #83-11, tephritic phonolite, Brenk
8 leucite, sample #83-12, tephritic phonolite, Brenk
9 leucite, sample #104-8, phonolite, Brenk
10 leucite, sample #104-9, phonolite, Brenk
11 leucite, sample #51-1, nephelinite, Southern Bell
12 leucite, sample #51-2, nephelinite, Southern Bell
13 leucite, sample #51-4, nephelinite, Southern Bell
14 leucite, sample #51-7, nephelinite, Southern Bell
15 leucite, sample #51-10, nephelinite, Southern Bell
16 leucite, sample #69-2, phonolite, Kempenich
17 leucite, sample #69-3, phonolite, Kempenich
18 leucite, sample 76-2, phonolite, Kempenich
19 leucite, sample #76-3, phonolite, Kempenich
20 leucite, sample #77-4, phonolite, Olbruck
21 leucite, sample #77-6, phonolite, Olbruck
22 pseudoleucite, sample 77-91, phonolite, Olbruck
23 leucite, sample 78-3, phonolite, olbruck

TABLE 5.8

NEPHELINE ANALYSES

	1	2	3	4	5	6	7	8	9	10	11
SiO_2	46.27	45.91	44.14	47.76	48.81	41.66	44.57	47.25	46.17	45.79	42.37
TiO_2	-	-	-	-	-	-	-	-	-	-	-
Al_2O_3	30.98	30.93	32.26	29.32	26.81	33.07	30.93	30.72	31.44	30.49	33.55
Fe_2O_3	2.025	1.89	1.74	1.57	3.02	.75	2.77	1.51	1.27	2.10	.61
MgO	-	-	-	-	-	-	-	-	-	-	-
CaO	-	0.35	.07	.44	.14	.30	.06	-	-	.07	-
Na_2O	16.17	15.79	15.77	15.91	13.25	16.06	15.89	16.31	15.99	15.88	15.92
K_2O	5.53	5.36	6.52	4.68	7.41	7.23	6.40	5.02	5.89	5.74	7.44
Total	100.89	100.13	100.51	99.60	99.02	99.03	100.48	100.73	100.69	99.96	99.86

Numbers of ions on the Basis of 32 Oxygens

Si	8.771	8.758	8.968	9.096	8.803	8.172	8.566	8.919	8.762	8.775	8.221
Ti	-	-	-	-	-	-	-	-	-	-	-
Al	6.922	6.955	7.295	6.582	7.030	7.667	7.006	6.835	7.033	6.887	7.673
Fe^{3+}	.289	.272	.251	.225	.102	.111	.401	.215	.182	.303	.089
Mg	-	-	-	-	-	-	-	-	-	-	-
Ca	-	.072	.014	.090	.058	.063	.012	-	-	.014	-
Na	5.943	5.840	5.865	5.875	5.615	6.107	5.920	5.968	5.883	5.900	5.988
K	1.338	1.305	1.597	1.138	1.664	1.810	1.570	1.209	1.427	1.404	1.843
Total	23.263	23.701	23.490	23.006	23.271	23.909	23.476	23.146	23.286	23.282	23.814

	12	13	14	15	16	17	18	19	20	21	22
SiO_2	42.85	42.58	42.36	48.46	45.50	44.29	45.24	44.55	44.19	44.46	45.06
TiO_2	-	-	.48	-	-	-	-	-	-	-	-
Al_2O_3	33.73	33.81	28.72	30.68	30.57	28.70	31.04	30.14	29.93	32.46	32.17
Fe_2O_3	.71	.69	2.40	.97	1.95	1.49	1.57	3.11	3.15	1.22	1.44
MgO	-	-	1.95	-	-	-	-	-	-	-	-
CaO	.18	-	4.72	.34	-	4.68	-	.04	-	.04	-
Na_2O	16.02	15.97	11.07	16.69	15.93	14.57	16.22	16.13	15.98	16.23	16.35
K_2O	7.50	7.48	9.07	3.36	5.80	5.92	5.69	6.11	5.89	6.60	6.00
Total	100.95	100.49	100.65	100.42	99.75	99.57	99.68	99.92	98.98	100.95	100.95

Si	8.228	8.210	8.295	9.071	8.741	8.646	8.695	8.615	8.617	8.485	8.567
Ti	-	-	.071	-	-	-	-	-	-	-	-
Al	7.634	7.684	6.629	6.769	6.945	6.604	7.032	6.870	6.879	7.302	7.210
Fe^{3+}	.103	.100	.354	.137	.282	.219	.227	.453	.463	.175	.206
Mg	-	-	.569	-	-	-	-	-	-	-	-
Ca	.037	-	.990	.068	-	.979	-	.008	-	.008	-
Na	5.464	5.969	4.203	6.057	5.933	5.514	6.044	6.047	6.091	6.005	6.027
K	1.838	1.841	2.267	.803	1.422	1.475	1.396	1.508	1.466	1.608	1.456
Total	23.804	23.804	23.378	22.906	23.323	23.437	23.395	23.501	23.466	23.583	23.466

1 nepheline - sample 79-8, Phonolite, Olbruck
2 nepheline - sample 79-9, Phonolite, Olbruck
3 nepheline - sample 79-10, Phonolite, Olbruck
4 nepheline - sample 82-113, Phonolite, Brenk
5 nepheline - sample 82-119, Phonolite, Brenk
6 nepheline - sample 82-124, Phonolite, Brenk
7 nepheline - sample 83-6, Tephritic Phonolite, Brenk
8 nepheline - sample 83-7, Tephritic Phonolite, Brenk
9 nepheline - sample 83-9, Tephritic Phonolite, Brenk
10 nepheline - sample 79-201, PHonolite, Olbruck
11 nepheline - sample 104-1, Phonolite, Brenk
12 nepheline - sample 104A, Phonolite, Brenk
13 nepheline - sample 104-2, Phonolite, Brenk
14 nepheline - sample 51-3, Nephelinite, Bell
15 nepheline - sample Neid3, Tephritic Phonolite, Niedermend
16 nepheline - sample 113-5, Phonolite, Perlerkopf
17 nepheline - sample 113-7, Phonolite, Perlerkopf
18 nepheline - sample 113-8, Phonolite, Perlerkopf
19 nepheline - sample 109-9, Tephritic Phonolite, Perlerkopf
20 nepheline - sample 107-9, Tephritic Phonolite, Perlerkopf
21 nepheline - sample 107-10, Tephritic Phonolite, Perlerkop
22 nepheline - sample 107-11, Tephritic Phonolite, Perlerkop

alkali ratio (K) is less than 0.2 in nephelinites, then only nepheline will crystallize. If the K ratio in phonolites is between 0.2 and 0.4, then nepheline will crystallise first, followed, in highly undersaturated rocks, by leucite. In phonolites where the K ratio is between 0.4 and 0.58, leucite will crystallize first, then nepheline. The K ratio in the nephelinites in this study is less than 0.2 and thus as predicted no leucite is present. Rittman (1973) has stated that the crystallization of nephelinites will increase the alkali ratio in the remaining melt. In this case nepheline will occur as phenocrysts and leucite will occur as anhedral infilling of interstices. The K ratio in some phonolites in this study falls between 0.2 and 0.4 and falls between 0.4 and 0.58 in other phonolites. In the former case the leucite and nepheline crystals occur as microphenocrysts. In the latter case leucite will crystallize as phenocrysts and nepheline will form small crystals in the groundmass as observed.

When plotted on the residua system (Fig. 5.2) one cluster of points lies in the nepheline-leucite-kalsilite triangle. These points may define the reaction line of the carnegeite field. The other set of points define a line probably corresponding to the degree of Na-K substitution in the structure of the crystal.

CHAPTER 6

DISCUSSION

6.1 Alkaline Magmatism

The generation of an alkaline magma is extremely complex and involves the combination of many processes. Some points to consider in the evolution of the magma body include the chemical, mechanical and physical responses of the enriched magma to its ascent. This enrichment may be enhanced by the upward migration of the more mobile elements as well as by the assimilation of the more silicic roof rocks.

Within the magma there are many processes which occur due to the chemical and physical nature of the ions and minerals present. As the magma strives for equilibrium, it is subjected to many processes which may include double diffusion, crystal fractionation, gravity settling and flowage differentiation.

External processes affecting a magma chamber include metasomatism, which may initiate partial melting, the mixing of two or more magma bodies, batch fractionation (O'Hara, 1977), zone refining (Harris, 1957), assimilation of bedrock (Rittman, 1973) and contamination by ionic exchange (O'Hara, 1980).

These processes however numerous and complex, are relatively unusual but must be reproducible to generate alkaline magmas which occur scattered throughout the crust.

6.2 Petrogenetic Models

As stated in Chapter one, magmatism is associated with rift zones in stable cratons.

Bailey (1974) has introduced a model which depicts the rising of geo-isotherms in the mantle, causing uplift and rifting of the crust. The movement of the isotherms is thought to be in response to the tectonic forces acting between plates - diverging in this case (Illies et al., 1979). The tectonic forces are generated by the interaction of two (or more) plates which are moving at different rates in different directions. Bailey (1974) believes that as the uplift occurs a zone of reduced pressure is produced at depth in the crust. Volatiles and other mobile elements migrate into this zone producing an alkaline magma which is subsequently extruded through the rift zone. Studies conducted on alkaline magmas in the East African Rift system concerning volatile enrichment and isotope and rare earth element ratios, led Bailey (1974) to believe that the magmas are derived from the mantle, not through a recycling episode of the crust.

Harris (1974) has indicated that the more mafic alkaline rocks eg. nephelinites, basanites and alkali basalts, are of mantle origin. Bailey (1974) indicates that the origin of the more felsic magmas eg. trachytes, phonolites and pantellerites is still in question. These are low temperature melts which may be produced by partial melting of the crust or by crystal fractionation of a mantle magma. The magmas are characterized by their peralkalic affinity and their enrichment in volatiles and incompatibles. Bailey (1974) concludes that the generation of alkaline magmas on a large scale can be attributed to the partial melting of the deep-seated crust. This conclusion is based on the reduction of pressure, facilitating the migration of volatiles and mobile elements from the mantle (as previously outlined). The presence of these elements reduces the melting range of the crustal rocks (Bailey, 1974). As this melting zone rises in the crust, the magmas generated become increasingly silicic eg. with increasing depth:

phonolite → trachyte → pantellerite

6.3 Eifel Magmatism

The samples in this study have been clearly divided into two major groups, a mafic one (M) and a felsic one (F). The mafic group contains nephelinites, phonolites and tephritic phonolites. The felsic group contains phonolites and

tephritic phonolites.

6.3.1 Group M

The petrogenetic model preferred (by the author) for the genesis of the nephelinites of Group M (M-1) is partial melting of the mantle. Evidence for this model includes the relative enrichment of LREE. The Rb/Sr ratios are similar to those for the mantle, indicating that this magma has not differentiated much from its original composition before extrusion. The highly alkalic nature of the samples is typical of 1 to 1.7% partial melting of a pyrolite (olivine + Al-poor pyroxene) mantle containing 0.1% water, at a depth of 80 to 120 km (Sood, 1981) (Fig. 6.1) (Table 6.1).

Since the REE data of the more leucocratic samples of Group M (M-2) follow the same trend as that of Group M-1, except being more enriched in REE's these two groups of samples should be related. The Rb/Sr ratio of Group M-2 is approximately the same for that of Group M-1. In many of the rare earth and trace element graphs, the samples of Group M-1 plot close to those of Group M-2, reinforcing the observed petrogenetic link.

The difference between Group M-1 and M-2 is more relevant in the abundances of major elements and thus in the mineralogy. Group M-2 is more alkalic than Group M-1 and as

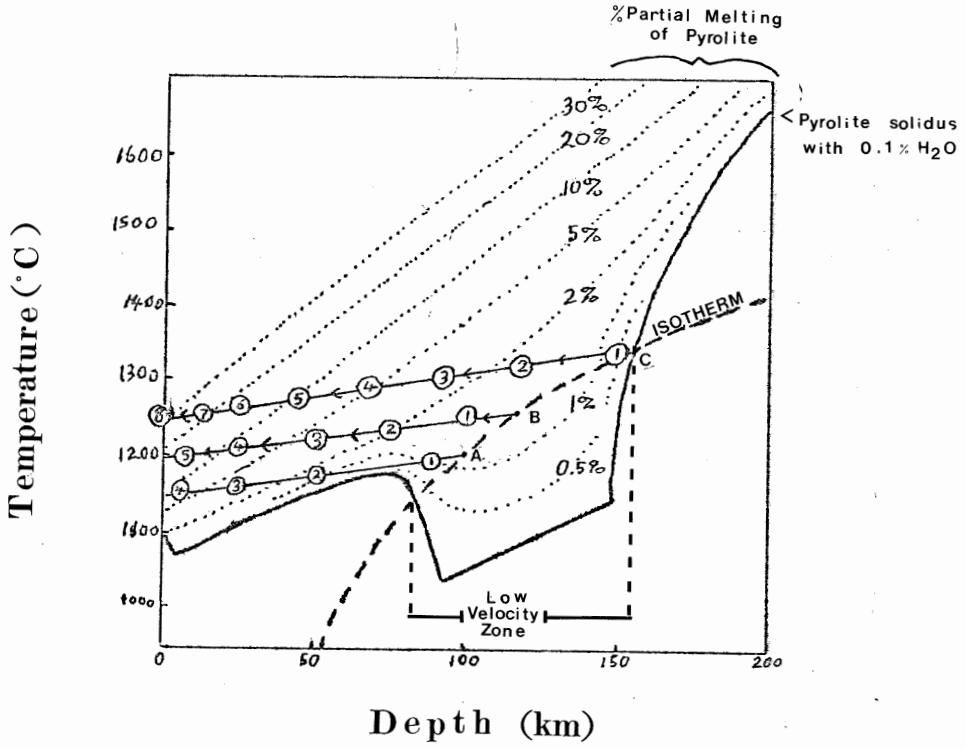

Figure 6.1. Relationships between the degree of melting and the depth of magma separation, to magma composition in the P-T field of the mantle solidus for rising geo-isotherms. Lines extending from the isotherm are P-T paths of the isotherms with percent partial melting of pyrolite. (After Sood, 1981).

Depth of Magma Separation	Diapir in Fig. 62		Magma Types	Partial Melting (%)
100 km ↓ 50 km ↓ Surface	A	1	Olivine nephelinite	1 ↓ 8
		2	Olivine basanite	
		3	High Al-alkali basalt	
		4	Quartz tholeiite	
120 km ↓ 50 km ↓ Surface	B	1	Olivine nephelinite	1 ↓ 15
		2	Olivine basanite	
		3	Alkali olivine basalt	
		4	High Al-basalt	
		5	Quartz tholeiite	
150 km ↓ 45 km ↓ Surface	C	1	Kimberlite	0.5 ↓ 5 ↓ 15 ↓ 30
		2	Olivine nephelinite	
		3	Olivine basanite	
		4	Alkali olivine basalt	
		5	Olivine basalt	
		6	High Al-olivine tholeiite	
		7	Olivine tholeiite	
		8	Tholeiitic picrite	

Table 6.1. Magma generation and low pressure liquid lines of descent, corresponding to Figure 6.1. (After Sood, 1981).

previously stated, it is more enriched in the LREE. This leads to the hypothesis that Group M-2 is a differentiate from Group M-1. During fractional crystallization, batch fractionation, zone refining, etc., the incompatibles, such as volatiles and REE are concentrated in the melt. Thus one of these processes or a combination of them may be responsible in the generation of Group M-2.

The clinopyroxenes of Group M-1 have cores richer in FeO, MnO and Na_2O than the rims. This suggests the influence of magma mixing. Since this process appears to influence only the clinopyroxenes of Group M-1, then a pulse of magma introduced would be of very similar composition to the original magma. An alternate hypothesis involves the remobilization of high pressure fractionated crystals (green cores) in the same magma which was altered at a lower pressure (development of lighter green rims).

Processes involving crystal fractionation and density settling are indicated by the presence of glomeroporphyritic masses of clinopyroxene, apatite and titaniferous oxides (Cox, et al., 1978). The fine oscillatory zoning present in the pyroxene, have probably been produced by the attempt of the crystal to equilibrate with a magma of slow, but constant compositional change ie. a change caused by fractionation of the melt.

Some of the samples show the effects of minor deformation. These effects are most evident in the straining of biotite (rare). The strained biotite crystals are present only in tuffs. It is probable then that these are xenocrysts from the country rock.

6.3.2 Group F

There are several alternatives for the genesis of this group in relation to the mafic group. 1) The two groups may have two totally unrelated sources. 2) Group F may be a felsic differentiate of the source magma for Group M, or 3) Group F may have been generated upon partial melting of the country rock overlying the magma chamber.

The first model probably does not apply in this case because the age of both groups is similar (Quaternary to Recent). The volcanic vents representing the two groups are intrically related (Fig. 6.2). It is thus unlikely that two unrelated bodies of magma would exist at the same time in a relatively small area.

The second model involves the processes of fractional crystallization or batch fractionation. The LREE trends are parallel to those of Group M, however they have become relatively depleted in the felsic group. If this process was involved the enrichment of LREE would be expected.

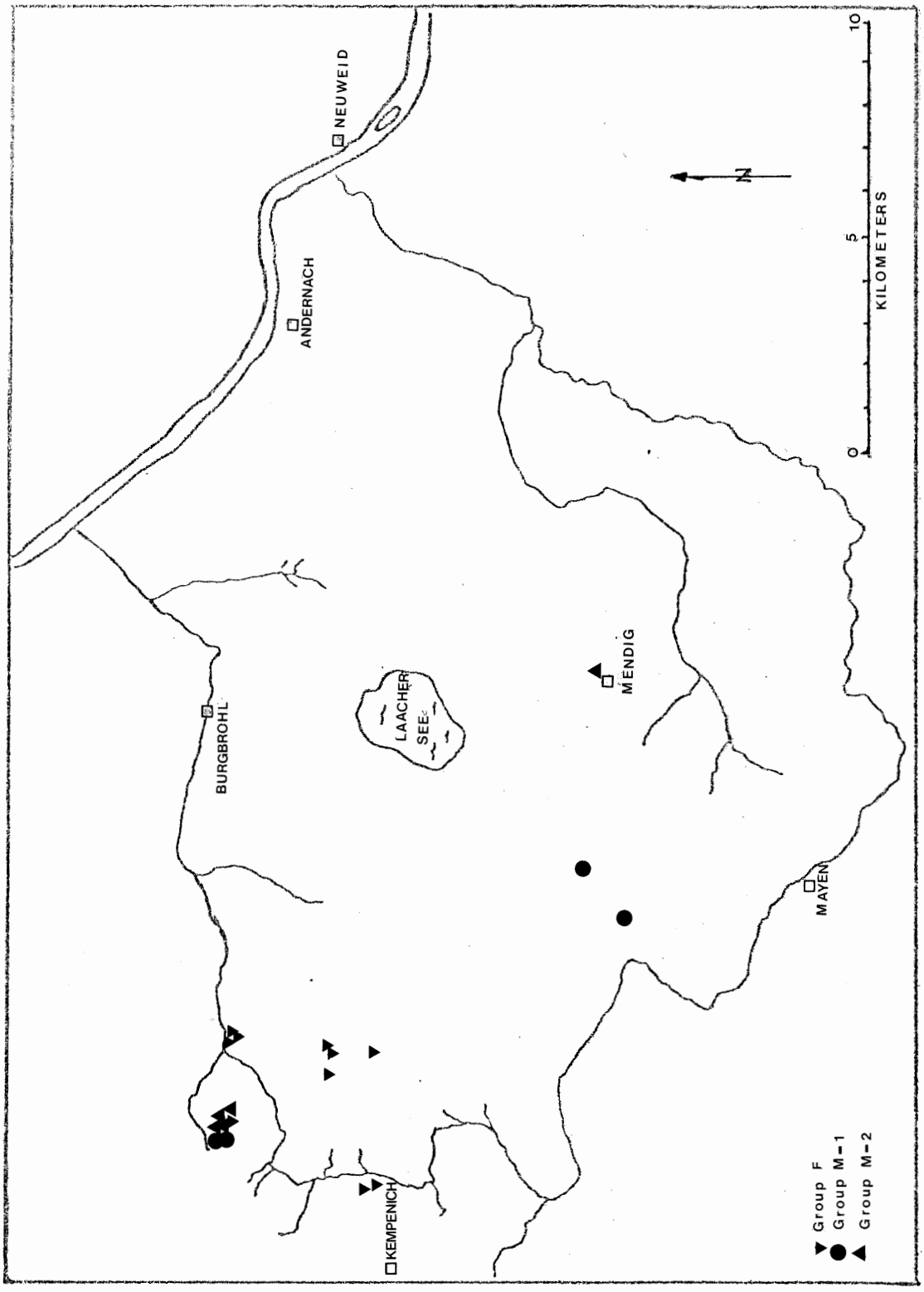

Figure 6.2. Map of the East Eifel volcanic field - Laacher See area. The relationships of Groups M-1, M-2 and F are depicted.

The third model is reinforced by the Rb/Sr graph which indicates a crustal source for this group.

The author feels that a combination of the second and third models best describes the petrogenesis of the felsic group. The Rb/Sr ratio may alternatively represent mantle material which has been exceptionally enriched in light trace elements. The lower values of LREE in the felsic group may be attributed to the assimilation of relatively LREE depleted crust. Metasomatism and gaseous transfer may be of subordinate importance.

In the residua system the mineral analysis of nepheline, sanidine and leucite form the apices of a triangle. The CIPW normative values of the whole rocks of the felsic group plot within this triangle as expected (Fig. 6.3). The conditions of formation as determined by this CIPW plot suggest that group F was last equilibrated at approximately 2 kilobars pressure. It is then under these conditions that the phenocrysts were stable and the magma was rapidly, sometimes explosively erupted to the surface and quenched upon extrusion.

Alteration is present to some degree in all the samples. The most obvious examples are the breakdown of leucite to pseudoleucite and the development of mantles around the hauyne phenocrysts. This alteration is generated as the minerals readjust to the changing conditions of equilibrium in the magma chamber.

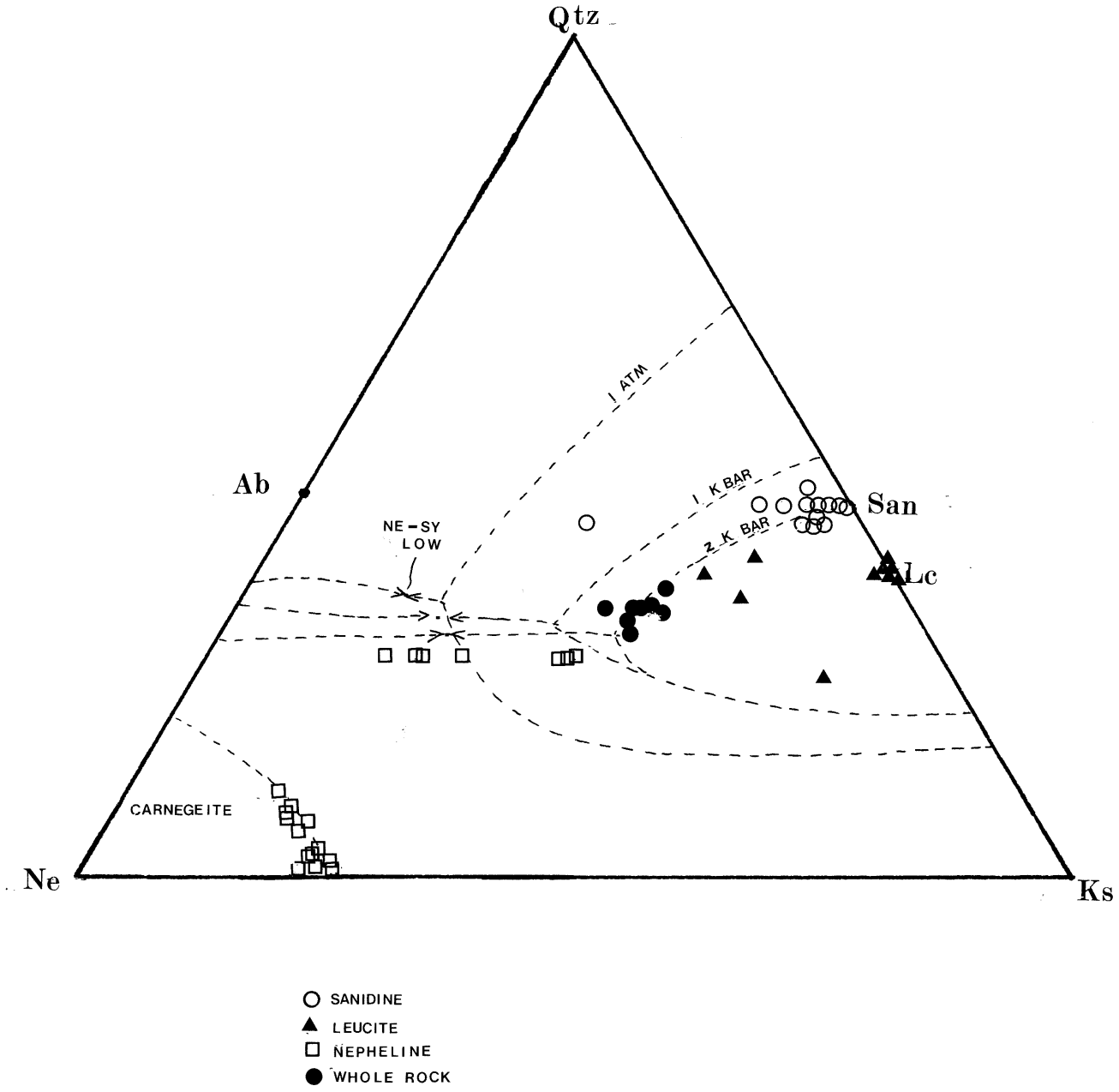

Figure 6.3. Quartz-Nepheline-Kalsilite Diagram-Residua System. Relationships are shown for P = latm, P_{H_2O} = 1 kbar, 2kbar. CIPW norm analyses of sanidine, nepheline, leucite and the whole rocks are plotted. (After Giffins, 1979).

6.3.3 Problems

There is a large compositional gap that exists between group M-1 and M-2. It is difficult to explain the absence of rocks of intermediate composition if these two groups are generated from different parts of the same magma chamber. If however, the rocks were genetically related and became differentiated from each other one magma could indeed be a felsic portion and the other, a mafic portion from the same parental magma.

The K/Rb vs K graph (Fig. 4.15) displays a trend which opposes that of Shaw (1968). Shaw's diagram indicates that as potassium increases, K/Rb increases which is to be expected since K and Rb have similar chemical properties and affinities for one another. The trend displayed by the samples in this study indicates that potassium increases relative to rubidium. A process responsible for this trend is not known at this point, however, a potassium rich, rubidium depleted metasomatic or hydrothermal event may be responsible.

The presence of xenoliths in Groups F and M indicate the violent nature of eruption and the possibility of mixing within the chamber. The xenoliths of country rock in the tuffs and some of the rocks of Group F indicate that the process of extrusion was one of disruption. In Group F there are also

xenoliths very similar in composition to the nephelinites. This may indicate that mixing has occurred within the magma chamber before extrusion. The felsic xenoliths in the rocks of Group M may have been incorporated in the mafic magma upon its ascent to the surface. The clinopyroxene cumulates in Group M may also indicate some degree of mixing within the magma.

6.3 Conclusions

Due to the time, space and compositional similarities of the two groups in this study it is concluded that they are petrogenetically related. Group M-1 is thought to have been derived from partial melting of the mantle and Group M-2 may represent a differentiate from the M-1 magma. Group F may also be a differentiate from the original M-1 magma, but had undergone partial melting of the overlying country rock?

CHAPTER 7

CONCLUSION

This thesis has incorporated the petrology, major and trace element geochemistry and the mineral chemistry of the samples, in an attempt to understand their petrogenesis.

The following is a list of conclusions from the above studies:

1) There are two distinct groups of rocks in this study, a mafic (M) one and a felsic (F) one.
2) The mafic group can be subdivided into nephelinites (M-1) and phonolites (M-2)
3) The fractionation of the olivine, clinopyroxene and feldspathoid crystals may be responsible for the element trends in the samples.
4) The rimming of the pyroxene may represent the attempt of the early stage crystals to equilibrate with a later stage melt.
5) The fine oscillatory zoning of the clinopyroxene represents the equilibration of the crystal with a constantly changing melt, this may indicate the influence of crystal fractionation or zone refining.
6) Groups F and M are enriched in LREE, which is typical of highly evolved magmas. Group M-2 is more enriched than

M-1 which may be expected from a lighter differentiate. Group F is relatively enriched in HREE.

7) The Rb/Sr ratio indicates that the source for Group M is the mantle and that for Group F is the crust.

8) The alkalic nature of the two groups as well as their relation in time and space, indicate that they must be petrogenetically related. The presence of xenoliths of Group F in the rocks of Group M, and visa versa, substantiate this assumption.

9) The enrichment of Rb, Zr and Nb in Group F and depletion in Group M is expected since the more mobile elements migrate to the lighter differentiate.

10) Group F is thought to have last equilibrated at 2 kilobars before extrusion, as indicated by the CIPW norm values of the feldspathoids and the whole rocks.

11) The alkalic nature of the nephelinites of Group M-1 indicate formation by 1-1.7% partial melting of pyrolite at 80 to 120 km.

12) Based on the above conclusions Group M-1 seems to have been derived by partial melting of the mantle. Group M-2 is thought to be a differentiate from the Group M-1 magma. Group F may also be a differentiate from the Group M-1 magma, but it has probably also undergone assimilation of the crust.

This study has been on a relatively small scale and if the nature of the petrogenesis of the magmas is to be more clearly defined, analyses must be performed on samples from many more vents. The combination of detailed field relations and more analyses may help clear the uncertainty. Further geochemical studies may also reveal important information eg. isotopes.

ACKNOWLEDGEMENTS

I would like to thank Dr. D.B. Clarke who was instrumental in the initiation, progress and completion of this thesis. I also greatly appreciate the instruction and expert help of Bob MacKay on the electron microprobe.

Heartfelt thanks goes to Dwight Kenney for help and support through all stages of the study. Many thanks are extended to Dianne Crouse who produced this final copy quickly and efficiently. The advice and encouragement of Jennifer Bates is greatly appreciated.

Finally, I would like to thank Hilda and Alex Dobson for their faith, prayers and support.

REFERENCES

Ahrens, W. (1978). IN Duda, A. and H-U. Schmincke. Quaternary Basanites, Melilite Nephelinites and Tephrites from the Laacher See Area (Germany). N.Jb. Mineral. Abh., 132, p. 1-33 (1978).

Bailey, D.K. (1974). The Alkaline Rocks. IN H. Sorensen (ed.). John Wiley and Sons, London, p. 53-66, 148-159, 436-441.

Bailey, D.K. (1982). Mantle metasomatism-continuing chemical change within the Earth. Nature, 296, p. 525.

Barker, D.S., and Long, L.E. (1969). Feldspathoidal syenite in quartz diabase sill, Brookville, New Jersey, J. Pet., 10, p. 202-221.

Brauns, R. (1921). Die phonolithischen Gesteine des Laacher-See-Gebietes und ihre Beziehungen zu anderen Gesteinen dieses Gebietes. Neues. Jb. Miner., Beilage-Band, 46, p. 1-116.

Cox, K. G., Bell, J.D. and Pankhurst, R.J. (1979). The Interpretation of Igneous Rocks. George Allen and Unwin, Boston.

Daly, R.A. (1933). Igneous Rocks and the Depths of the Earth. McGraw-Hill, New York.

Deer, W.A., Howie, R.A. and Zussman, J. (1980). An Introduction to the Rock Forming Minerals. Longman, London.

Duda, A. and Schmincke, H.U. (1978). Quaternary Basanites, Melilite Nephelinites and tephrites from the Laacher See Area (Germany). N. Jb. Mineral. Abh., 132, p. 1-33.

Frechen, J. (1962). Fuhrer zu Vulkanologisch-petrographischen Exhursianen im siebengebirge am Rhein, Laacher Vulkangebiet und Maargebiet der Westeifel. Schweizerbart: Stuttgart.

Frechen, J. and Lippolt, H.J. (1965). K-Ar-Daten zum Alter des Laacher Vulkanisinus, der Rheinterrassen und der Eiszeiten. Eiszeitalter Ggw., 16, p. 5-30.

Frechen, J. (1971). Siebengebirge am Rhein Laacher Vulkangebeit det Westeifel. Gebt. Bointraeger: Berlin.

Fudali, R.F. (1963). Experimental studies bearing on the origin of pseudoleucite and associated problems of alkali rock systems. Geol. Soc. Am. Bull., 74, p. 1101-1126.

Giffins, J. (1979). The Evolution of the Igneous Rocks. IN H.S. Yoder, Princeton, University Press: Princeton, p. 351-390.

Harker, A. (1909). The Natural History of the Igneous Rocks. MacMillan, New York.

Harris, P.G. (1957). Zone refining and the origin of the potassic basalts. Geochim. et Cosmochim. Acta, 12, p. 195-208.

Harris, P.G. IN The Alkaline Rocks. H. Sorensen (ed.), John Wiley and Sons, London, p. 427-436 (1974).

Hughes, C.J. (1982). Igneous Petrology. Elsevier Scientific Publishing Company, Amsterdam.

Illies, J.H., Prodehl, C., Schmincke, H.-U. and Semmel, A. (1979). The Quaternary Uplift of the Rheinish Shield in Germany. Tect. 51, p. 197-225.

Kogarko, L.N., Ryabchikov, I.D. and Sorensen, H. (1974). IN The Alkaline Rocks, H. Sorensen (ed.), John Wiley and Sons, London, p. 488-500.

Korzhinsky, D.S. (1955). Problems of petrography of the magmatic rocks related to transmagmatic solutions and granitization (in Russian). IN Magmatism isvyaz's nim paleznykh iskopaemykh. Izd. Akad. Nauk USSR.

Kushiro, I. (1972). Determinations of liquidus relations in synthetic silicate systems with electron probe analysis: the system forsterite-diopside-silica at 1 atmosphere. Am. Min. 57, p. 1260-1271.

Lorenz, V. (1975). IN Physics and Chemistry of the Earth. Ahrens, L.H., J.B. Dawson, A.R. Duncan, and A.J. Erlank (ed.), Pergamon Press, Oxford, vol. 9.

Morse, S.A. (1980). Basalts and Phase Diagrams. Springer-Verlag, New York.

O'Hara, M.J. (1968). The bearing of phase equilibria studies on the origin and evolution of basic and ultrabasic rocks. Earth Sciences Revs., 4, p. 69-133.

O'Hara, M.J. (1977). Geochemical evolution during fractional crystallization of a periodically refilled magma chamber. Nature 266, p. 503-507.

O'Hara, M.J. (1980). Nonlinear nature of the unavoidable long-lived isotopic, trace and major element contamination of a developing magma chamber. Phil. Trans. Roy. Soc. London, 297A, p. 215-227.

Okrusch, M., Schroder, B. and Schnutgen, A. (1979). Granulite-facies metabasalt ejecta in the Laacher See area, Eifel, West Germany. Lithos 12, p. 251-270.

Ringwood, A.E. (1975). Composition and Petrology of the Earth's Mantle. McGraw-Hill, New York.

Rittman, A. (1973). Stable Mineral Assemblages of Igneous Rocks. Springer-Verlag, New York.

Sahama, Th. G. (1974). IN The Alkaline Rocks, H. Sorensen (ed.), John Wiley and Sons, London, p. 96-109.

Schmincke, H.U. (1977b). Phreatomagmatic Phasen in quartaren Vulkanen der Osteifel. Geol Jahrb., A 39, p. 3-45.

Schmincke, H.U., Mertes, H., Staudigel, H., Zindler, A., Gijbels, R. and Bowman, H. (1978). Geochemische and tektonische Kontraste zwischen den quartaren Vulkanfeldern der E-und W-Eifel. Fortschr. Mineral., 56, Beih. 1, p. 124-125.

Shaw, D.M. (1968). A review of K-Rb fractionation trends by covariance analysis. Geochim. et Cosmochim. Acta, 32, p. 573-602.

Sood, M.K. (1981). Modern Igneous Petrology. John Wiley and Sons, New York.

Sorensen, H. (1974). The Alkaline Rocks. John Wiley and Sons, London.

Taylor, S.R. (1964). The abundance of chemical elements in the continental crust - a new table. Geochim. Cosmochim. Acta, 28, p. 1273-1285.

Taylor, H.P., Frechen, J. and Degens, E.T. (1967). Oxygen and carbon isotope studies of carbonatites from the Laacher See District, West Germany and the Alno District, Sweden. Geochim. Cosmochim. Acta, 31, p. 407-430.

Wimmenaur, W. (1964). IN The Alkaline Rocks. H. Sorensen (ed.), John Wiley and Sons, London, p. 238-271.

Wimmenaur, W. (1972). Gesteinassoziationen des jungen Magmatismus in Mitteleuropa. tschermaks miner. petrogr. Mitteil., 3, Folge, 18, p. 56-63.

Wood, C.P. (1974). A geochemical study of E. African alkaline lavas and its relevance to the petrogenesis of nephelinites. IN The Alkaline Rocks, H. Sorensen (ed.), John Wiley and Sons, London, p. 238-271.

Wyllie, P.J. (1974). IN The Alkaline Rocks, H. Sorensen (ed.), John Wiley and Sons, London, p. 238-271.

GROUP M

51 - Nephelinite, 57 - Nephelinite

Texture
- porphyritic, holocrystalline
- groundmass - pilotaxitic, aphanitic
- phenocrysts - moderately poikilitic

Phenocrysts

Titanaugite
- (30-35%) subhedral to euhedral phenocrysts
- oscillatory zoning, also overgrowth of augite
- few simple twins

Biotite
- (2-3%), zoned crystals; well fractured
- golmeroporphyritic, strained crystals
- crystals 1 cm to 0.2 mm

Olivine
- (1%) iddingsite rims phenocrysts
- phenocrysts highly fractured

Groundmass
- 50% of total mineral content
- nepheline - inclusions in augite, olivine and in groundmass
  - anhedral to subhedral crystals
- augite - fine grained felty mass of crystals
- sanidine - fibrous, acicular crystals
- magnetite - subhedral to anhedral

Xenolith
- leucocratic, crystal tuff, similar to 52

Plates I, II

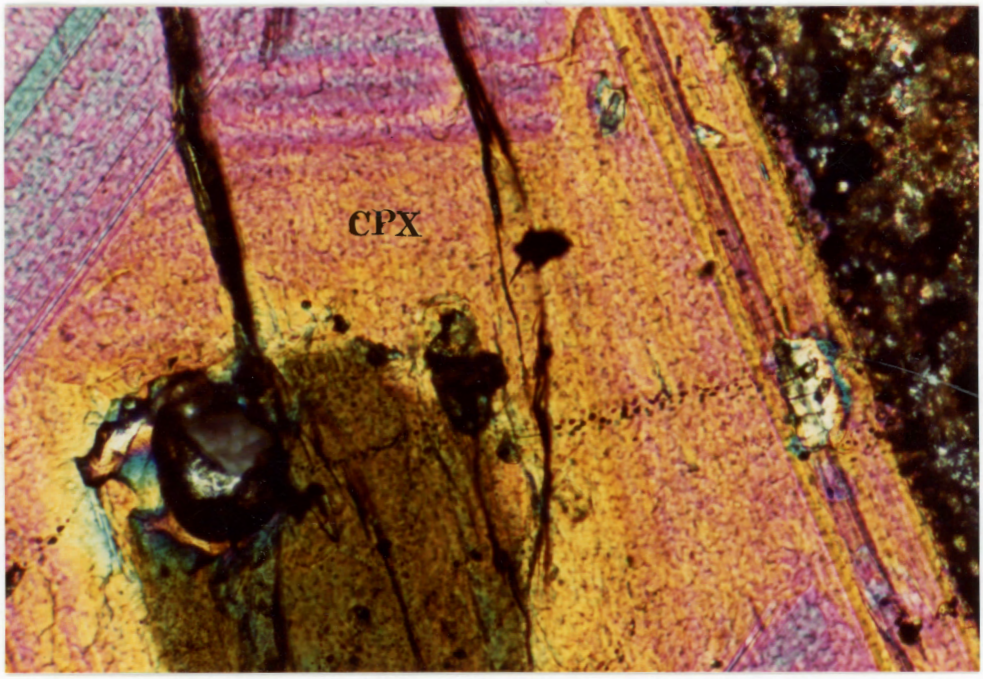
CPX

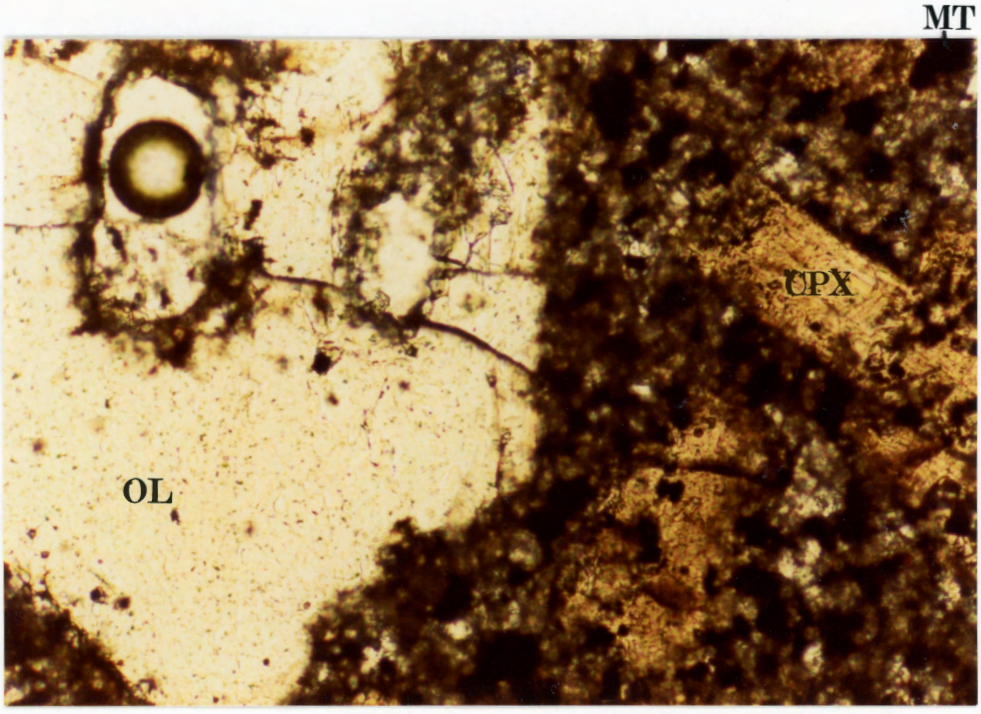
MT
CPX
OL

Plate I: 51 - Nephelinite (porphyritic) Mag. x80 (x-nicols) Group M-1
- core of original pyroxene rimmed by a more stable pyroxene
- rim displays fine oscillatory zoning

Plate II: 51 - Nephelinite (porphyritic) Mag. x80 (ppl) Group M-1
- phenocryst of olivine (ol) surrounded by laths of clinopyroxene (cpx) and irregular grains of magnetite (mt)

GROUP M

116 - Nephelinite, 117 - Nephelinite

Texture
- vesicular lava flow
- aphanitic groundmass, holocrystalline
- granular groundmass
- subophitic texture
- green, brown weathering on surface

Mineralogy

Main constituents

- Augite (40%) laths, some zoning displayed, irregularly fractured
- Nepheline (30%) acicular crystals in groundmass, subhedral - some simple twins
- Magnetite (15-20%) granules in groundmass, irregular grain boundaries

Minor constituents (10%)

- Leucite - minimal, highly altered
- Calcite - secondary, found in fractures and voids
- Aegirine-augite - secondary, euhedral laths, protrude into cavities

Xenolith: glomeroporphyritic clinopyroxene

Plates III

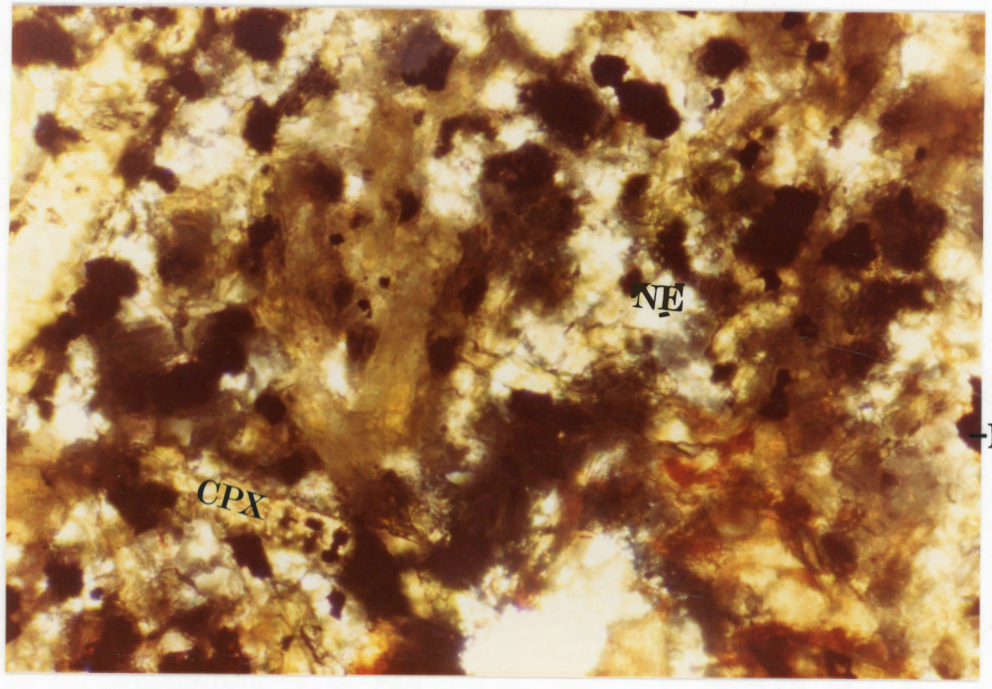
NE
MT
CPX

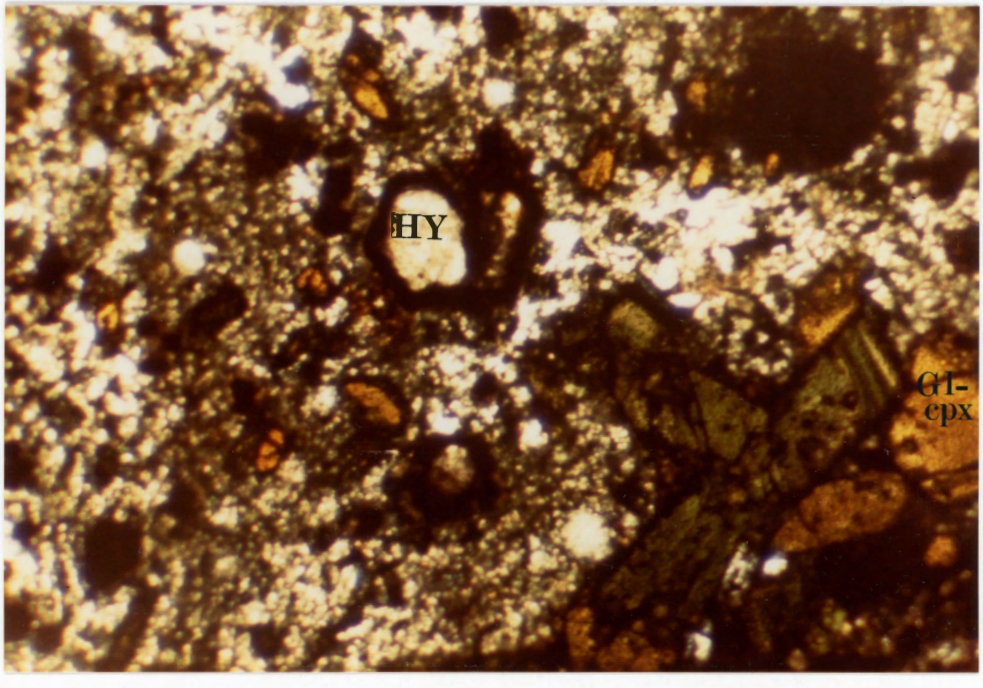
HY
GI-
cpx

Plate III: 117 - Nephelinite (flow) Mag. x20 (ppl) Group M-1
- irregular magnetite grains (mt), clinopyroxene laths (cpx), nepheline crystals (ne)

Plate IV: 113 - Selbergite Mag. x20 (ppl) Group M-2
- Glomeroporphyritic clinopyroxene (Gl-cpx)
- hauyne (Hy)
- felty groundmass of nepheline and clinopyroxene

GROUP M

108 - Selbergite, 109 - Selbergite, 113 - Selbergite

Texture - holocrystalline, porphyritic, voids present
- groundmass, pilotaxitic, aphanitic

Phenocrysts

- Augite (35-40%) - good oscillatory zoning, subhedral to euhedral crystals
  - poikilitic, fractured, alteration mantle
- Leucite (20%) - highly altered to pseudoleucite and clays
  - hexagonal outline evident
- Hauyne (5%) - generally well altered, highly fractured
  - some cleavage evident
- Sanidine (5%) - altered, displays carlsbad twinning, highly fractured

Groundmass (30-35%)

- Augite - felty mass of acicular crystals
- Nepheline - small rectangular outline
- Sanidine - felty, acicular mass of crystals
- Magnetite - irregular and rare
- Apatite - subhedral to anhedral, minimal

Xenolith - in 108 - hauyne, augite, apatite cumulate

Plates IV, V, VI

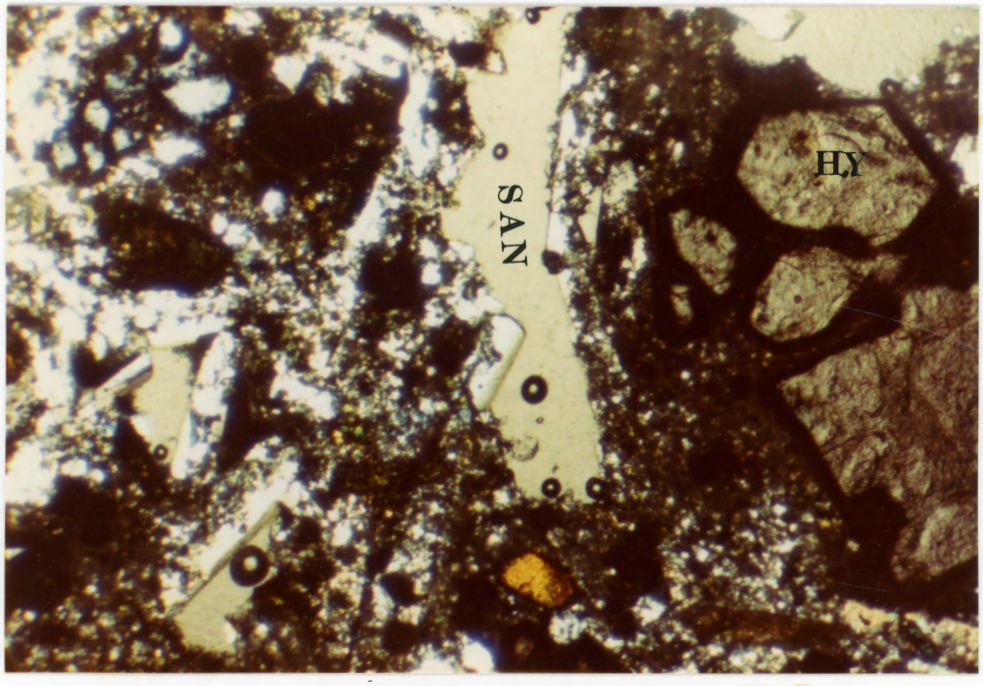
SAN
HY

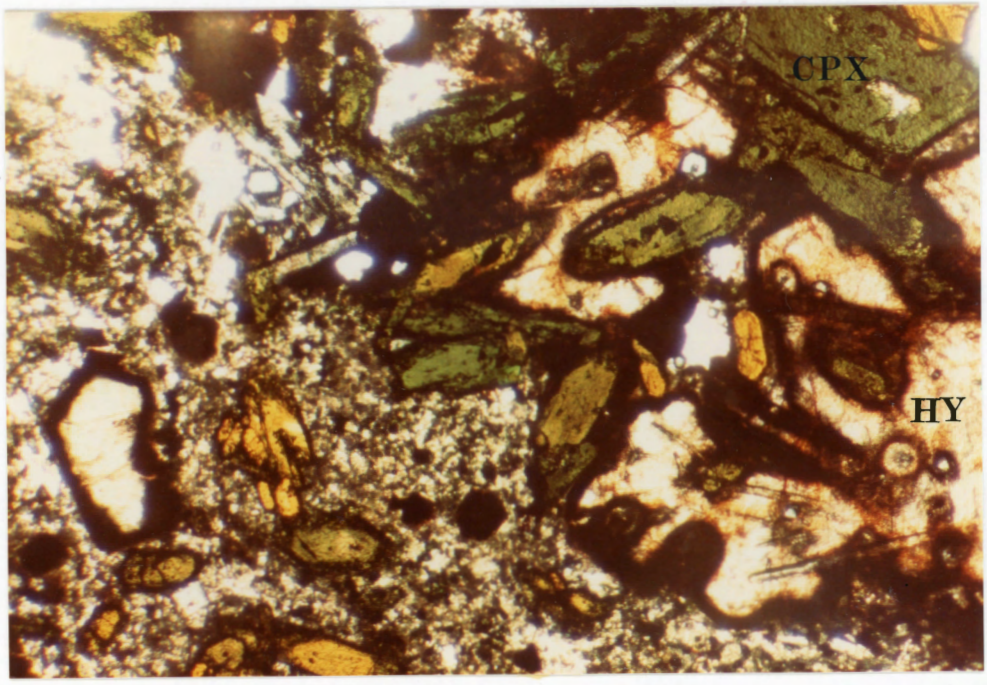
CPX
HY

Plate V: 109 - Selbergite Mag. x20 (x-nicols) Group M-2
- sanidine (SAN) and hauyne (Hy) phenocrysts in pilotaxitic groundmass

Plate VI: 108 - Selbergite Mag. x20 (ppl) Group M-2
- clinopyroxene (CPX) and hauyne (HY) cumulate in fine grained groundmass

GROUP M

107 - Tephritic Phonolite

Texture
- holocrystalline, porphyritic, subhedral to euhedral crystals
- groundmass - pilotaxitic, aphanitic

Phenocrysts

- Augite (40%) dark green, light green, red in ppl.
  - glomeroporphyritic, subhedral, twinned
  - altered rims
- Sanidine - (20%) lath shaped crystals
  - carlsbad twinning
  - altered rims
- Leucite - (2-3%) anhedral, generally entirely altered to red-brown clay
- Hauyne - (2-3%) alteration mantles, highly fractured
  - glomeroporphyritic

Groundmass (30-35%)

- nepheline - euhedral rectangles
- sanidine - felty, acicular crystals
- augite - acicular laths
- magnetite - irregular crystals - minimal
- apatite - highly fractured, poikilitic, euhedral

Plate VII

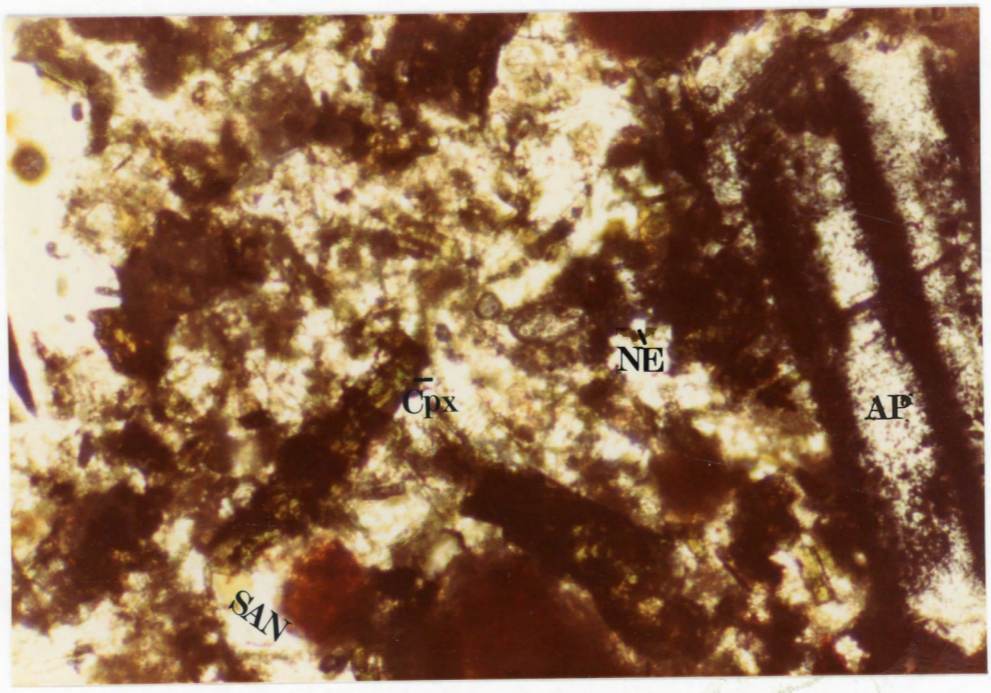
NE
Cpx
AP
SAN

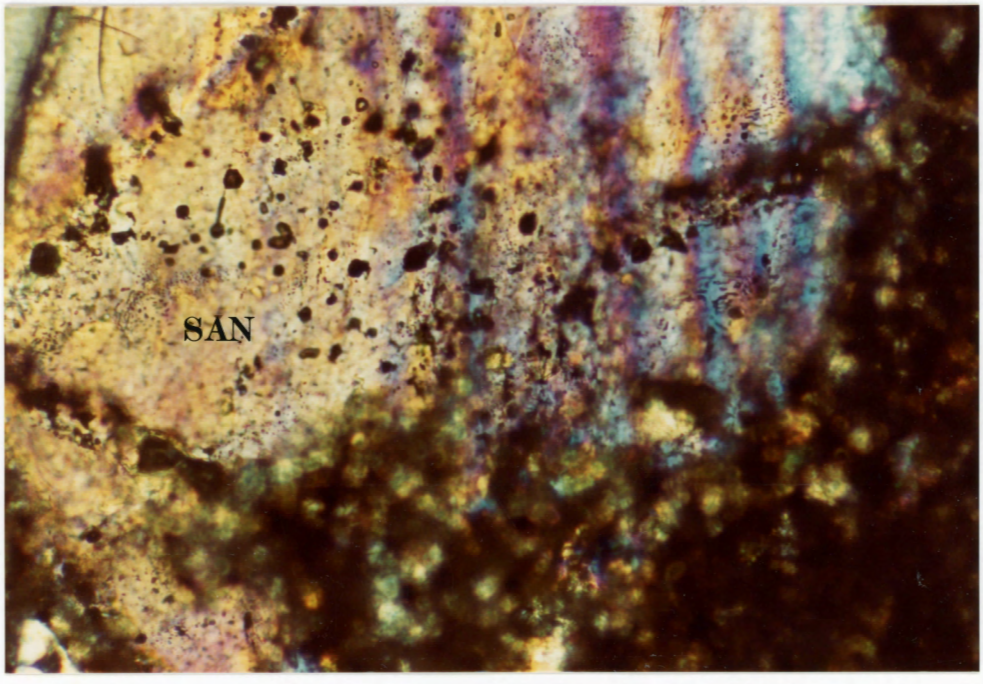
SAN

Plate VII: 107 - Tephritic phonolite Mag. x80 (ppl)
Group M-2
- apatite (AP) phenocryst in groundmass of clinopyroxene (CPX) sanidine (SAN) and nepheline (NE)

Plate VIII: 50 - Tephritic phonolite Mag. x80 (x-nicols)
Group M-2
- zoned poikilitic sanidine (SAN) phenocryst

GROUP M

50 - Tephritic Phonolite

Texture
- vesicular lava flow
- porphyritic
- groundmass - aphanitic, holocrystalline
- highly altered to clays

Mineralogy

Main constituents

- Augite (40%) zoned phenocrysts, irregularly fractured
- Hauyne (5%) 2 mm phenocrysts, altered rims
- Magnetite (10-15%) anhedral to euhedral - rectangular - about .01 mm in groundmass
- Nepheline (15-20%) acicular felty crystals in groundmass

Minor constituents (25-30%)

- Sanidine - minimal, zoned crystals, well fractured
- Aergine-Augite - secondary, euhedral crystals found in fractures, voids
- Calcite - secondary, fills fractures, voids

Plate VIII

GROUP F

77, 78, 79, 101, 104 - Selbergite

Texture
- porphyritic, holocrystalline
- alteration generally to clays and fine grained alkali feldspar
- groundmass - aphanitic
- generally subhedral to anhedral crystals

Phenocrysts

Leucite: (30-40%) euhedral to subhedral crystals
- alteration of small crystals to pseudoleucite
- some crystals fresh, complex twinning
- poikilitic

Hauyne: (5-7%) altered crystals - dark rims, light cores
- generally euhedral, fractured
- some indication of cleavage

Sanidine: (5%) - euhedral to subhedral, some fracturing
- carlsbad twinning

Augite: (1%) - zoned crystals, green in ppl.

Groundmass (40-45%)

- nepheline - euhedral, rectangular crystals, often containing rows of inclusions
- sanidine - fine, acicular lath-shaped crystals
- magnetite - minimal, irregular grains
- augite - fine grained acicular crystals
- calcite - secondary - fills voids and fractures
- zeolite - secondary - also found in fractures and voids

Xenolith - in 79 - very fine grained - metased/volcanic (?)

Plates IX, X, XI

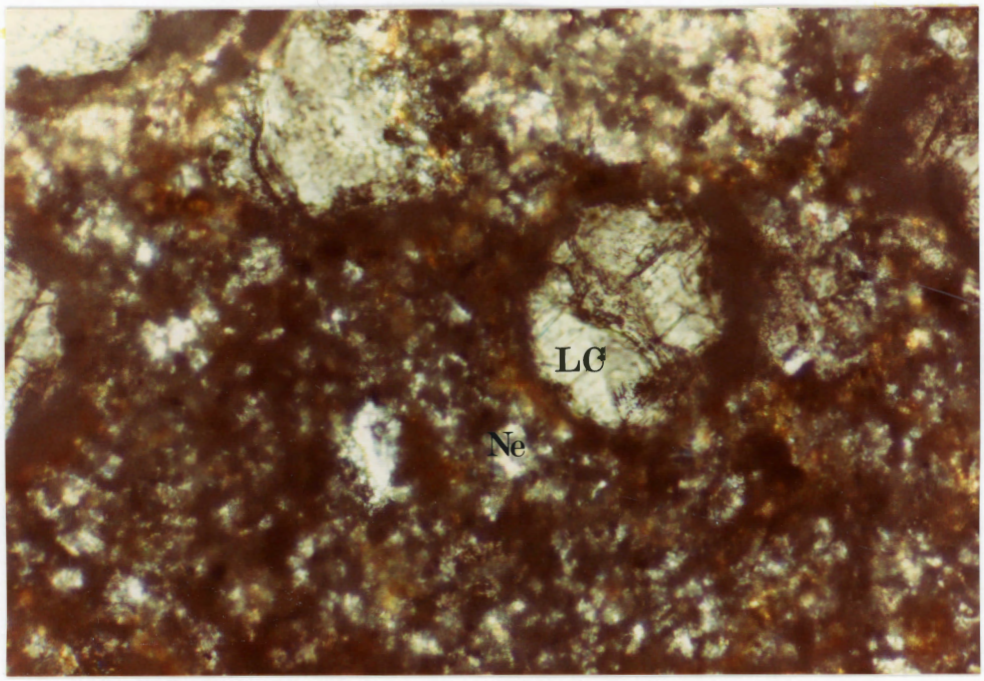
LC
Ne

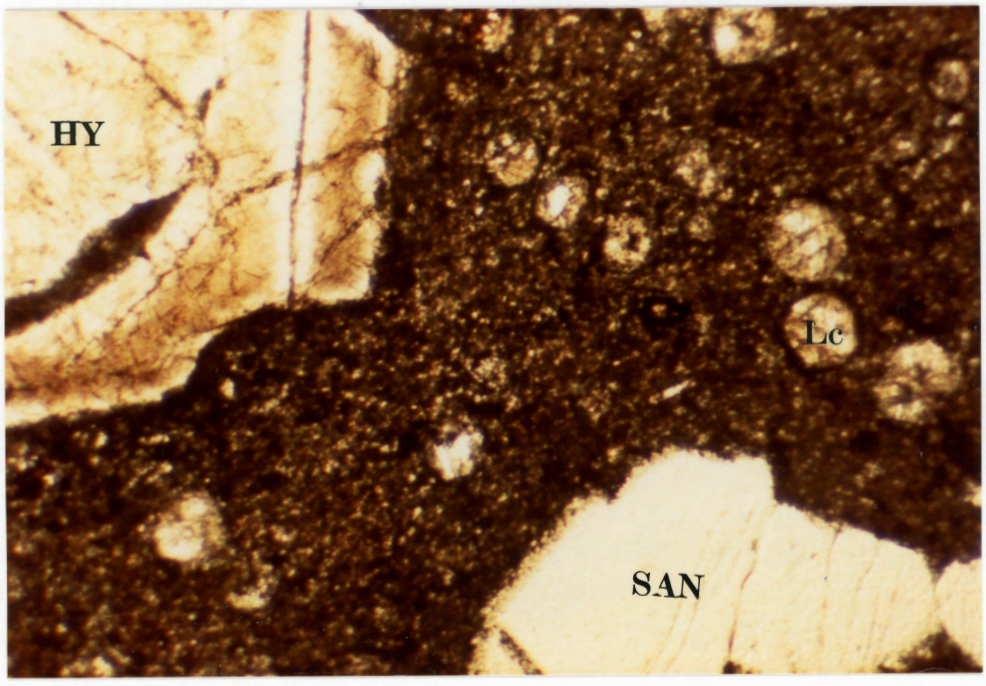
HY
Lc
SAN

Plate IX: 77 - Selbergite Mag. x80 (x-nicols) Group F
- leucite phenocrysts (LC) with altered rims and displaying complex twinning
- nepheline (NE) in groundmass

Plate X: 78 - Selbergite Mag. x20 (ppl) Group F
- hauyne (HY), sanidine (SAN) and leucite (LC) phenocrysts in fine grained crystalline groundmass

GROUP F

69, 76, 82 - Porphyritic Phonolites

Textures
- holocrystalline, porphyritic
- groundmass - aphanitic, pilotaxitic
- crystals are generally euhedral to subhedral
- much alteration to clays

Phenocrysts

Leucite: (20-30%) generally euhedral crystals, complex twinning
- largely altered to pseudoleucite
- slightly poikilitic

Hauyne: (2%) - euhedral phenocrysts, alteration around rim and along fractures, rarely altered core
- poikilitic
- rare aggregates

Sanidine: (2%) - lath shaped
- irregular fracturing perpendicular to length
- some alteration

Augite: (1%) - highly altered, subhedral
- rarely glomeroporphyritic

Biotite: (1%) - very minimal, highly altered to clays

Groundmass (60-65%)

- nepheline - small rectangular, euhedral crystals, generally altered
- sanidine - felty groundmass, some twinning, good cleavage
- magnetite - minimal, irregular crystals
- augite (?) - minimal, needle-like crystals
- zeolite - secondary, fibrous, fan extinction, found in cavities and veins
- calcite - secondary, associated with hauyne in cavities

Xenolith - 69 - melanocratic - similar in composition to #51
- 76 - fine grained metased/volcanic

Plates XII, XIII

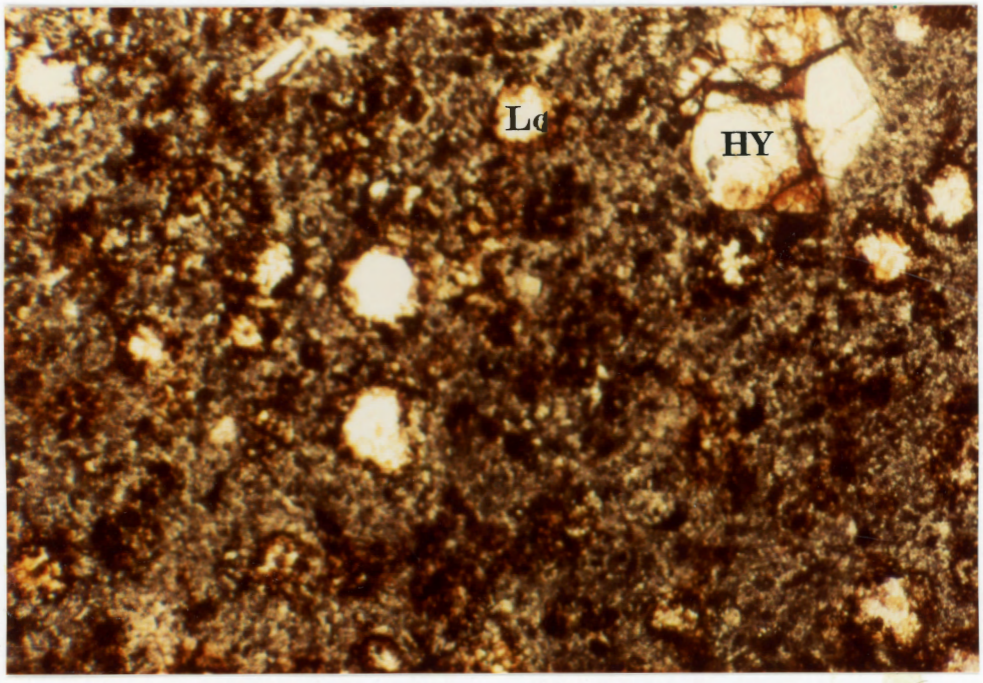
Lc
HY

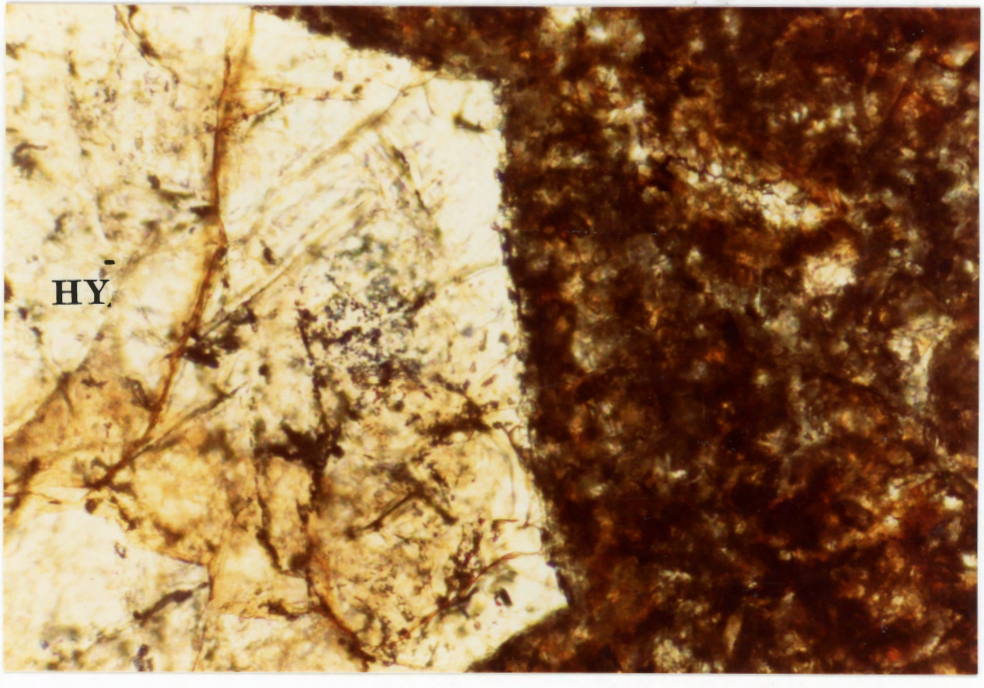
HY

Plate XI: 79 - Selbergite Mag. x20 (ppl) Group F
- altered rim around hauyne phenocryst, altered rims of leucite phenocrysts
- pilotaxitic groundmass

Plate XII: 69 - Phonolite (porphyry) Mag. x80 (ppl) Group F
- fractured hauyne phenocryst (HY)
- fine grained crystalline groundmass, alteration evident

GROUP F

83 - Tephritic Phonolite

Texture
- porphyritic, holocrystalline
- groundmass - aphanitic, pilotaxitic
- highly altered to light brown and reddish brown clays
- crystals are generally idiomorphic, some display corrosion

Phenocrysts

Leucite: (10-15%) complex twinning, rims are largely altered to pseudoleucite

Hauyne: (5%) - euhedral crystals, hexagonal in shape
- felty microcrystalline center, altered rims

Sanidine: (5%) - lath shaped phenocrysts up to 4 mm long
- conchoidal fractures across width
- Carlsbad twinning, corroded crystals

Groundmass (70-75%)

- nepheline - rectangular crystals
  - displays rows of inclusions parallel to crystal faces
- sanidine - acicular, felty crystals
- aergine-augite - secondary, acicular crystals which grow along cracks and in voids
- zeolite - radial habit, filling voids and fractures
- calcite - secondary, fills veins

Plate XIV

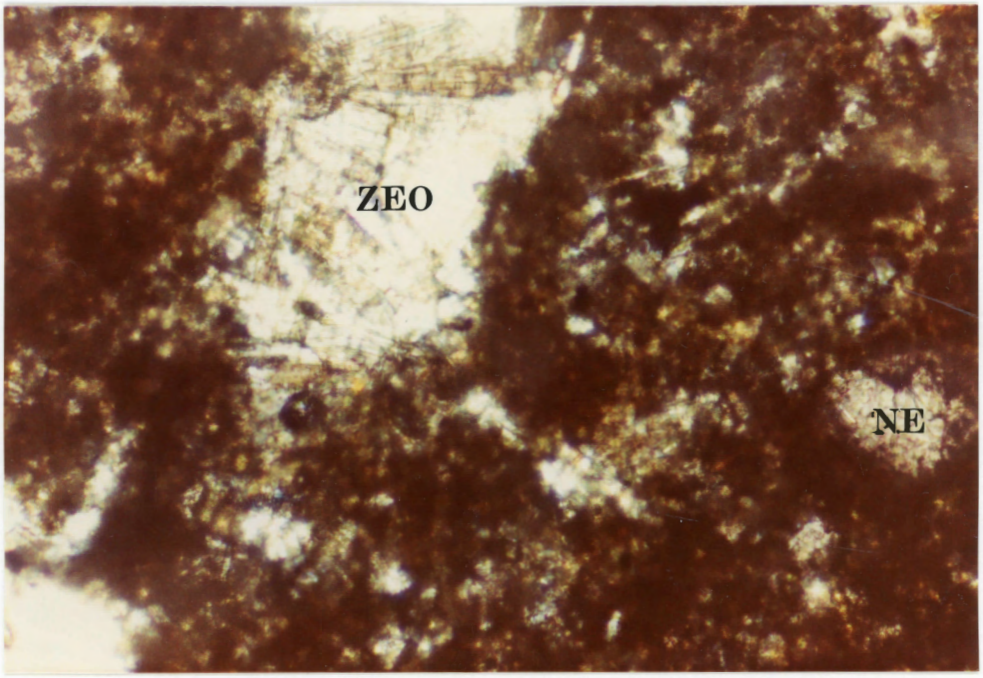
ZEO
NE

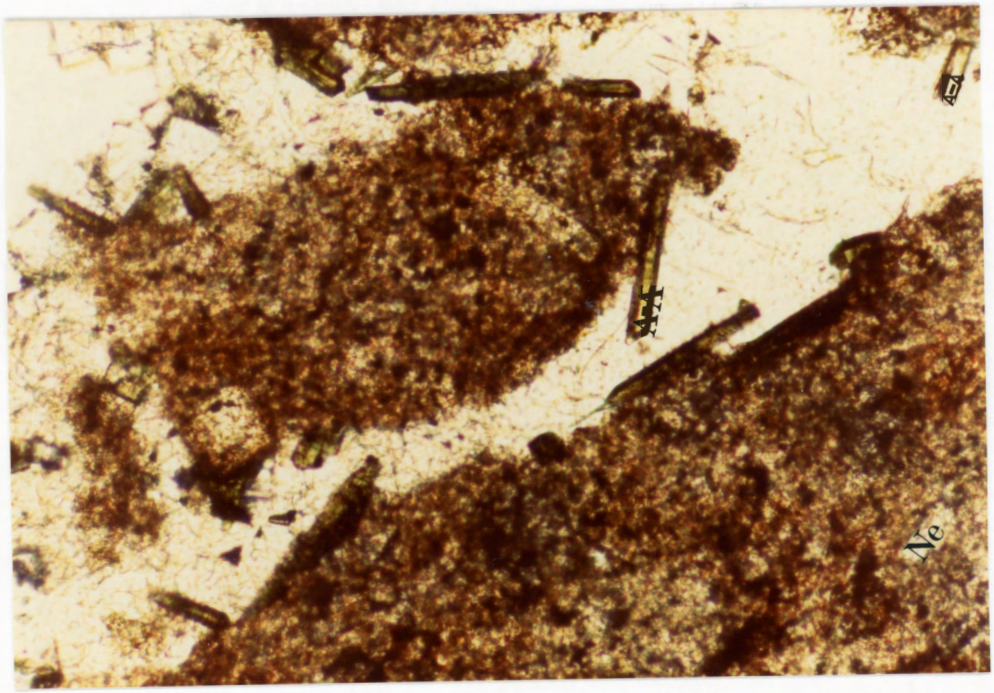
Ne

Plate XIII: 76 - Phonolite (porphyry) Mag. x80 (x-nicols)
Group F
- secondary zeolite (ZEO) in fracture
- nepheline (NE) in groundmass

Plate XIV: 83 - Tephritic Phonolite Mag. x80 (ppl)
Group F
- secondary aegirine-augite crystals (A-A) along fractures
- rectangular nepheline (NE) crystals in crystalline groundmass

GROUP T

52, 96 - Phonolitic Tuff

Texture
- pyroclastic, holocrystalline
- ∿50% rock fragments and crystal fragments
- poorly consolidated - numerous voids
- aphanitic to medium grain size
- highly altered

Mineralogy

Titanaugite and augite: (3-4%) well zoned, green in ppl, well fractured
- some inclusions of magnetite
- subhedral, good cleavage displayed rarely

Leucite: (5-7%) - euhedral to rounded crystals
- some entirely altered to pseudoleucite, some fresh

Nepheline: (2%) - euhedral to subhedral crystals, grow in cavities

Magnetite: (5%) - irregular to euhedral grains
- occur as phenocrysts and in the groundmass

Biotite: (<1%) - minimal, excellent cleavage

Amphibole: (<1%) - brown lath-like crystals, good cleavage

Sanidine: (1-2%) - phenocrysts, generally altered
- poikilitic
- also in groundmass as felty laths

Lithic Fragments

Silicic - quartz 70 to 80%, feldspar, probably derived from the country rock

Leucocratic - fragments of approximately trachytic composition (?)

Melanocratic - fragments possibly nephelinitic in composition

Mafic - possibly metasediments/volcanics
- well lineated, probably derived from the country rock

Plates XV, XVI

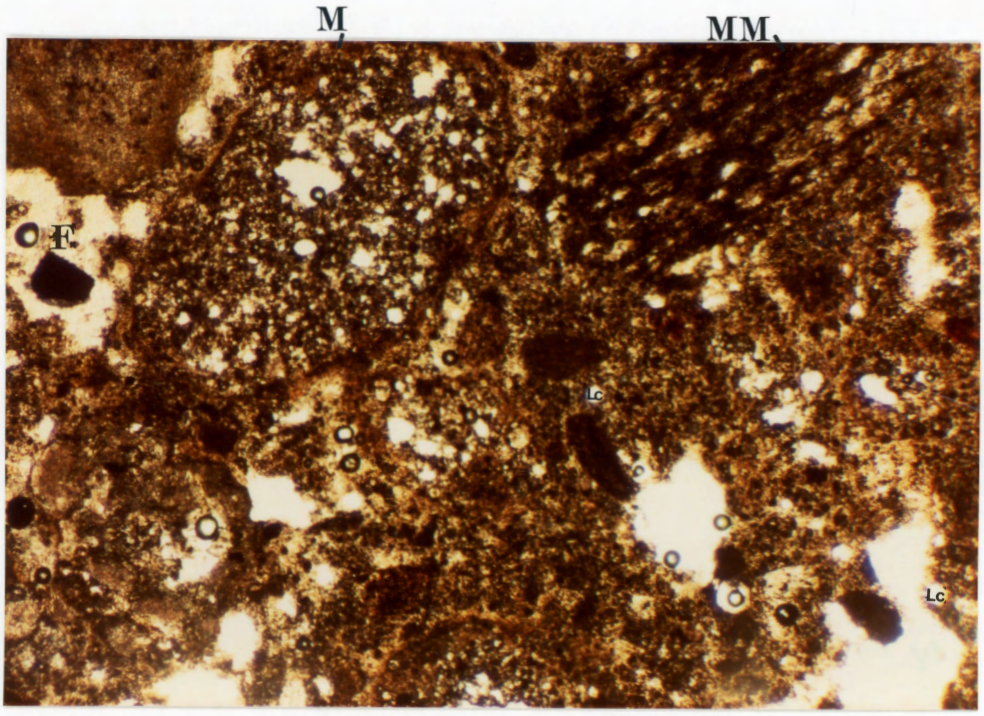
M
MM
F
Lc
Lc

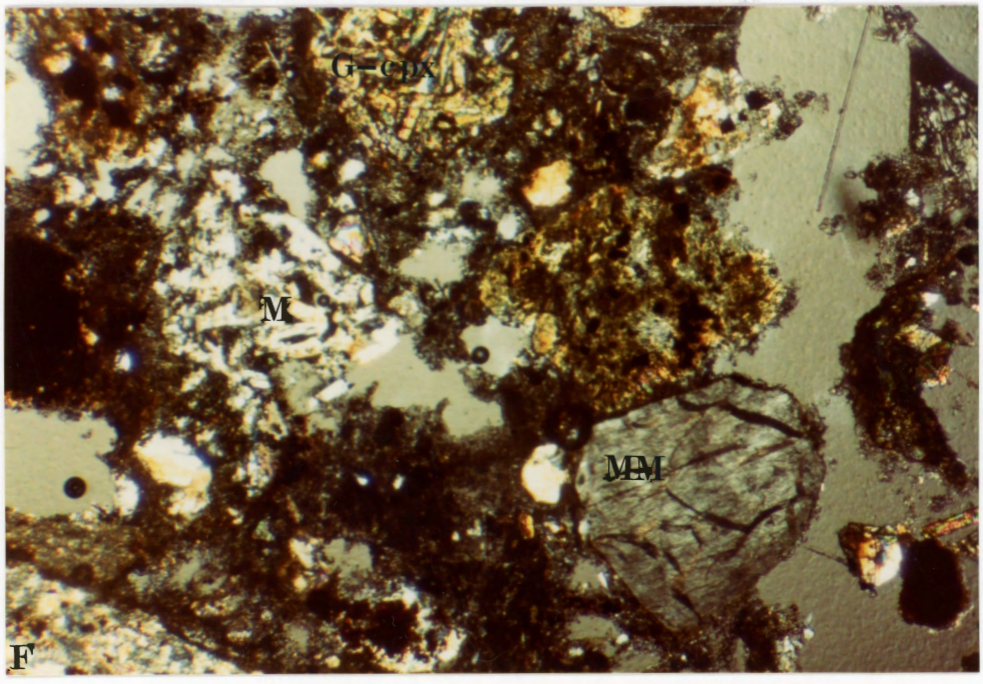
G=CPX
M
MM
F

Plate XV: 52 - Selbergite Tuff Mag. x20 (ppl)
- felsic (F), mafic (M) and metamorphic (MM) rock fragments
- groundmass is mainly fine grained ash
- microphenocrysts of leucite (LC)

Plate XVI: 96 - Selbergite Tuff Mag. x20 (x-nicols)
- felsic (F), mafic (M) and metamorphic (MM) rock fragments again present
- fragments of glomeroporphyritic clino-pyroxene crystals (G-cpx)

GROUP T

64 - Trachyte Tuff

Texture
- pyroclastic, tuffaceous, holocrystalline
- vesicular
- highly altered to clays
- all rock fragments have altered rims
- 80 - 90% lithic fragments

Mineralogy

Sanidine: (2%) - short, rectangular, subhedral prisms
- phenocrysts 1.3mm to 0.1mm
- some zoning present, Carlsbad twinning

Clinopyroxene: (1%) - zoning, subhedral crystals
- green to brown in ppl - pleochroic

Biotite: (<1%) subhedral, irregular flakes

Nepheline: (1%) - small rectangular prisms in groundmass
- crystals protrude into cavities

Leucite: (<1%) - altered to pseudoleucite
- euhedral crystals present in some lithic fragments

Calcite - secondary, fills cavities

Lithic Fragments: as in 52 and 96

- lithic fragments and fine grained ash have been kaolinized

Plate XVII

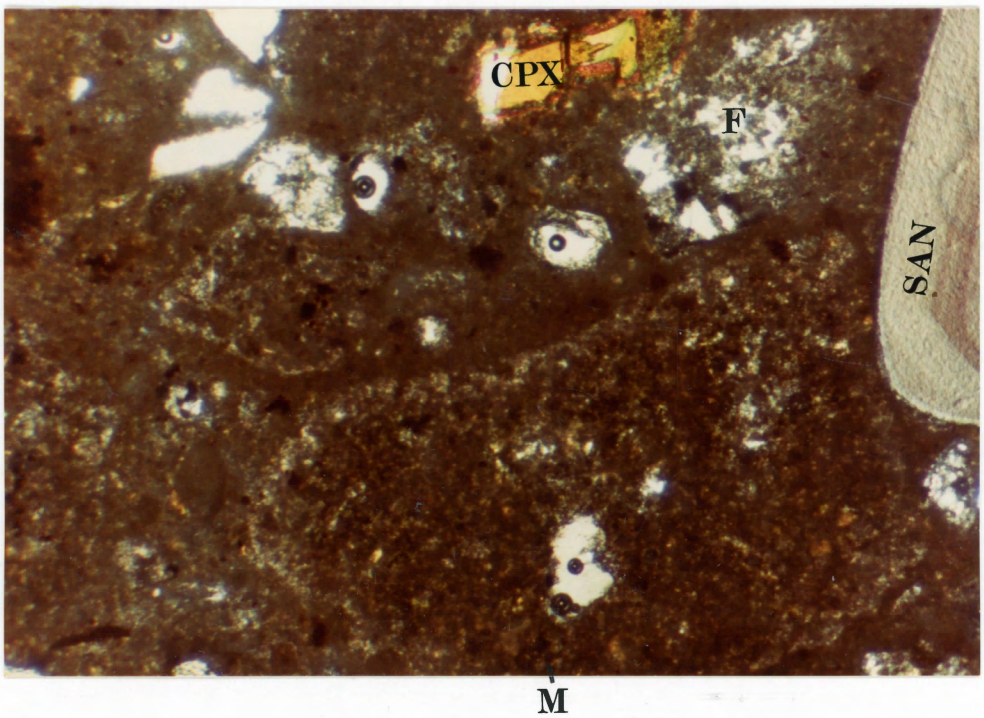

Plate XVII. 64 Trachyte Tuff Mag. x20 (x-nicols)

- zoned sanidine (SAN) phenocrysts
- clinopyroxene (CPX) crystal fragments
- mafic (M) and felsic (F) rock fragments
- groundmass is fine grained ash